

Introduction

In the past two decades, significant advances have been made in the description of the sensory anatomy of the head and neck, mostly in the cosmetic surgery literature. This progress was driven in large part by the discovery that compression of sensory nerves in the head and neck may contribute to the pathogenesis of migraine headaches.

Migraine headaches are a robust clinical challenge that affects 17.1% of women and 5.6% of men in the United States.¹ Traditional pharmacologic treatment is often insufficient. New surgical options for the treatment of migraine headache have been developed based on the finding that extracranial sensory branches of the trigeminal and cervical spinal nerves can be irritated, entrapped, or compressed at multiple points along their anatomical course, ultimately leading to a cascade of physiologic events that results in migraine headaches.^{2–5}

In addition to the abundant clinical studies that have been published in support of the surgical treatment of migraine headaches, complementary anatomical studies have been performed that describe the detailed anatomy of the sensory nerves involved, as well as the compression points along their course. These include the frontal trigger point (supraorbital and supratrochlear nerves, or STNs), the temporal trigger point (zygomaticotemporal nerve [ZTN] and auriculotemporal nerve [ATN]), the occipital trigger point (greater occipital, third occipital, and lesser occipital nerves [LONs]), and the nasoseptal trigger point. In this chapter, we begin by summarizing the hypotheses on the pathogenesis of migraine headaches and then describe the detailed anatomy of the sensory nerves involved, along with their compression points.

Pathogenesis of Migraine Headaches

The final common pathway in the pathogenesis of migraine headaches appears to be hyperexcitability of cerebral neurons resulting from lower than normal threshold to excitation of the neuronal membrane,⁶ which is believed to be due to localized dural inflammation and vasodilation of meningeal vessels that are supplied by the trigeminal nerve. The mechanism of aura is believed to be cortical spreading depression, characterized by cortical neuronal excitation, followed by depression of normal neuronal activity.⁶

Irritation of the trigeminal nerve, from either a central⁷ or peripheral source, causes inflammation and vasodilation in the region of the dura mater supplied by the trigeminal nerve via release of nociceptive mediators such as calcitonin gene-related peptide, substance P, and neurokinin A.^{6,8} The central trigger theory of migraine headache postulates that central neurovas-

cular events cause irritation of the trigeminal nerve, leading to the release of nociceptive substances from the nerve, triggering dural inflammation and the migraine pain cascade. This theory ascribes the proven ability of botulinum toxin A to reduce the frequency and severity of migraine headaches^{9,10} to its ability to be taken up by the trigeminal nerve peripherally, travel downstream through the axon, and block the release of nociceptive substances at the synaptic interface of the trigeminal nerve with the dura. In an in vitro study, Durham et al found that botulinum toxin A decreased the amount of calcitonin gene-related peptide released from activated rat trigeminal neurons.¹¹

In contrast, the peripheral trigger theory of migraine headache postulates that irritation of the trigeminal nerve occurs peripherally via compression of one of the sensory branches of the trigeminal or cervical nerves by muscle, fascia, bone, artery, or mucosa. This theory attributes the efficacy of botulinum toxin A to its ability to weaken temporarily the muscles by blocking acetylcholine release at the neuromuscular junction, thus reducing muscular compression of branches of the trigeminal nerve.¹² This theory is also validated by the efficacy of surgical trigger-point decompression. Indeed, surgical release of branches of the trigeminal nerve entrapped in muscle, fascia, bone, artery, and mucosa has been shown to be effective at reducing the frequency, intensity, and severity of migraine headaches in most patients who have been refractory to medical management through retrospective chart reviews,^{5,13} prospective cohort studies,^{2,3} and a prospective randomized trial using sham surgery as a placebo control.⁴ In addition, patients with migraine headaches often have tenderness to palpation that precisely localizes to their trigger points, which further lends credence to the peripheral trigger theory.¹⁴

The central and peripheral theories of the pathogenesis of migraine headaches may not, in fact, be incompatible. A combination of peripheral and central sensitization may act in synergy to produce migraine headaches,¹⁵ and current therapeutic strategies—including medications, botulinum, and surgical decompression—may prove to be multimodal in their mechanism of action.

Peripheral Trigger Points in Migraine Headaches

Frontal Trigger Point

Supraorbital Nerve

Origin and Course

The supraorbital nerve (SON) is one of the two terminal cutaneous branches of the frontal nerve, which is a branch of the oph-

thalmic division of the trigeminal nerve (V1). The frontal nerve

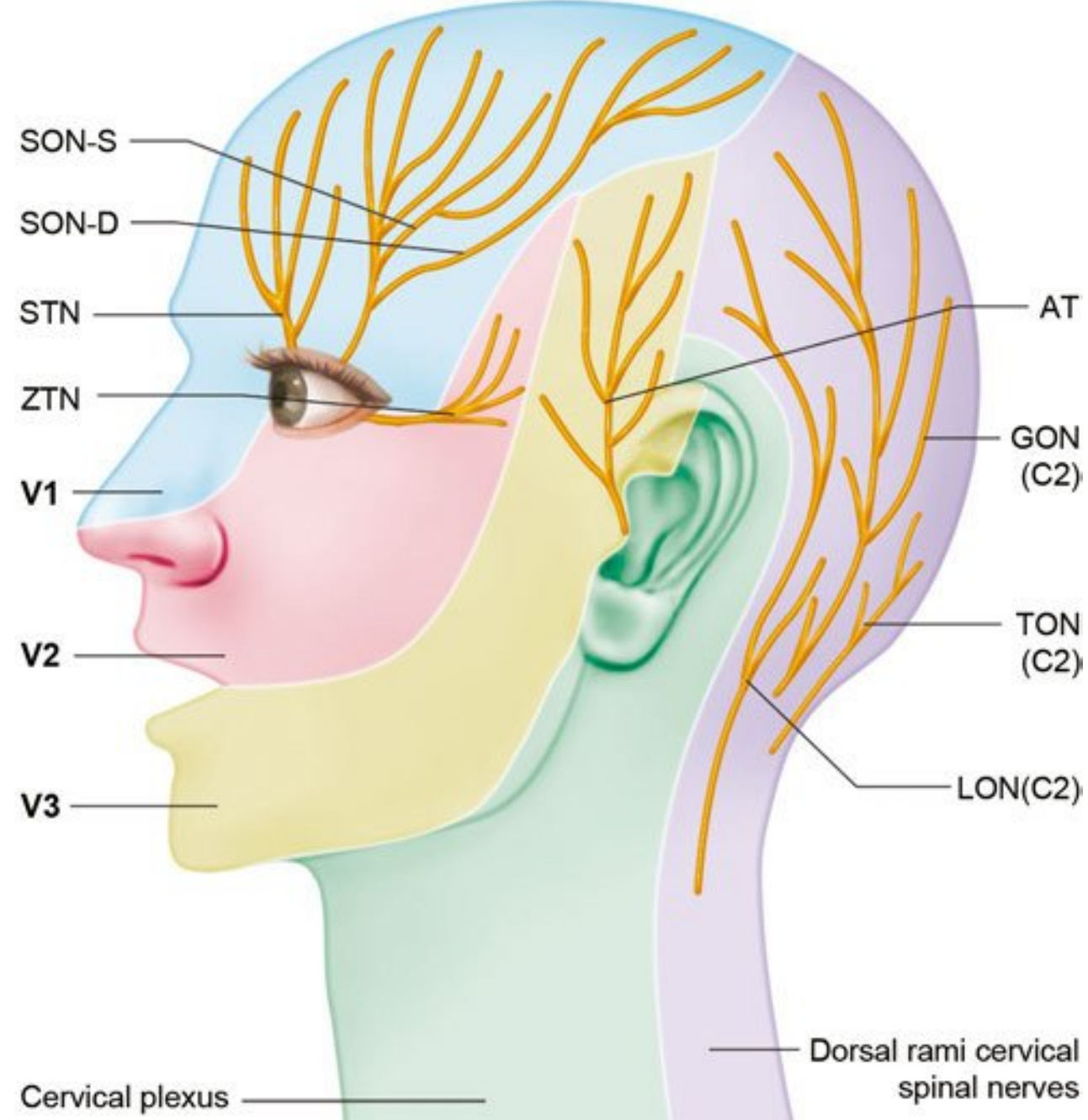


Fig. 10.1 Sensory distributions of nerves involved in migraine trigger points: AT, auriculotemporal nerve; GON, greater occipital nerve; LON, lesser occipital nerve; SON-D, deep branch of the supraorbital nerve; STN, supratrochlear nerve; TON, third occipital nerve; SON-S, superficial branch of the supraorbital nerve; V1, ophthalmic branch of the trigeminal nerve; V2, maxillary branch of the trigeminal nerve; V3, mandibular branch of the trigeminal nerve; ZTN, zygomaticotemporal nerve.

passes through the superior orbital fissure and divides into two branches: the SSTN and the SON, both of which run beneath the orbital roof. The SON proceeds laterally and most commonly exits the orbit through a supraorbital notch located on the supraorbital rim, but it can also exit through a foramen located cephalad to the supraorbital rim.

After exiting the orbit, the SON divides into a deep (lateral) branch and a superficial (medial) branch. The deep branch has a more consistent course and runs between the galea aponeurotica and the periosteum toward the temporal fusion line laterally¹⁶ and provides sensation to the frontoparietal scalp (**Fig. 10.1**). Cuzalina and Holmes described the reproducible location of the deep branch of the SON in a study that examined 75 patients undergoing endoscopic brow lift¹⁷ and found the deep branch of the SON to be located an average of 0.56 mm from a vertical line drawn tangentially to the medial limbus of the iris. The superficial branch of the SON is more variable in location. It pierces the frontalis muscle in a fanlike pattern with numerous branches and provides sensory innervation to the forehead skin and anterior scalp.¹⁶

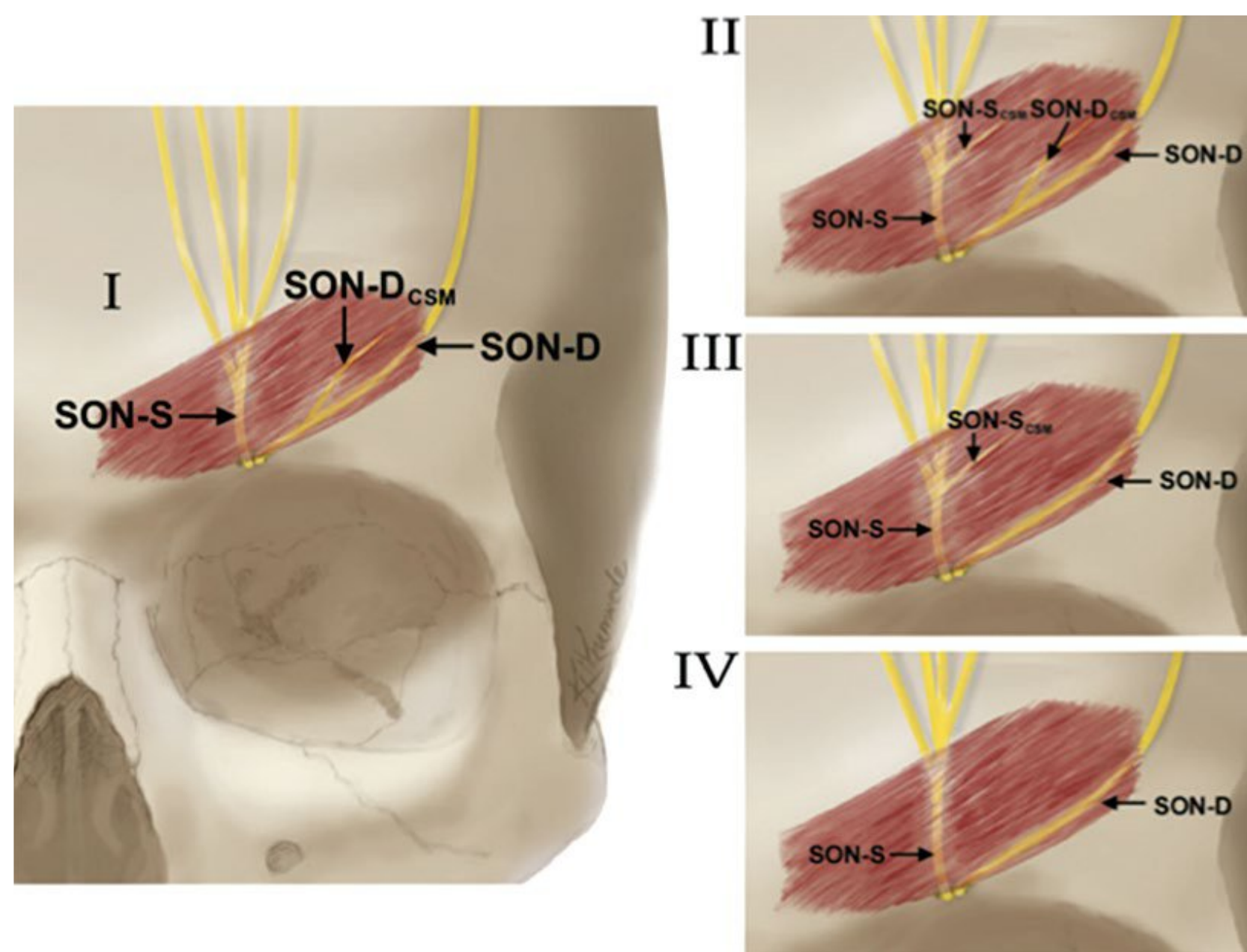
Points of Compression and External Landmarks

The first compression point of the SON consists of either the supraorbital notch or foramen (**Fig. 10.2**, **Table 10.1**). When a supraorbital notch is present as the SON exits from the superior orbital rim, there is frequently a fascial band that completes the

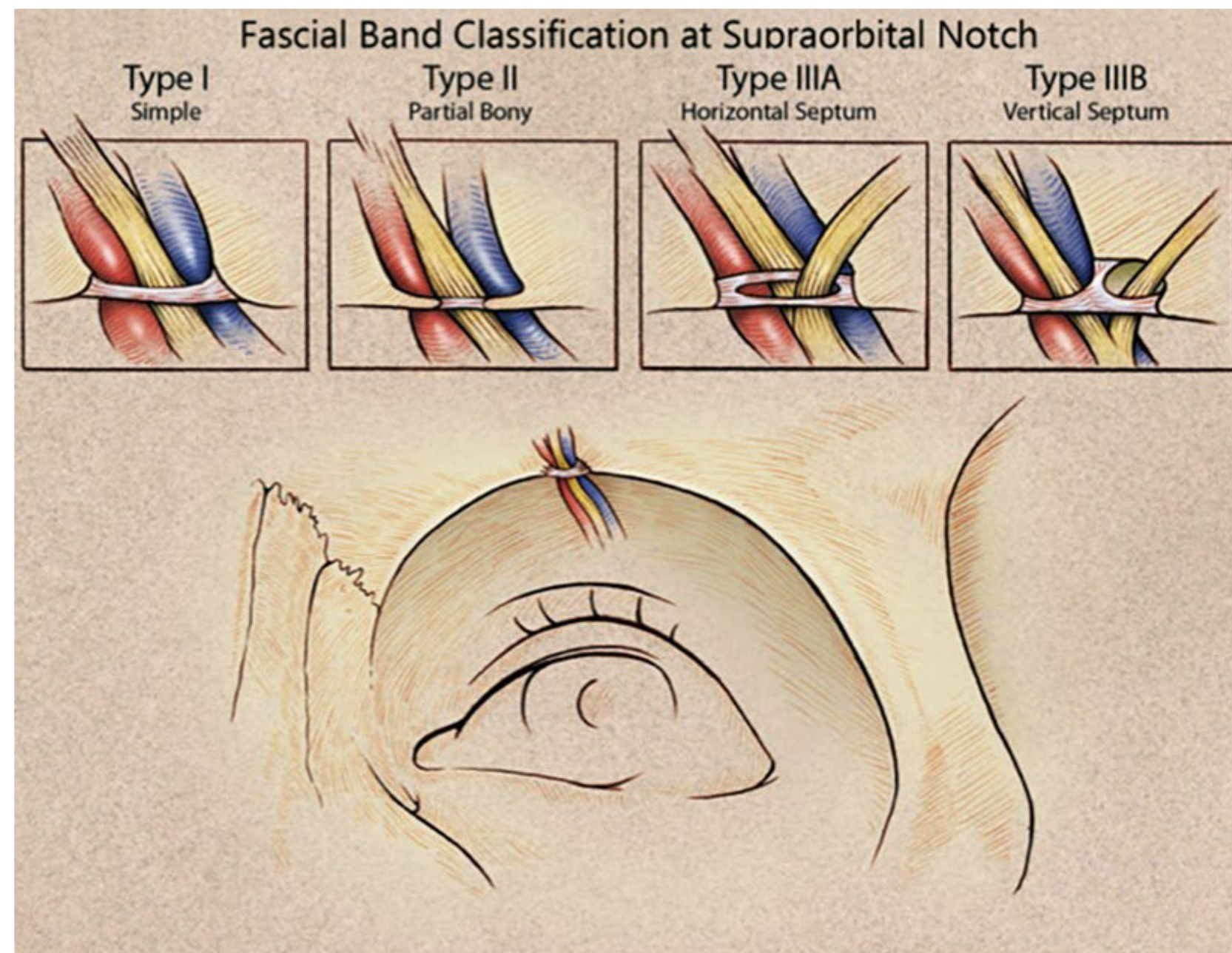
circular shape of the notch and can compress the SON against the frontal bone, as observed by Janis et al¹⁸ and then studied extensively by Fallucco et al,¹⁹ who found that a supraorbital notch was present 83% of the time and a foramen 27% of the time (10% of specimens had both a notch and a foramen). They found that 86% of supraorbital notches had a fascial band. The fascial bands were further divided into three classifications. Type 1 bands, which occurred in 51.2% of specimens, were described as “simple” and consisted of a single fascial band. Type 2 bands, occurring in 30.2% of specimens, consisted of bony spicules with a fascial band completing the bridge overlying the supraorbital notch. Type 3 bands, occurring in 18.6% of specimens, contained a septum that allowed for more than a single passageway for the neurovascular bundle through the supraorbital notch.

These were further divided into types 3A and 3B classification, depending on whether the septum was horizontal or vertical, with each occurring 9.3% of the time (**Fig. 10.2**).¹⁹ When present, a supraorbital foramen can act as a bony compression point.²⁰ Beer et al described the SON exit from 507 European skulls and discovered that in 74% of cases, the location of the exit was asymmetric between sides in the same person.²¹ The average distance from the nasion to either a supraorbital notch or foramen was 31 mm. A single exit point exists in most circumstances, but in approximately 10 to 15% of people, more than one exit point exists.^{21,22} Agthong et al examined specimens from 70 men and 40 women in an Asian population and noted that when measured from the midline, the nerve exit trended toward a more lateral location in men (25.1 mm) than in women (24.1 mm).²² Interestingly, this study demonstrated an equal rate of supraorbital notch versus foramen in this population. Conversely, Cutright et al examined 20 specimens each from white versus black and male versus female populations and found that a notch was present 92.5% of the time and a foramen present in the remaining specimens.²³ They also noted a more lateral location in men versus women and in blacks versus whites (24.1 mm in white men, 26.1 mm in black men, 22.3 mm in white women, and 25.5 mm in black women). Saylam et al described the presence of a supraorbital notch in 71.6% of specimens, with an average distance of 25.2 mm from the midline.²⁴ Webster et al examined the variability in nerve exit patterns between sides within the same person in a study with 111 skulls.²⁵ In approximately 50% of specimens, a bilateral supraorbital notch was found, in 25% a bilateral supraorbital foramen, and in 25% a notch on one side with a foramen on the contralateral side. Extrapolating definitive conclusions about the presence of a notch versus a foramen as well as a precise location of nerve exit from the data reviewed here is limited by the fact that no two studies examined comparable populations in sufficient numbers with comparable reference points to measure nerve exit; however, the data highlight the importance of appreciating the frequent variability within different people and even within the same patient.

The second compression point of the SON is the corrugator supercilii muscle (CSM), where branches of the nerve course directly through the muscle in 78% of people.^{18,26} In an anatomical study of 25 cadavers, Janis et al described the branching patterns of the SON in relation to the CSM and discovered four unique patterns.¹⁸ In a type I branching pattern, which occurred in 40% of specimens, the deep branch of the SON interacted with the CSM. In a type 2 pattern, occurring in 34% of specimens,



a



b

Fig. 10.2 (a) Compression points of the supraorbital nerve. (Reproduced with permission from Bindingnavele VKI, Bresnick SD, Urata MM, et al. Superior results using the islandized hemipalatal flap in palatoplasty: experience with 500 cases. Reproduced from Plast Reconstr Surg 2008; 122(1):232.) **(b)** Supraorbital nerve course through the corrugator supercilii muscle. Fascial band classification at the supraorbital notch. (Reproduced with permission from Fallucco M1, Janis JE, Hagan RR. The anatomical morphology of the supraorbital notch: clinical relevance to the surgical treatment of migraine headaches. (Reproduced with permission from Plast Reconstr Surg 2012;130(6):1227–1233.)

branches of both the superficial and deep branches of the SON interacted with the CSM. In a type 3 pattern, which occurred in 4% of specimens, only the superficial branch of the SON interacted with the CSM. Lastly, in a type 4 pattern, occurring in 22% of specimens, the branching of the SON occurred more cephalad to the CSM, without any interaction with the muscle (Fig. 10.2, lower left).

Clinical Correlation

The supraorbital and STNs constitute the frontal trigger point, the most commonly described trigger point among migraine patients. Patients with a frontal trigger point typically have a strong CSM, as indicated by deep frown lines. They often have tender-

ness over the SON, and they experience headaches that are “imploding” and are worse in the afternoon and with stress.²⁷

The first compression point is decompressed via a supraorbital foraminotomy (for a foramen) or fasciotomy (for a notch). The second trigger point is addressed by resection of the corrugator myofascial unit through either subtotal resection of the CSMs or more effectively by resection of the entire glabellar muscle group, including the CSM and portions of the depressor supercilii and procerus muscles. This resection is achieved through either a transpalpebral approach or with an endoscopic approach through small hairline incisions,² although the endoscopic approach has been shown to visualize more of the muscle and therefore may lead to more successful complete resection and better decompression.^{28,29}

Table 10.1 Compression points of the supraorbital nerve

Compression point	Name	Type	Frequency	Horizontal location (from midline)	Craniocaudal location	Reference
1	Supraorbital notch	Fascial/bony	83.3% ^a (51.2%fascial band, 30.2% partial bony band, 9.3%horizontal septum, 9.3% vertical septum)		At the superior orbital rim	Fallucco et al ¹⁹
	Supraorbital foramen	Bony	26.7% ^a	31 mm 25.1 mm in men, 24.1 mm in women 24.1 mm in white men, 26.1 mm in black men, 22.3 mm in white women, and 25.5 mm in black women 25.2 mm		Beer et al ²¹ Agthong et al ²² Cutright et al ²³ Saylam et al ²⁴
2	Corrugator supercilii	Muscular	78%(40%deep branch, 34%deep and superficial branch, 4% superficial branch)	2.9 –43.3 mm ^b	9.8–32.6 mm cranial to nasion ^b	Janis et al ¹⁸

^a10%of specimens had both a supraorbital notch and a foramen.

^bThese measurements indicate the extent of the corrugator supercilii muscle.

Multiple clinical studies have been completed that address muscular, fascial or bony release of the frontal trigger point.^{5,13,30} Success rates of migraine headache improvement or migraine headache elimination have been high when performed independently or concurrently with decompression of other trigger points. Interestingly, the proportion of patients who benefit from surgical decompression (79.2%)⁵ closely mirrors the percentage of patients who have interaction between the SON and the CSM (78%).¹⁸

Supratrochlear Nerve

Origin and Course

The STN is one of the two terminal cutaneous branches of the frontal branch of the ophthalmic division of the trigeminal nerve (V1). It provides sensory innervation to the midline forehead (**Fig. 10.1**). Much less has been published about the anatomy of the smaller STN compared with the larger SON. The STN proceeds medially to exit the superior orbital rim via a notch or a foramen, then travels cranially through the CSM. Miller et al examined the anatomy of the STN in 10 cadavers and found that

the nerve coursed between 1.6 and 2.3 cm lateral to the midline at the level of the superior orbital rim.³¹ After exiting the orbital rim, the STN courses through the CSM as it travels cephalad.

Points of Compression and External Landmarks

The first compression point of the STN occurs as it exits the orbit via either a notch or a foramen (**Table 10.2**). In a dissection of 50 cadaver hemiheads by Janis et al, the STN was found to exit the orbit via a notch in 72%of specimens, located an average of 1.75 cm from the midline.³² The floor of the notch consisted of a fibrous band in all cases. In 68%of specimens, the nerve was observed to pass directly through the notch; however, in 8% the nerve pierced the fascial band and coursed directly through the connective tissue. In another 8% the fascial band was very broad and flattened the nerve against the bony surroundings. A true bony foramen occurred in 18%of specimens and was located an average of 4 mm cranial to the superior orbital rim.

The second compression point occurs as the STN interacts with the CSM. Janis et al found that 84%of the time, the STN

Table 10.2 Compression points of the supratrochlear nerve

Compression Point	Name	Type	Frequency	Horizontal location (from midline)	Craniocaudal location	Reference
1	Frontal notch	Fascial/bony	72%	17.5 mm	At the superior orbital rim	Janis et al ³²
	Frontal foramen	Bony	18%		4 mm cranial to superior orbital rim	Janis et al ³²
2	Corrugator supercilii	Muscular	88%(84%two branches, 4%one branch)	Enters muscle 18.7 mm, exits muscle 19.6 mm	15 mm cranial to superior orbital rim	Janis et al ³²

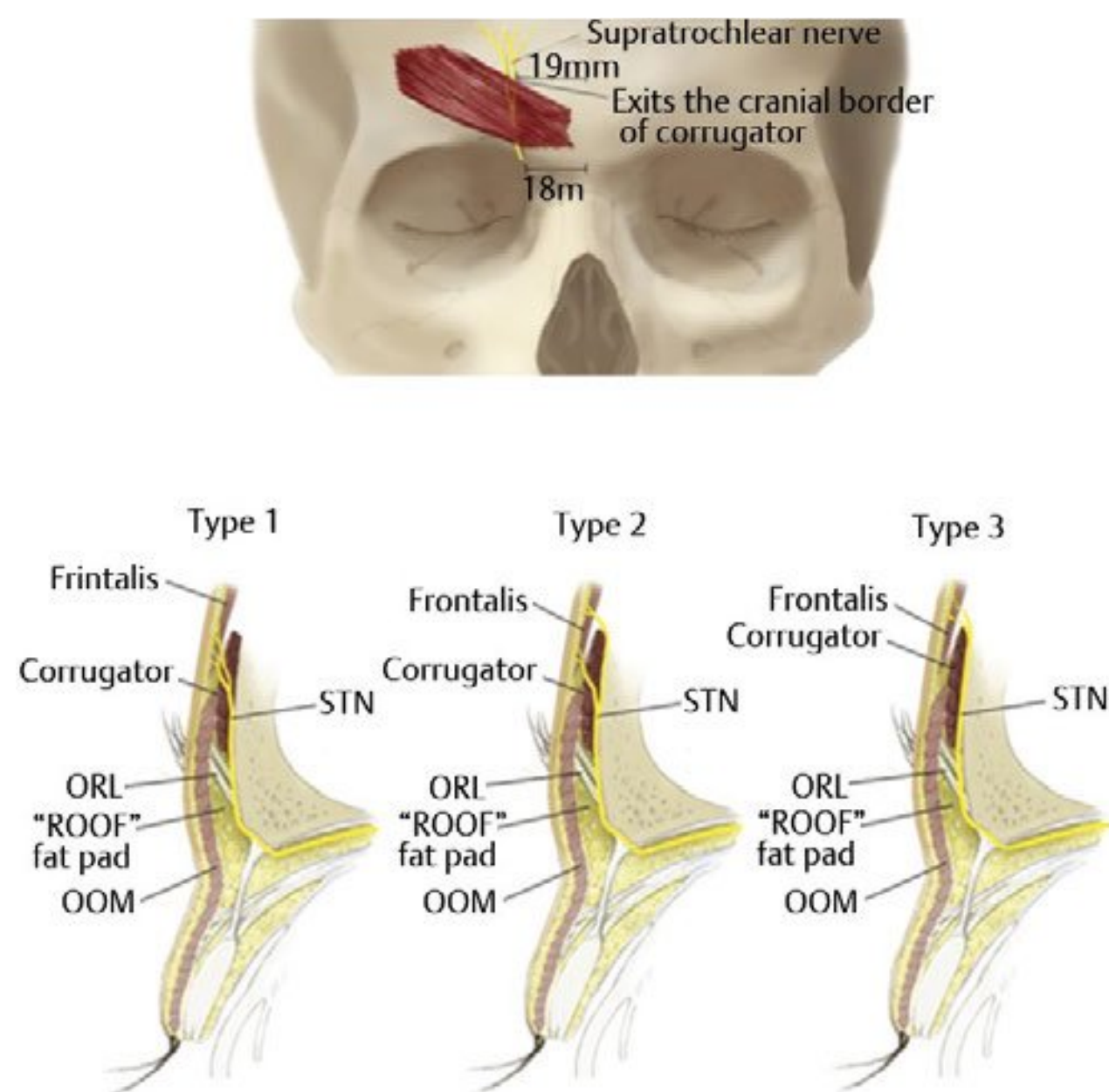


Fig. 10.3 Compression points of the supratrochlear nerve. (Reproduced with permission from Janis JE1, Hatef DA, Hagan R, et al. Anatomy of the supratrochlear nerve: implications for the surgical treatment of migraine headaches. *Plast Reconstr Surg* 2013;131(4): 743–750.)

divided into two branches within the retro-orbicularis fat, which then both entered the CSM at an average of 18.7 mm lateral to the midline, and exited it 19.6 mm lateral to the midline and 15 mm cranial to the superior orbital rim (**Fig. 10.3**).³² In 4% of specimens, only one STN branch entered the CSM, and the other one stayed deep; in 12% of specimens, neither branch traveled through the CSM, but rather both remained deep to the muscle.

Clinical Correlation

The STN and the SON constitute the frontal trigger point, and release of both nerves is usually achieved simultaneously. Anatomical studies involving the STN have highlighted the importance of extending surgical dissection medially to fully decompress it. It has been hypothesized that failure to fully decompress the most medial aspect of the frontal trigger site may have resulted in early clinical failures.³²

Temporal Trigger Point Zygomaticotemporal Nerve

Origin and Course

The ZTN is one of the two terminal branches of the zygomatic nerve, which is a branch of the maxillary division of the trigeminal nerve (V2).³³ The zygomatic nerve enters the orbit via the inferior orbital fissure, travels along the lateral orbital wall,³⁴ then divides into the zygomaticofacial nerve (ZFN) and ZTN. The ZTN provides sensation to the skin of the temple (**Fig. 10.1**), as well as parasympathetic innervation to the lacrimal gland.³⁴

In a study by Janis et al, 30% of subjects were found to have two ZTN branches.³³ Among those, 20% had branching of the ZTN within the orbit, with the two branches exiting via two separate zygomaticotemporal foramina. In the remaining 80%, the ZTN branched after exiting the orbit. Accessory branches of the ZTN were found in 50 to 55% of patients. Among those with accessory ZTN branches, the ZTN branches were cranial to the main branch in 30% on the left (located an average of 16mm lateral and 12.2 mm cranial to the lateral palpebral commissure) and in 55% on the right (located an average of 15.7 mm lateral and 16.5 mm cranial to the lateral palpebral commissure). The ZTN branches were immediately adjacent to the main branch in 30% on the left (located an average of 17.7 mm lateral and 6 mm cranial to the lateral palpebral fissure) and in 9% on the right (located an average of 19.0 mm lateral and 5.0 mm cranial to the lateral palpebral commissure). The ZTN branches were lateral to the main branch in 40% on the left (located an average of 34.2 mm lateral and 6.7 mm cranial to the lateral palpebral commissure), and in 36% on the right (located an average of 28.7 mm lateral and 6.0 mm cranial to the lateral palpebral commissure). In all cases with a lateral branch, this branch travelled horizontally to join the ATN. Tubbs et al have confirmed this communication with the ATN in 13% of hemiheads.³⁵ In addition, Odobescu et al found that 82% of individuals had small connections between the ZTN and the frontal division of the facial nerve.³⁶

Points of Compression and External Landmarks

The first compression point occurs as the ZTN enters the temporal fossa. The nerve exits the lateral orbit via a bony canal and emerges in the temporal fossa via a bony foramen (**Fig. 10.4**, **Table 10.3**)³⁴; 94% of individuals have one zygomaticotemporal foramen, and the remaining 6% have two foramina.³³ The foramen is located in the frontal bone within the temporal fossa and is found an average of 6.7 ± 6.12 mm lateral to the lateral orbital rim and 7.88 ± 6.9 mm cranial to the nasion. In an anatomical study of 400 hemiskulls, Loukas et al found that the location of the zygomaticotemporal foramen varied widely depending on ethnic background and that up to 50% of individuals lacked a zygomaticotemporal foramen.³⁷

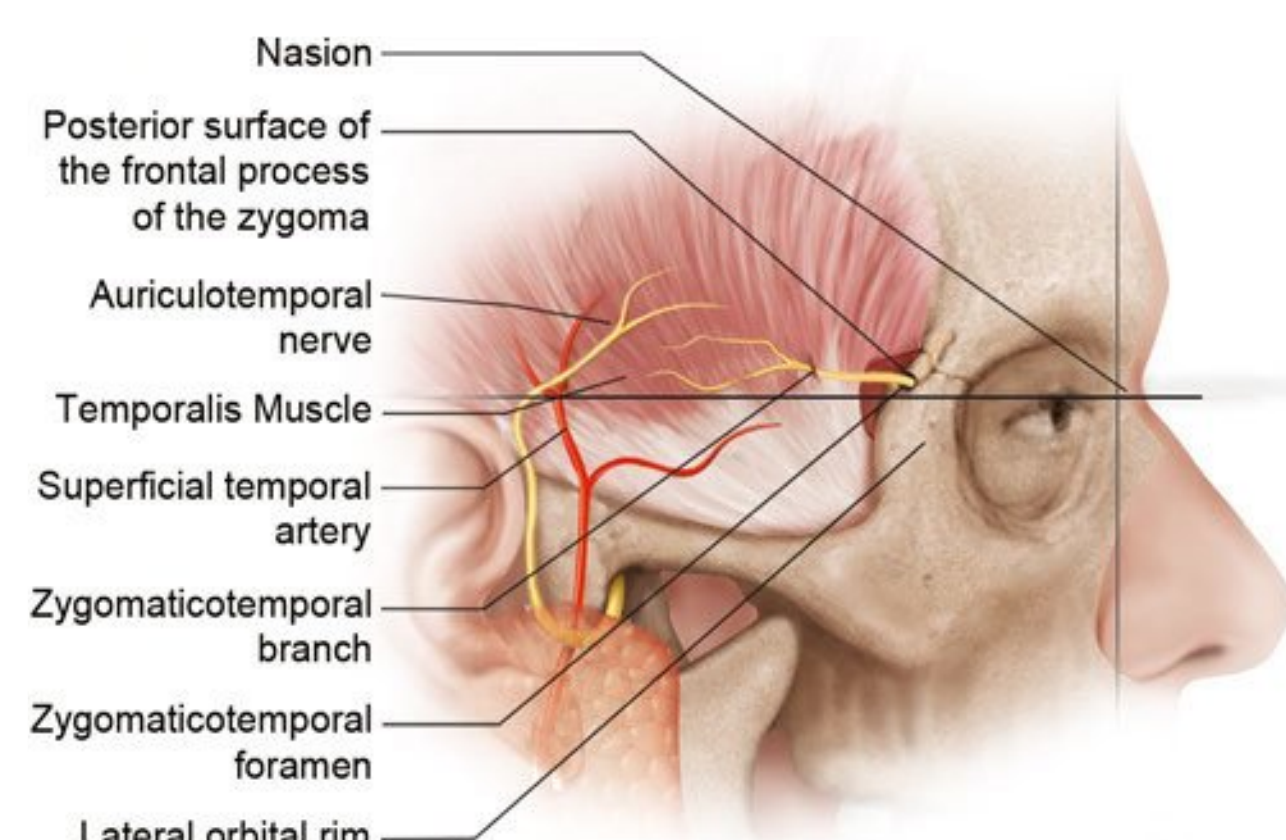


Fig. 10.4 Compression points of the zygomaticotemporal nerve.

Table 10.3 Compression points of the zygomaticotemporal nerve

Compression point	Name	Type	Frequency	Horizontal location	Craniocaudal location	Reference
1	Zygomaticotemporal foramen	Bony	100%	6.7 ± 6.12 mm lateral to the lateral orbital rim	7.88 ± 6.9 mm superior to the nasion	Janis et al ³³
2	Temporalis muscle Deep temporal fascia	Muscular Fascial	50% 50%	16.9 mm lateral to the lateral ocular commissure 10.1 ± 1.5 mm lateral to the zygomaticofrontal suture	6.5 mm superior to the lateral ocular commissure 22.2 ± 3.1 mm superior to upper margin of zygomatic arch 23 mm cranial to the zygomatic arch	Janis et al ³³ Janis et al ³³ Totonchi et al ³⁴ Jeong et al ³⁸ Tubbs et al ³⁵

The second compression point is the temporalis muscle/deep temporal fascia. After exiting the orbit, the ZTN enters the deep aspect temporalis muscle and travels intramuscularly in 50% of individuals.³³ Among those whose ZTN has an intramuscular course, this course is short and direct in 44% and long and tortuous in 56%. In the 50% of individuals who have no intramuscular course, the ZTN travels between the temporal periosteum and the temporalis muscle before piercing the deep temporal fascia. In an intraoperative endoscopic anatomical study of 20 patients, Totonchi et al found that the ZTN pierced the deep temporal fascia 16.9 mm lateral and 6.5 mm cranial to the lateral palpebral commissure,³⁴ whereas Jeong et al found that it pierced the deep temporal fascia 10.1 ± 1.5 mm lateral to the zygomaticofrontal suture and 22.2 ± 3.1 mm cranial to the upper margin of the zygomatic arch.³⁸ This was confirmed by Tubbs et al, who found that the ZTN pierced the deep temporal fascia an average of 23 mm cranial to the zygomatic arch.³⁵

Clinical Correlation

Patients with migraine headaches originating from the ZTN tend to have temporal pain, usually in the morning, associated with stress, grinding, clenching, or temporomandibular joint dysfunction.²⁷ Murillo first described open resection of the ZTN and of the superficial temporal artery (STA) for temporal migraine headaches in 34 patients in 1968³⁹; results were positive in 88.2% of patients. The technique for ZTN decompression has since been refined by Guyuron and is now usually performed via an endoscopic approach. Dissection is performed just superficial to the deep temporal fascia until the ZTN is identified. It is then avulsed, with resection of approximately 3 cm of the nerve, allowing the proximal end of the nerve to retract and get buried into the temporalis muscle.⁴⁰ Avulsion of the ZTN may cause temporary paresthesia and anesthesia in the temporal region, which are usually temporary.⁴¹ The method of ZTN decompression has been examined by Chim et al.⁴² In an animal study on rat sural nerves, they found that nerve avulsion and burying in muscle led to the lowest rate of neuroma formation.

In a study of 246 patients undergoing endoscopic decompression of the ZTN, Kurlander et al found that at 1 year postoperatively 55% of patients had complete elimination of temporal migraine headaches, with an additional 30% of patients having

significant improvement.⁴¹ In a prospective evaluation of 71 patients with a temporal trigger site undergoing surgical avulsion of the ZTN, with a mean 396-day follow-up, Guyuron et al demonstrated complete migraine elimination in 63% with at least 50% improvement in migraine severity, duration, and frequency in an additional 35%.³ In a single-blinded, randomized controlled trial comparing actual decompression of the ZTN in 19 patients with sham surgery in nine patients, those undergoing actual decompression had significant improvements in migraine intensity, frequency, and duration from baseline, which was not the case for those undergoing sham surgery.⁴ In a review of 19 patients undergoing ZTN avulsion for the treatment of migraine headaches from a temporal trigger site, with a mean follow-up of 661 days, Janis et al demonstrated complete migraine elimination in 52.6% of patients, with an additional 36.8% having at least 50% improvement.⁵

Auriculotemporal Nerve

Origin and Course

The ATN is a branch of the mandibular division of the trigeminal nerve (V3). It is a sensory nerve that provides sensation to the tragus and anterior ear, as well as to the posterior temporal region (Fig. 10.1). It also carries autonomic nervous fibers, providing sympathetic innervation to the scalp and parasympathetic innervation to the parotid gland.

The ATN emerges within the superficial parotid gland along the posteromedial aspect of the temporomandibular joint⁴³ and travels cranially within the temporoparietal fascia, crossing the posterior aspect of the zygomatic arch.⁴⁴ It travels as a single branch in 50% of people, and up to four branches in the remainder.⁴⁵ As the nerve travels cephalad, it parallels and runs lateral to the STA.⁴⁴ In the upper temporal area, the nerve becomes more superficial, lying superficial to the temporoparietal fascia.

Points of Compression and External Landmarks

In an anatomical study of 10 cadavers, Chim et al found that in all specimens the ATN traveled under a fascial compression

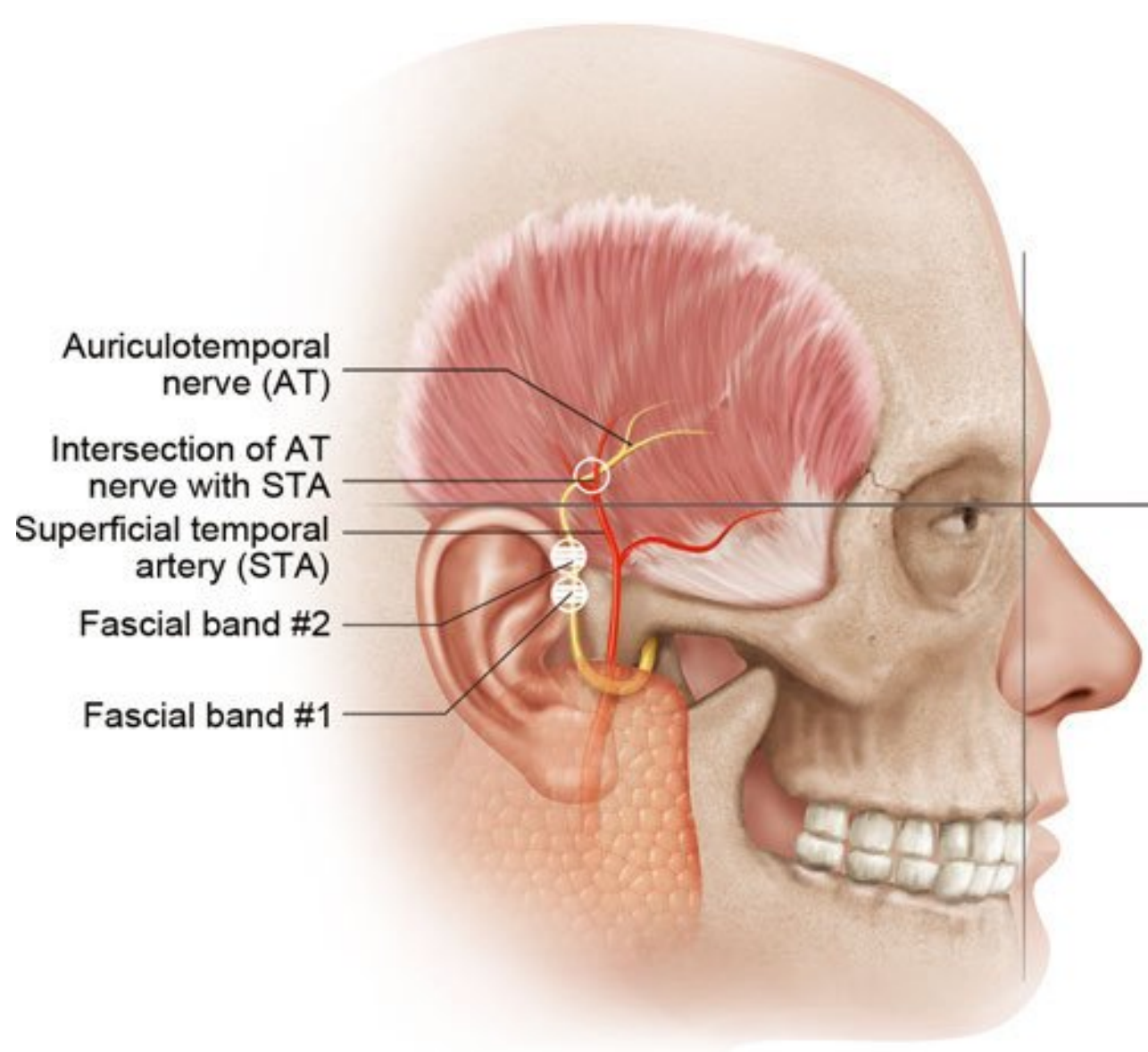


Fig. 10.5 Compression points of the auriculotemporal nerve.

band (compression point 1), present an average of 13.1 ± 5.9 mm anterior and 5.0 ± 7.0 mm cranial to the most anterosuperior point of the external acoustic meatus (**Fig. 10.5, Table 10.4**).⁴⁶

They also showed that in 85% of specimens, a second, more cranial, fascial compression band (compression point 2) was

present an average of 11.9 ± 6.0 mm anterior and 17.2 ± 10.4 mm cranial to the most anterosuperior point of the external acoustic meatus.

The third potential compression point consists of the intersection with the STA, found in up to 80% of specimens; 81.2% of those specimens demonstrated a simple intersection. Most commonly in this situation, the artery crossed superficial to the nerve (62.5%), at a point 19.2 ± 10.0 mm anterior and 39.5 ± 16.6 mm superior to the most anterosuperior point of the external acoustic meatus. In the remaining 18.8% of the simple intersection specimens, multiple branches of the nerve crossed superficial to the artery at multiple points, with variable anatomy among the specimens. In 18.8% of the specimens with an AT-STA intersection, helical intertwining over an average distance of 10.3 ± 0.4 mm was noted to extend between 20.0 ± 15.6 mm and 24.7 ± 17.9 mm anterior and 53.7 ± 4.7 mm and 62.7 ± 3.8 mm cranial to the most anterosuperior point of the external acoustic meatus.⁴⁶ In a study of 25 fresh cadavers, Janis et al also described the third compression point of the ATN in detail⁴⁴: it was present in 34% of specimens at a point located an average of 107.88 ± 17.73 mm lateral to the facial midline and 37.53 ± 15.29 mm cranial to a horizontal line passing through the nasion. Among the specimens that demonstrated an intersection between the ATN and STA, the intersection consisted of a simple crossing in 88.2% and a helical intertwining in 11.8%. In cases of a helical intertwining, this extended from 123 mm to 117 mm lateral to the midline and from 25 mm to 38 mm cranial to a horizontal line through the nasion.

Table 10.4 Compression points of the auriculotemporal nerve

Compression point	Name	Type	Frequency	Horizontal location	Craniocaudal location	Reference
1	Fascial band 1	Fascial	100%	13.1 ± 5.9 mm anterior to anterosuperior EAC	5.0 ± 7.0 mm superior to anterosuperior EAC	Chim et al ⁴⁶
2	Fascial band 2	Fascial	85%	11.9 ± 6.0 mm anterior to anterosuperior EAC	17.2 ± 10.4 mm superior to anterosuperior EAC	Chim et al ⁴⁶
3	Superficial temporal artery	Arterial	Simple intersection: 65%	19.2 ± 10.0 mm anterior to anterosuperior EAC	39.5 ± 16.6 mm superior to anterosuperior EAC	Chim et al ⁴⁶
			Helical intertwining: 15%	20.0 ± 15.6 mm to 24.7 ± 17.9 mm anterior to anterosuperior EAC	53.7 ± 4.7 mm to 62.7 ± 3.8 mm superior to anterosuperior EAC	Janis et al ⁴⁴
			Simple intersection: 30%	107.88 ± 17.73 mm lateral to midline	37.53 ± 15.29 mm superior to nasion	
			Helical intertwining: 4%	$123-117$ mm lateral to midline	$25-38$ mm superior to nasion	

Abbreviations: EAC, external acoustic canal.

Clinical Correlation

The ATN has been hypothesized to be the trigger point in patients with persistent temporal migraine headaches who underwent ZTN release.⁴⁴ Patients with an ATN trigger point typically have pain along the course of the ATN in the high temporal region.^{27,46} This pain may be pulsatile if nerve compression is due to impingement of the superficial temporal artery on the AT.⁴⁴

Although a surgical technique directly addressing the first two fascial compression points has not been described yet, decompression of the ATN intersection with the STA involves making a short incision over the point of maximal tenderness⁴⁶ or in the temporal hairline⁴⁴ and exposing the ATN. If the STA artery is found to be crossing over the nerve, the artery is ligated. If the artery is not crossing over the nerve, the nerve is transected, and its ends are buried in the temporalis muscle.

Nasoseptal Trigger Point

Pathophysiology

Nasoseptal headaches are attributed to intranasal mucosal contact points that are present in up to 4% of the population.⁴⁷

The contact areas are believed to cause neural irritation, leading to the release of inflammatory mediators, specifically substance P. This causes nociceptive signals to be transmitted along afferent C fibers to the dura mater, which then lead to vasodilation and perivascular inflammation in the dura, generating a migraine headache.

Points of Compression

Intranasal contact points can usually occur between the septum and the superior turbinate, middle turbinate, or medial wall of the ethmoid sinus (Fig. 10.6). Causes of these contact points include septal deformities, such as septal deviation and septal spurs; turbinate deformities such as turbinate hypertrophy; and concha bullosa,⁴⁸ which refers to a pneumatized turbinate that may impinge on the nasal septum.⁴⁹

In patients with migraine headaches attributed to a nasoseptal trigger point, Ferrero et al found that the frequency of intranasal mucosal contact points was the following: septum-middle turbinate plus septum-superior turbinate in 42.8%, septum-middle turbinate in 36%, septal spur in 7.1%, septal spur plus septum-middle turbinate in 7.1%, septal spur plus septum-middle turbinate plus septum-superior turbinate in 7.1%.⁵⁰

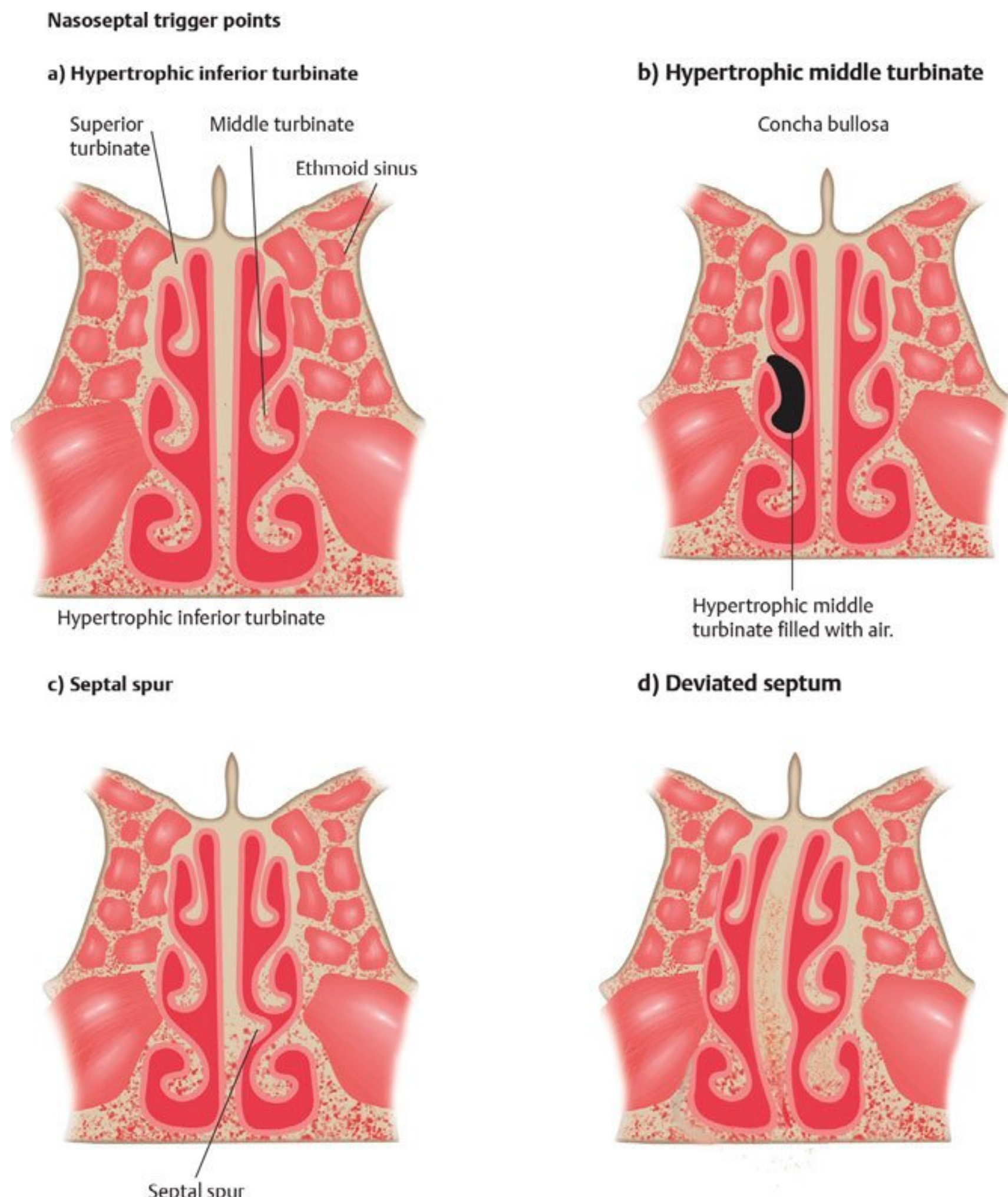


Fig. 10.6 Nasoseptal trigger points: (a) Hypertrophic inferior turbinate. (b) Hypertrophic middle turbinate with concha bullosa. (c) Septal spur. (d) Deviated septum.

Clinical Correlation

Patients with a nasoseptal migraine trigger point typically complain of retrobulbar pain, usually worse in the early morning, and related to weather, allergies, and hormonal cycles and associated with rhinorrhea.²⁷ Confirmation of the nasoseptal trigger point as the causative agent in migraine may take the form of application of topical local anesthetic or injection of local anesthetic into the contact point during an active headache. Improvement or elimination of the headache confirms the contact point as a trigger.⁵¹ Another modality for diagnosis would be a combination of constellation of symptoms (as above) combined with computed tomographic scan findings of anatomical contact points (usually most easily seen on coronal images). Rhinosinusitis must also be excluded.⁴⁷

Surgical techniques to address nasoseptal trigger points must address the underlying anatomical abnormality to eliminate the mucosal contact point and include septoplasty, middle turbinectomy, and medial ethmoidectomy.

In a study of 12 patients with migraine headaches attributed to the nasoseptal trigger point, Behin et al found that surgery reduced headache frequency from 17.7 days per month to 7.7 days per month and mean headache severity from 7.8 to 3.6.⁴⁷ Headache severity improved by 50% or more in 76.2% of subjects and was eliminated in 42.9%. In a study of 30 patients with migraine headaches from a nasoseptal trigger point, endoscopic nasal surgery achieved complete headache relief in 43% and significant improvement in 47%.⁵² Welge-Luessen followed up on 20 patients with migraine headaches from a nasoseptal trigger point for a period of 10 years after endoscopic septoplasty, partial ethmoidectomy, and turbinectomy (if indicated) and found that 30% had complete headache resolution and an additional 35% had significant improvement.⁵³ In a study of eight patients with a nasoseptal trigger point who underwent septoplasty or inferior and/or middle turbinectomies, either alone or in conjunction with other trigger sites, with a follow-up of 661 days, Janis et al demonstrated significant overall improvement in 100% with 62.5% having complete elimination of migraine headaches.⁵ In a prospective evaluation of 62 patients with a nasoseptal trigger point undergoing surgical treatment, with a mean follow-up of 396 days, Guyuron et al demonstrated complete migraine elimination in 34% of patients, with an additional 55% experiencing at least 50% improvement.³

Occipital Trigger Point

Greater Occipital Nerve

Origin and Course

The greater occipital nerve (GON) is the medial branch of the dorsal ramus of the C2 spinal nerve. It measures approximately 5 mm in diameter as it enters the semispinalis capitis muscle.⁵⁴ The GON initially travels in a caudal, posterior, and lateral direction until it reaches the lower border of the obliquus capitis inferior muscle. It then hooks around this muscle and travels cranially, superficial to the obliquus capitis inferior muscle, and deep to the semispinalis capitis muscle. The nerve then crosses the semispinalis capitis muscle from deep to superficial and runs cranially deep to the trapezius muscle. It then pierces the tra-

pezius muscle to become subcutaneous and provides sensory innervation to the posterior scalp (Fig. 10.1).

Points of Compression and External Landmarks

Janis et al studied the potential compression points of the GON in 50 cadaver hemiheads.⁵⁵ They identified six potential points of compression of the GON as it traveled cranially through the posterior neck (Fig. 10.7, Table 10.5). The first compression point occurred as the GON crossed tight fascial bands between the obliquus capitis inferior and semispinalis muscles before continuing its cranial course. This point occurred at an average 20.13 mm lateral and 77.38 mm caudal to the external occipital protuberance (EOP).

The second compression point occurred when the GON entered the deep surface of the semispinalis capitis 17.46 mm lateral and 59.71 mm caudal to the EOP. The GON pierced the semispinalis capitis muscle in 90% of specimens by Bovim et al.⁵⁶

The third compression point occurred when the GON emerged from the superficial surface of the semispinalis capitis 15.52 mm lateral and 34.52 mm caudal to the EOP. This point of compression has been studied extensively and confirmed by several other authors. Mosser et al conducted an anatomical study and found that point of emergence of the GON from the semispinalis capitis muscle could be found 29.1 mm (right) to 28.7 mm (left) caudal to the EOP and 14.1 mm (right) to 13.8 mm (left) lateral to the EOP.⁵⁴ This was also confirmed by Ducic et al,⁵⁷ who found the point of emergence to be 14.9 mm lateral and 30.2 mm inferior to the EOP and who also noted that the course of the GON was asymmetric in 43.9% of individuals. Tubbs et al found that the GON pierced the semispinalis capitis muscle 2 cm cranial to the intermastoid line.⁵⁸ The mean intramuscular course in the semispinalis capitis muscle was 7.6 mm (right) and 8.9 mm (left).

The fourth compression point, as demonstrated by Janis et al,⁵⁵ occurred as the GON entered the trapezius muscle, 24.0 mm lateral and 21.0 mm caudal to the EOP. The fifth compression point occurred as the GON pierced the tendinous insertion of the trapezius into the nuchal line, 37.07 mm lateral and 4.36 mm caudal to the EOP.

The sixth compression point consisted of the interaction of the GON with the occipital artery,⁵⁹ identified in 54% of specimens. This took the form of a simple intersection in 29.6% (with the nerve always crossing superficial to the artery) and of helical intertwining in 70.4%. In cases where there was a single point of intersection, this occurred $30.27 \text{ mm} \pm 6.83 \text{ mm}$ lateral and $10.67 \text{ mm} \pm 8.25 \text{ mm}$ caudal to the EOP. In cases where there was a helical intertwining, this occurred between $25.34 \text{ mm} \pm 12.16 \text{ mm}$ and $42.09 \text{ mm} \pm 25.61 \text{ mm}$ lateral and between $24.91 \text{ mm} \pm 12.87 \text{ mm}$ and $0.97 \text{ mm} \pm 8.34 \text{ mm}$ caudal to the EOP, with a total length of helical intertwining of $37.6 \text{ mm} \pm 14.5 \text{ mm}$. The location of the interaction between the GON and the occipital artery is quite variable, as evidenced by the high standard deviations reported. In fact, although it is referred to as the sixth compression point, it often occurs proximal to point 5 along the course of the GON. It may be superficial or deep to the trapezius muscle. In a review of 272 patients undergoing GON decompression, Junewicz et al noted that the GON branched in 7.4% of patients, most often into two branches.⁶⁰ They noted

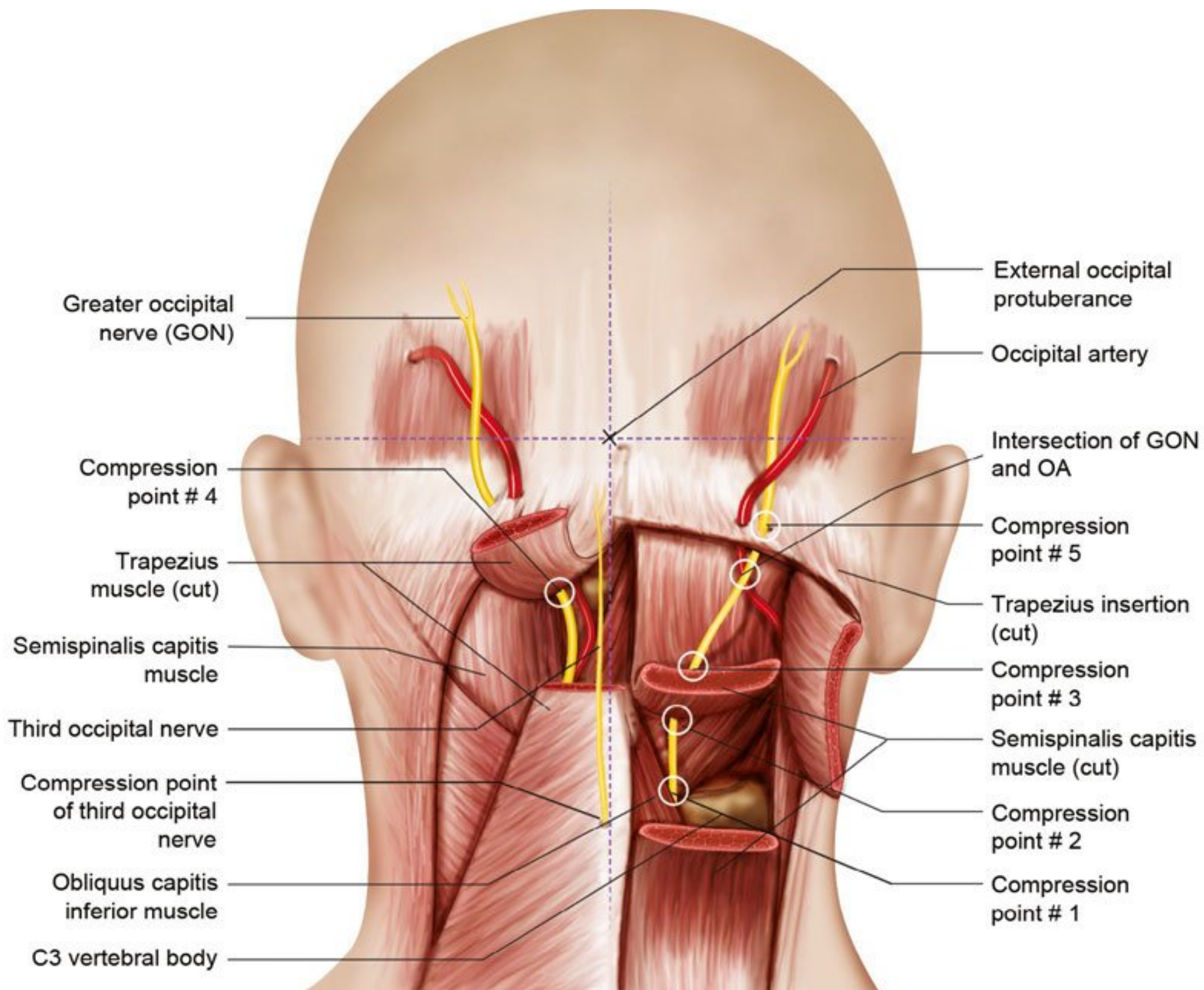


Fig. 10.7 Compression points of greater occipital and third occipital nerves.

Table 10.5 Compression points of the greater occipital nerve

Compression point	Name	Type	Frequency	Horizontal location (from midline)	Craniocaudal location	Reference
1	Bands between obliquus capitis and semispinalis	Fascial		20.1 mm	77.38 mm below EOP	Janis et al ⁵⁵
2	Entrance into semispinalis	Muscular	90%	17.46 mm	59.71 mm	Janis et al ⁵⁵ Bovim et al ⁵⁶
3	Exit from semispinalis	Muscular	90%	11.5 mm 14.1 ± 4.4 mm on right, 13.8 ± 4.3 mm on left 14.9 ± 4.5 mm 15.52 mm	37.3 mm below EOP 29.1 ± 7.8 mm on right, 28.7 ± 6.6 mm on left below EOP 30.2 ± 5.1 mm 34.52 mm 2 cm above intermastoid line	Vital et al ⁶¹ Mosser et al ⁵⁴ Ducic et al ⁵⁷ Janis et al ⁵⁵ Tubbs et al ⁵⁸
4	Entrance into trapezius	Muscular		24 mm	21 mm	Janis et al ⁵⁵
5	Through trapezius insertion	Musculo-tendinous		37.07 mm	4.36 mm	Janis et al ⁵⁵
6	Occipital artery	Arterial	16% 38%	Simple intersection: 30.27 ± 6.83 mm Helical intertwining: 25.34 ± 12.16 mm– 42.09 ± 25.61 mm	Simple intersection: 10.67 ± 8.25 mm Helical intertwining: 24.91 ± 12.87 mm– 0.97 ± 8.34 mm	Janis et al ⁵⁵

Abbreviations: EOP, external occipital protuberance.

an interaction between the GON and the occipital artery in 64% of patients

Clinical Correlation

Patients with migraine headaches from a GON trigger point usually have upper cervical and occipital pain related to heavy exercise and strain. They may also have cervical muscle tightness and tenderness over the GON.²⁷

There are multiple reports of “occipital neuralgia” occurring for various reasons,⁵⁸ from whiplash to C2 osteophytes and arthritis causing compression of the GON. GON compression may be static or dynamic, as demonstrated by Vital et al, who demonstrated that the GON may be compressed by its musculofascial surroundings during neck flexion and rotation.⁶¹

Diagnosis of the occipital trigger point as a cause of migraine headaches has traditionally focused on compression point 3, the point of emergence of the GON from the semispinalis capitis muscle. Anthony found that injection of local anesthetic around the GON 1.5 cm lateral to the midline and 3 cm inferior to the EOP during a migraine attack led to migraine resolution in 88% of patients.⁶²

Traditional treatments have focused on nerve ablation, including C2 dorsal rhizotomy, C2 dorsal ganglionectomy, or radio-frequency ablation of the C2 dorsal root. Anthony et al. found that greater occipital neurectomy led to resolution of migraine headaches in 70% of patients for a mean duration of 8.1 months.⁶² Such ablative treatment, however, often resulted in significant numbness in the occipital region.

Modern nerve-preserving treatments of migraine headaches with an occipital trigger point revolve around decompression of the six potential compression points. Either a midline vertical or a horizontal incision is performed in the posterior nuchal area through the skin and subcutaneous tissue. The trapezius fascia is exposed and incised just lateral to the midline. The GON is exposed and dissected free from the semispinalis capitis muscle. A segment of semispinalis capitis muscle is removed medial to the nerve, and a triangular segment of trapezius muscle and fascia is removed lateral to the nerve. Fascial bands overlying the GON are released. If the occipital artery crosses the nerve, it is ligated.

Long-term outcomes of GON decompression have been favorable. In a prospective evaluation of 34 patients with an occipital trigger site undergoing GON decompression, with a mean 396-day follow-up, Guyuron et al. achieved at least 50% improvement in migraine intensity, duration, and frequency in 100% of patients, with 62% of them having complete migraine elimination.³ In a single-blinded, placebo-controlled, randomized trial, Guyuron et al randomized 18 patients with migraine headaches stemming from a GON trigger point to actual or sham surgery.⁴ There was a significant improvement in migraine headache frequency, intensity, and duration in the actual surgery group, which was significantly greater than the improvement experienced by the sham surgery group ($P=0.03$). Janis et al studied 16 patients with migraine headaches from an occipital trigger site who underwent GON decompression, either alone or in combination with other trigger sites.⁵ After a follow-up period of 661 days, 93.8% demonstrated significant improvement, with 56.3% having complete migraine elimination.

Ducic et al followed up on 202 patients who underwent GON decompression, either alone or in conjunction with CSM excision, with a minimum follow-up of 12 months¹⁵; 80.5% of the patients had significant improvement, with 43.4% having complete migraine headache relief.

The role of occipital artery ligation is still unclear. Chmielewski et al analyzed 170 patients who underwent GON decompression.⁶³ Among them, 55 patients underwent occipital artery resection, and 115 did not. Patients undergoing occipital artery resection had significantly lower rates of surgery success, defined as 50% or more reduction in migraine headaches (80.0% vs. 91.3% $P=0.047$) and migraine elimination (38.2% vs. 64.3%, $P=0.002$), which suggests that occipital artery resection may not always be beneficial in patients undergoing GON decompression. Further studies may be needed, but what can be stated is that some patients who have a high suspicion of symptoms related to this area (geographic location, pulsatile nature, positive Doppler signal at the point of maximal pain) likely would benefit from decompression of this trigger point.

Lesser Occipital Nerve

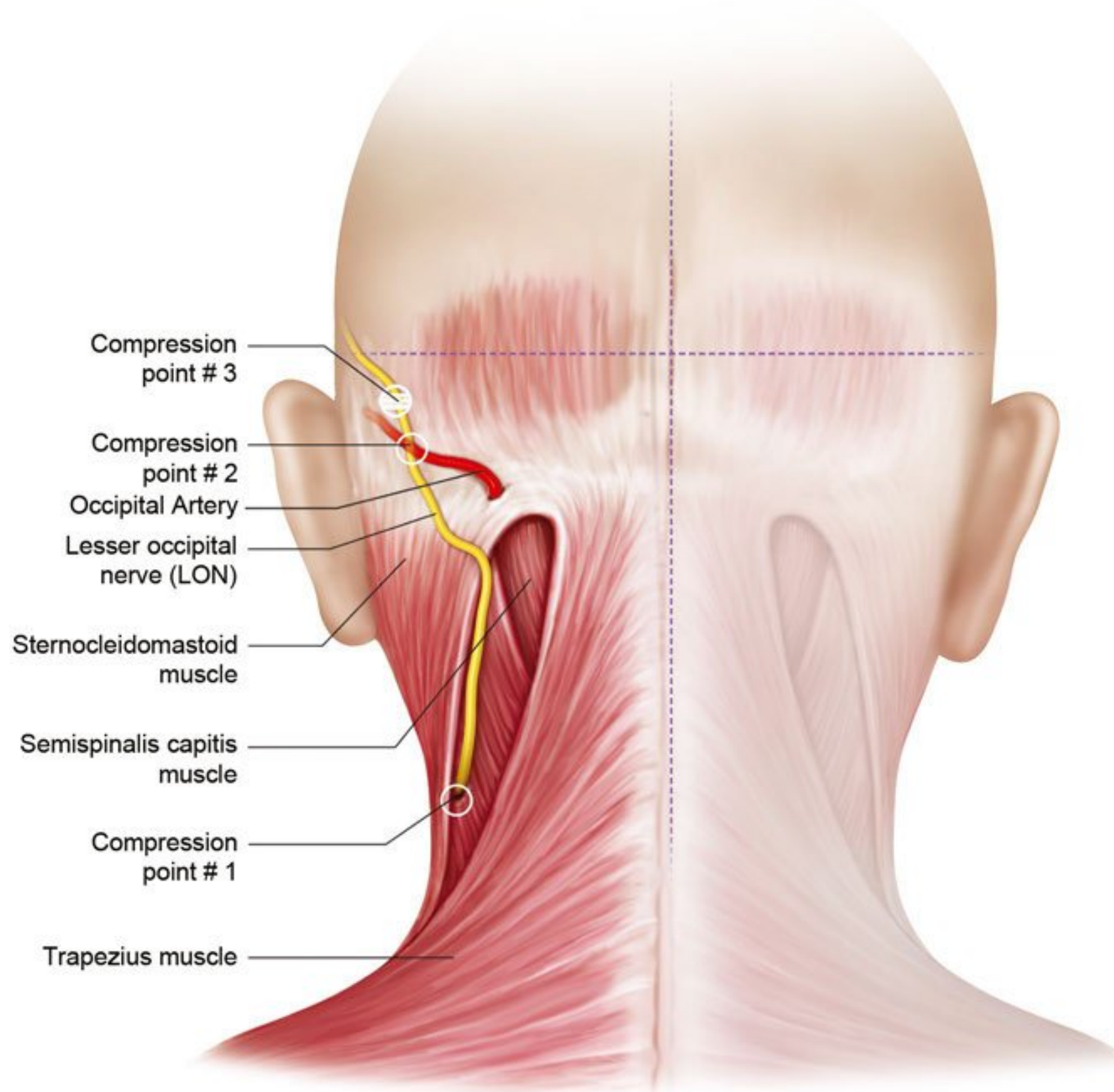
Origin and Course

The LON originates from the ventral ramus of the C2, and sometimes C3, spinal nerves. It is a cutaneous nerve that innervates the superior ear, as well as the postauricular and lateral neck areas (Fig. 10.1). It emerges from beneath the posterior border of the sternocleidomastoid (SCM).⁶⁴ The LON then travels superolaterally along the posterior border of SCM. Ducic et al found that in 85% of specimens, the LON can be located along the posterior border of the SCM, 3 cm inferior to occipital protuberance.⁵⁷ It is more variable in the remaining 15%. It then crosses over the SCM and travels superolaterally to the postauricular region at a point 7 cm lateral to the EOP and 3 cm medial to mastoid.⁵⁸ The nerve then branches into a medial and lateral component at the midpoint between the EOP and the intermastoid line.

Points of Compression and External Landmarks

The LON's point of emergence from beneath the posterior border of the SCM is located an average of 61.3 ± 12.3 mm (right) or 68.9 ± 10.1 mm (left) lateral to the posterior midline and 53.2 ± 16.1 mm caudal to a horizontal line drawn through the inferior aspect of the external acoustic meatuses (Fig. 10.8, Table 10.6).⁶⁴ Most of the time, the nerve simply emerges around the muscle edge, but in 13.3% of specimens, the LON actually pierces it. This is the first potential compression point. Lee et al located this point of emergence from the SCM an average of 64 ± 14 mm lateral to the posterior midline and 50 ± 9 mm caudal to a line drawn through the most anterosuperior aspects of the external acoustic meatuses.⁶⁵ Unlike Dash et al, Lee et al found no compression at the point of emergence from the SCM. This muscular compression point can be treated with neuromuscular blockade or nerve block. Dash et al suggest addressing the LON with botulinum toxin in a region approximately 3 cm in diameter centered at a point 6.5 cm from midline and 5.3 cm below the line between the external acoustic meatuses.⁶⁴

Fig. 10.8 Compression points of lesser occipital nerve.



In 55% of cadavers, the LON had an intersection with the occipital artery, constituting the second potential compression point.⁶⁵ This intersection was located 51 ± 9 mm lateral to the midline and 20 ± 14.5 mm inferior to a horizontal line through the most anterosuperior points of the external acoustic meatuses. In 82% of those cases, the intersection was a simple crossing located 50.7 ± 10.9 mm lateral to the midline and 22.5 ± 16.3 caudal to the horizontal line through the most anterosuperior

points of the external acoustic meatuses. In the remaining 18% there was a helical intertwining between the two structures, the midpoint of which was located 52.2 ± 6.8 mm lateral to the midline and 15.7 ± 11.2 mm caudal to the x-axis.

The third compression point, observed in 20% of specimens, consisted of a fascial band located 47 ± 8.1 mm lateral to the midline and 13.1 ± 15.2 mm inferior to a horizontal line through the most anterosuperior points of the external acoustic meatuses.⁶⁵

Table 10.6 Compression points of the lesser occipital nerve

Compression point	Name	Type	Frequency	Horizontal location (from midline)	Craniocaudal location	Reference
1	Emergence from SCM	Muscular	13.3%	61.3 \pm 12.3 mm (right) or 68.9 \pm 10.1 mm	53.2 \pm 16.1 mm caudal to inferior EAC	Dash et al ⁶⁴
				64 \pm 14 mm	50 \pm 9 mm caudal to anterosuperior EOP	Lee et al ^{65a}
2	Occipital artery	Arterial	Simple intersection: 45.1%	50.7 \pm 10.9 mm	22.5 \pm 16.3 mm caudal to anterosuperior EAC	Lee et al ⁶⁵
				Helical intertwining: 9.9%	15.7 \pm 11.2 mm caudal to anterosuperior EAC	
3	Fascial band	Fascial	20%	47 \pm 8.1 mm	13.1 \pm 15.2 mm caudal to anterosuperior EAC	Lee ⁶⁵

Abbreviations: EAC, external acoustic meatus; EOP, external occipital protuberance; SCM, sternocleidomastoid.

^aDid not find compression at this point.

Table 10.7 Compression points of the third occipital nerve

Compression point	Name	Type	Frequency	Horizontal location (from midline)	Craniocaudal location	Reference
1	Emergence from semispinalis	Muscular	100%	13.0 ± 5.0 mm (left), 13.3 ± 5.8 mm (right)	60.7 ± 20.2 mm (left), $63.4 \pm 20.8 \pm$ mm (right) caudal to inferior external acoustic meatus	Dash et al ⁶⁴

Clinical Correlation

Patients with LON compression typically have symptoms similar to those seen with GON compression, but the pain is more lateral along the course of the LON. The LON may be implicated in patients with migraine headaches resulting from an occipital trigger point who undergo GON release without complete relief.⁵

To decompress the LON, it is released from all muscular and fascial attachments, ligated, and its ends are implanted into the SCM muscle. Guyuron et al also recommend injecting triamcinolone in the area intraoperatively in order to minimize the risk of neuroma formation.³⁰

Few clinical studies have reported the outcomes of LON release, and most patients in those studies underwent concomitant GON release, which makes quantification of the outcomes of isolated LON release difficult.

of the external acoustic meatuses and a second injection 1 cm below.⁶⁴

Clinical Correlation

Similar to the lesser occipital nerve, the third occipital nerve may be implicated in some patients with occipital trigger points who do not fully respond to release of the GON.^{5,64} Cervicogenic headaches stemming from third occipital nerve irritation can be due to osteoarthritis of the C2-C3 zygapophysial joint or whiplash. Lord et al found that 27% incidence of TON-induced headaches in post-whiplash patients.⁶⁷

In the past, patients were successfully treated with third occipital nerve blockade,^{67,68} radiofrequency ablation,⁶⁹ or neurectomy.⁶⁶ Recently described surgical release methods of TON release involve releasing it from the surrounding semispinalis capitis muscle and then avulsing the nerve. Avulsion of the TON is performed by applying traction to it and avulsing it, thus allowing it to retract into the musculature instead of being trapped in the scar of the surgical field.¹⁵

Like the LON, few clinical studies have clearly outlined the outcomes of isolated TON release in migraine decompression surgery. Lee et al conducted a retrospective review of patients undergoing GON release and compared those in whom the TON was encountered and avulsed with those in whom it was not⁷⁰; no difference in outcomes between the two groups was found.

Third Occipital Nerve

Origin and Course

The third occipital nerve (TON), also known as the dorsal occipital nerve, originates from the medial branch of the dorsal ramus of the C3 spinal nerve.⁶⁴ It is a sensory nerve that innervates the posterior medial scalp and neck (Fig. 10.1).

The TON always emerges from the semispinalis capitis muscle by piercing it and then travels cranially in the subcutaneous plane towards the posterior medial scalp. The average diameter of the TON is 1.3 mm.⁶⁶ Each TON has multiple interconnections with the ipsilateral GON and the contralateral TON.

Points of Compression and External Landmarks

Dash et al found that the TON pierces the semispinalis capitis muscle at a point 13.0 ± 5.0 mm (left) to 13.3 ± 5.8 mm (right) lateral to the posterior midline and 60.7 ± 20.2 mm (left) to $63.4 \pm 20.8 \pm$ mm (right) inferior to a horizontal line drawn through the inferior aspect of the external acoustic meatuses (Fig. 10.7, Table 10.7).⁶⁴ Tubbs et al found that point approximately 5 to 6 cm caudal to the external occipital protuberance, 3 cm caudal to the intermastoid line, and 3 to 7 mm lateral to the midline.⁶⁶

The vertical location of the TON varies significantly; therefore, to reliably block this nerve, Dash et al suggest performing two injections 1.3 cm lateral to the midline, with one injection 1 cm above a horizontal line drawn through the inferior aspect

Summary

The peripheral trigger theory postulates that compression of sensory branches of the trigeminal and cervical nerves in the head and neck generates the nociceptive signals responsible for migraine headaches. Surgical decompression of those compression points has been proven, in multiple studies, to be effective at reducing the frequency, severity, and duration of migraine headaches. In a systematic review comparing various nerve decompression modalities in migraine headaches, surgical decompression showed the highest efficacy and the lowest complication rate.⁷¹ To perform adequate and safe surgical decompression, however, a thorough and detailed knowledge of the anatomy of those compression points, their external landmarks, and their anatomical variants is essential. This chapter summarizes the published anatomical data on the known migraine trigger sites.

References

1. Lipton RB, Bigal ME, Diamond M, Freitag F, Reed ML, Stewart WF; AMPP Advisory Group. Migraine prevalence, disease burden, and the need for preventive therapy. *Neurology* 2007;68(5):343–349 [PubMed](#)
2. Guyuron B, Tucker T, Davis J. Surgical treatment of migraine headaches. *Plast Reconstr Surg* 2002;109(7):2183–2189 [PubMed](#)
3. Guyuron B, Kriegler JS, Davis J, Amini SB. Comprehensive surgical treatment of migraine headaches. *Plast Reconstr Surg* 2005;115(1):1–9 [PubMed](#)
4. Guyuron B, Reed D, Kriegler JS, Davis J, Pashmini N, Amini S. A placebo-controlled surgical trial of the treatment of migraine headaches. *Plast Reconstr Surg* 2009;124(2):461–468 [PubMed](#)
5. Janis JE, Dhanik A, Howard JH. Validation of the peripheral trigger point theory of migraine headaches: single-surgeon experience using botulinum toxin and surgical decompression. *Plast Reconstr Surg* 2011;128(1):123–131 [PubMed](#)
6. Welch KMA. Contemporary concepts of migraine pathogenesis. *Neurology* 2003;61(8, Suppl 4)S2–S8 [PubMed](#)
7. Bolay H, Reuter U, Dunn AK, Huang Z, Boas DA, Moskowitz MA. Intrinsic brain activity triggers trigeminal meningeal afferents in a migraine model. *Nat Med* 2002;8(2):136–142 [PubMed](#)
8. Moskowitz MA. The neurobiology of vascular head pain. *Ann Neurol* 1984;16(2):157–168 [PubMed](#)
9. Silberstein S, Mathew N, Saper J, Jenkins S; For the BOTOX Migraine Clinical Research Group. Botulinum toxin type A as a migraine preventive treatment. *Headache* 2000;40(6):445–450 [PubMed](#)
10. Relja M, Poole AC, Schoenen J, Pascual J, Lei X, Thompson C; European BoNTA Headache Study Group. A multicentre, double-blind, randomized, placebo-controlled, parallel group study of multiple treatments of botulinum toxin type A (BoNTA) for the prophylaxis of episodic migraine headaches. *Cephalgia* 2007;27(6):492–503 [PubMed](#)
11. Durham PL, Cady R, Cady R. Regulation of calcitonin gene-related peptide secretion from trigeminal nerve cells by botulinum toxin type A: implications for migraine therapy. *Headache* 2004;44(1):35–42, discussion 42–43 [PubMed](#)
12. Kung TA, Guyuron B, Cederna PS. Migraine surgery: a plastic surgery solution for refractory migraine headache. *Plast Reconstr Surg* 2011;127(1):181–189 [PubMed](#)
13. Guyuron B, Varghai A, Michelow BJ, Thomas T, Davis J. Corrugator supercilii muscle resection and migraine headaches. *Plast Reconstr Surg* 2000;106(2):429–434, discussion 435–437 [PubMed](#)
14. Calandre EP, Hidalgo J, García-Leiva JM, Rico-Villademoros F. Trigger point evaluation in migraine patients: an indication of peripheral sensitization linked to migraine predisposition? *Eur J Neurol* 2006;13(3):244–249 [PubMed](#)
15. Ducic I, Hartmann EC, Larson EE. Indications and outcomes for surgical treatment of patients with chronic migraine headaches caused by occipital neuralgia. *Plast Reconstr Surg* 2009;123(5):1453–1461 [PubMed](#)
16. Knize DM. Transpalpebral approach to the corrugator supercilii and procerus muscles. *Plast Reconstr Surg* 1995;95(1):52–60, discussion 61–62 [PubMed](#)
17. Cuzalina AL, Holmes JD. A simple and reliable landmark for identification of the supraorbital nerve in surgery of the forehead: an in vivo anatomical study. *J Oral Maxillofac Surg* 2005;63(1):25–27 [PubMed](#)
18. Janis JE, Ghavami A, Lemmon JA, Leedy JE, Guyuron B. The anatomy of the corrugator supercilii muscle: part II. Supraorbital nerve branching patterns. *Plast Reconstr Surg* 2008;121(1):233–240 [PubMed](#)
19. Fallucco M, Janis JE, Hagan RR. The anatomical morphology of the supraorbital notch: clinical relevance to the surgical treatment of migraine headaches. *Plast Reconstr Surg* 2012;130(6):1227–1233 [PubMed](#)
20. Chepla KJ, Oh E, Guyuron B. Clinical outcomes following supraorbital foraminotomy for treatment of frontal migraine headache. *Plast Reconstr Surg* 2012;129(4):656e–662e [PubMed](#)
21. Beer GM, Putz R, Mager K, Schumacher M, Keil W. Variations of the frontal exit of the supraorbital nerve: an anatomic study. *Plast Reconstr Surg* 1998;102(2):334–341 [PubMed](#)
22. Agthong S, Huanmanop T, Chentanez V. Anatomical variations of the supraorbital, infraorbital, and mental foramina related to gender and side. *J Oral Maxillofac Surg* 2005;63(6):800–804 [PubMed](#)
23. Cutright B, Quillopa N, Schubert W. An anthropometric analysis of the key foramina for maxillofacial surgery. *J Oral Maxillofac Surg* 2003;61(3):354–357 [PubMed](#)
24. Saylam C, Ozer MA, Ozek C, Gurler T. Anatomical variations of the frontal and supraorbital transcranial passages. *J Craniofac Surg* 2003;14(1):10–12 [PubMed](#)
25. Webster RC, Gaunt JM, Hamdan US, Fuleihan NS, Giandello PR, Smith RC. Supraorbital and supratrochlear notches and foramina: anatomical variations and surgical relevance. *Laryngoscope* 1986;96(3):311–315 [PubMed](#)
26. Janis JE, Ghavami A, Lemmon JA, Leedy JE, Guyuron B. Anatomy of the corrugator supercilii muscle: part I. Corrugator topography. *Plast Reconstr Surg* 2007;120(6):1647–1653 [PubMed](#)
27. Liu MT, Armijo BS, Guyuron B. A comparison of outcome of surgical treatment of migraine headaches using a constellation of symptoms versus botulinum toxin type A to identify the trigger sites. *Plast Reconstr Surg* 2012;129(2):413–419 [PubMed](#)
28. Liu MT, Chim H, Guyuron B. Outcome comparison of endoscopic and transpalpebral decompression for treatment of frontal migraine headaches. *Plast Reconstr Surg* 2012;129(5):1113–1119 [PubMed](#)
29. Walden JL, Brown CC, Klapper AJ, Chia CT, Aston SJ. An anatomical comparison of transpalpebral, endoscopic, and coronal approaches to demonstrate exposure and extent of brow depressor muscle resection. *Plast Reconstr Surg* 2005;116(5):1479–1487, discussion 1488–1489 [PubMed](#)
30. Guyuron B, Kriegler JS, Davis J, Amini SB. Five-year outcome of surgical treatment of migraine headaches. *Plast Reconstr Surg* 2011;127(2):603–608 [PubMed](#)
31. Miller TA, Rudkin G, Honig M, Elahi M, Adams J. Lateral subcutaneous brow lift and interbrow muscle resection: clinical experience and anatomic studies. *Plast Reconstr Surg* 2000;105(3):1120–1128 [PubMed](#)
32. Janis JE, Hatef DA, Hagan R, et al. Anatomy of the supratrochlear nerve: implications for the surgical treatment of migraine headaches. *Plast Reconstr Surg* 2013;131(4):743–750 [PubMed](#)
33. Janis JE, Hatef DA, Thakar H, et al. The zygomaticotemporal branch of the trigeminal nerve: Part II. Anatomical variations. *Plast Reconstr Surg* 2010;126(2):435–442 [PubMed](#)
34. Totoni A, Pashmini N, Guyuron B. The zygomaticotemporal branch of the trigeminal nerve: an anatomical study. *Plast Reconstr Surg* 2005;115(1):273–277 [PubMed](#)
35. Tubbs RS, Mortazavi MM, Shoja MM, Loukas M, Cohen-Gadol AA. The zygomaticotemporal nerve and its relevance to neurosurgery. *World Neurosurg* 2012;78(5):515–518 [PubMed](#)
36. Odobescu A, Williams HB, Gilardino MS. Description of a communication between the facial and zygomaticotemporal nerves. *J Plast Reconstr Aesthet Surg* 2012;65(9):1188–1192 [PubMed](#)

37. Loukas M, Owens DG, Tubbs RS, Spentzouris G, Elochukwu A, Jordan R. Zygomaticofacial, zygomaticoorbital and zygomaticotemporal foramina: anatomical study. *Anat Sci Int* 2008;83(2): 77–82 [PubMed](#)
38. Jeong SM, Park KJ, Kang SH, et al. Anatomical consideration of the anterior and lateral cutaneous nerves in the scalp. *J Korean Med Sci* 2010;25(4):517–522 [PubMed](#)
39. Murillo CA. Resection of the temporal neurovascular bundle for control of migraine headache. *Headache* 1968;8(3):112–117 [PubMed](#)
40. Guyuron B, Becker DB. Surgical treatment of migraine headaches. In: Guyuron B, Eriksson E, Persing JA, et al, eds. *Plastic Surgery: Indications and Practice*. Philadelphia, PA: Saunders Elsevier; 2009:1655–1665
41. Kurlander DE, Punjabi A, Liu MT, Sattar A, Guyuron B. In-depth review of symptoms, triggers, and treatment of temporal migraine headaches (site II). *Plast Reconstr Surg* 2014;133(4):897–903 [PubMed](#)
42. Chim H, Miller E, Gliniak C, Cohen ML, Guyuron B. The role of different methods of nerve ablation in prevention of neuroma. *Plast Reconstr Surg* 2013;131(5):1004–1012 [PubMed](#)
43. Schmidt BL, Pogrel MA, Necoechea M, Kearns G. The distribution of the auriculotemporal nerve around the temporomandibular joint. *Oral Surg Oral Med Oral Pathol Oral Radiol Endod* 1998;86(2):165–168 [PubMed](#)
44. Janis JE, Hatef DA, Ducic I, et al. Anatomy of the auriculotemporal nerve: variations in its relationship to the superficial temporal artery and implications for the treatment of migraine headaches. *Plast Reconstr Surg* 2010;125(5):1422–1428 [PubMed](#)
45. Gülekon N, Anil A, Poyraz A, Peker T, Turgut HB, Karaköse M. Variations in the anatomy of the auriculotemporal nerve. *Clin Anat* 2005;18(1):15–22 [PubMed](#)
46. Chim H, Okada HC, Brown MS, et al. The auriculotemporal nerve in etiology of migraine headaches: compression points and anatomical variations. *Plast Reconstr Surg* 2012;130(2):336–341 [PubMed](#)
47. Behin F, Behin B, Bigal ME, Lipton RB. Surgical treatment of patients with refractory migraine headaches and intranasal contact points. *Cephalgia* 2005;25(6):439–443 [PubMed](#)
48. Harley DH, Powitzky ES, Duncavage J. Clinical outcomes for the surgical treatment of sinonasal headache. *Otolaryngol Head Neck Surg* 2003;129(3):217–221 [PubMed](#)
49. Clerico DM. Pneumatized superior turbinate as a cause of referred migraine headache. *Laryngoscope* 1996;106(7):874–879 [PubMed](#)
50. Ferrero V, Allais G, Rolando S, Pozzo T, Allais R, Benedetto C. Endonasal mucosal contact points in chronic migraine. *Neurol Sci* 2014;35(Suppl 1):83–87 [PubMed](#)
51. Homsioglou E, Balatsouras DG, Alexopoulos G, Kaberos A, Katotomichelakis M, Danielides V. Pneumatized superior turbinate as a cause of headache. *Head Face Med* 2007;3:3–8 [PubMed](#)
52. Tosun F, Gerek M, Ozkaptan Y. Nasal surgery for contact point headaches. *Headache* 2000;40(3):237–240 [PubMed](#)
53. Welge-Luessen A, Hauser R, Schmid N, Kappos L, Probst R. Endonasal surgery for contact point headaches: a 10-year longitudinal study. *Laryngoscope* 2003;113(12):2151–2156 [PubMed](#)
54. Mosser SW, Guyuron B, Janis JE, Rohrich RJ. The anatomy of the greater occipital nerve: implications for the etiology of migraine headaches. *Plast Reconstr Surg* 2004;113(2):693–700 [PubMed](#)
55. Janis JE, Hatef DA, Ducic I, et al. The anatomy of the greater occipital nerve: Part II. Compression point topography. *Plast Reconstr Surg* 2010;126(5):1563–1572 [PubMed](#)
56. Bovim G, Bonamico L, Fredriksen TA, Lindboe CF, Stolt-Nielsen A, Sjaastad O. Topographic variations in the peripheral course of the greater occipital nerve. Autopsy study with clinical correlations. *Spine* 1991;16(4):475–478 [PubMed](#)
57. Ducic I, Moriarty M, Al-Attar A. Anatomical variations of the occipital nerves: implications for the treatment of chronic headaches. *Plast Reconstr Surg* 2009;123(3):859–863, discussion 864 [PubMed](#)
58. Tubbs RS, Salter EG, Wellons JC III, Blount JP, Oakes WJ. Landmarks for the identification of the cutaneous nerves of the occiput and nuchal regions. *Clin Anat* 2007;20(3):235–238 [PubMed](#)
59. Janis JE, Hatef DA, Reece EM, McCluskey PD, Schaub TA, Guyuron B. Neurovascular compression of the greater occipital nerve: implications for migraine headaches. *Plast Reconstr Surg* 2010;126(6): 1996–2001 [PubMed](#)
60. Junewicz A, Katira K, Guyuron B. Intraoperative anatomical variations during greater occipital nerve decompression. *J Plast Reconstr Aesthet Surg* 2013;66(10):1340–1345 [PubMed](#)
61. Vital JM, Grenier F, Dautheribes M, Baspeyre H, Lavignolle B, Sénergas J. An anatomic and dynamic study of the greater occipital nerve (n. of Arnold). Applications to the treatment of Arnold's neuralgia. *Surg Radiol Anat* 1989;11(3):205–210 [PubMed](#)
62. Anthony M. Headache and the greater occipital nerve. *Clin Neurol Neurosurg* 1992;94(4):297–301 [PubMed](#)
63. Chmielewski L, Liu MT, Guyuron B. The role of occipital artery resection in the surgical treatment of occipital migraine headaches. *Plast Reconstr Surg* 2013;131(3):351e–356e [PubMed](#)
64. Dash KS, Janis JE, Guyuron B. The lesser and third occipital nerves and migraine headaches. *Plast Reconstr Surg* 2005;115(6):1752–1758, discussion 1759–1760 [PubMed](#)
65. Lee M, Brown M, Chepla K, et al. An anatomical study of the lesser occipital nerve and its potential compression points: implications for surgical treatment of migraine headaches. *Plast Reconstr Surg* 2013;132(6):1551–1556 [PubMed](#)
66. Tubbs RS, Mortazavi MM, Loukas M, et al. Anatomical study of the third occipital nerve and its potential role in occipital headache/neck pain following midline dissections of the craniocervical junction. *J Neurosurg Spine* 2011;15(1):71–75 [PubMed](#)
67. Lord SM, Barnsley L, Wallis BJ, Bogduk N. Third occipital nerve headache: a prevalence study. *J Neurol Neurosurg Psychiatry* 1994; 57(10):1187–1190 [PubMed](#)
68. Bogduk N, Marsland A. On the concept of third occipital headache. *J Neurol Neurosurg Psychiatry* 1986;49(7):775–780 [PubMed](#)
69. Hamer JF, Purath TA. Response of cervicogenic headaches and occipital neuralgia to radiofrequency ablation of the C2 dorsal root ganglion and/or third occipital nerve. *Headache* 2014;54(3):500–510 [PubMed](#)
70. Lee M, Lineberry K, Reed D, Guyuron B. The role of the third occipital nerve in surgical treatment of occipital migraine headaches. *J Plast Reconstr Aesthet Surg* 2013;66(10):1335–1339 [PubMed](#)
71. Ducic I, Felder JM III, Fantus SA. A systematic review of peripheral nerve interventional treatments for chronic headaches. *Ann Plast Surg* 2014;72(4):439–445 [PubMed](#)

Yoko Tabira, Joe Iwanaga, Tsuyoshi Saga, and Koichi Watanabe

Introduction

The soft tissue layers of the face from the surface down are generally made up of the skin, subcutaneous fat, superficial fascia (superficial musculocutaneous system [SMAS]), mimetic muscles, and deep tissue layers. Structurally, these layers vary among the different regions of the face. For example, the subcutaneous fat layer does not exist in the eyelid, lip, or nose. The deep tissue layer is covered by deep fascia and includes the parotid gland, masseter muscle, buccal fat pad, deep temporal fascia, and temporalis muscle. The structures within the deep tissue layer also vary among the different facial regions. Each layer is connected to adjacent layers and supports proper anatomical positioning of the facial soft tissue against gravity. Among the soft tissue layers of the face, the SMAS is the key structure of the facial fascial system. This chapter describes the basic structure of each layer and presents cadaver dissections and microscopic images.

Subcutaneous Fat Layer

The subcutaneous fat is located beneath the dermis and is present throughout most of the entire body. In body regions other than the face, the subcutaneous fat layer is divided into two layers by the superficial fascia, and each layer exhibits different characteristics. The superficial fat layer contains many fibrous septa and is involved in protection from external forces. Nakajima et al¹ termed this fat layer the protective adipofascial system. In contrast, the deep fat layer provides flexibility to musculoskeletal movement and is termed the lubricant adipofascial system. The facial subcutaneous fat contains many fibrous septa and has a structure similar to that of the protective adipofascial system. The subcutaneous fat layer has an intimate relationship with the SMAS. Many connective tissue fibers rise upward to the dermis and provide a strong connection between the dermis and SMAS. Each lobule of the subcutaneous fat is small and surrounded by dense fibrous septa. In the cheek region, a thick fat tissue layer lies on the SMAS and is distinct from the subcutaneous fat layer. This fat tissue is called the malar fat pad.

Malar Fat Pad

The malar fat pad is the fat tissue that lies superficial to the SMAS in the cheek region. It is triangular shaped and bound medially along the nasolabial crease, superiorly along the orbital rim, and laterally along the convex curved line connecting the lateral canthus and nasolabial crease around the corner of the mouth. At the location of the malar fat pad, the upper half of the SMAS comprises the orbicularis oculi muscle, and the

lower half comprises the superficial upper lip elevator muscles. The lower half of the SMAS is quite thin and almost discontinuous and has no mechanical bearing capacity. The malar fat pad is firmly fixed to the dermis and relatively loosely fixed to the SMAS layer in this region. The zygomatic ligament, which is an osteocutaneous ligament located on the zygoma lateral to the origin of the zygomatic minor muscle, inserts in the overlying dermis and pierces and anchors the malar fat pad to connect it to the deeper tissue layers.

Cosmetically, the malar fat pad slides downward and inward over the SMAS with aging, deepening the nasolabial crease. Fat tissue is also present beneath the orbicularis oculi muscle. This fat tissue is called the suborbicularis oculi fat pad and lacks continuity with the malar fat pad.

SMAS

The SMAS is the fascial tissue layer located just beneath the subcutaneous fat layer. It connects the facial muscles with the dermis, transmits contraction of the facial muscles to the skin, and assists in creating facial expression. The SMAS is the key structure in surgical treatment of the face, and an accurate knowledge of its anatomy is extremely important. The existence of superficial fascia in the head and neck region has been discovered in fragments; for example, the superficial temporal fascia and galea aponeurotica were not originally recognized as a continuous layer. The concept of a fascia layer that spreads throughout the entire head and neck region in one sheet and is integrated with the conventional fragmental fascial structures (i.e., the concept of the SMAS) was first advocated by Mitz and Peyronie in 1976.² The SMAS is a fascial layer that is connected superiorly to the frontalis muscle and inferiorly to the platysma muscle. Its thickness decreases as it continues to the anterior cheek area. Although some opinions differ, the generally prevailing thoughts regarding the SMAS are almost identical to those proposed by Mitz and Peyronie.²

The SMAS lies on the same horizontal plane as the platysma muscle and extends superiorly to the superficial temporal fascia, galea aponeurotica, and frontalis muscle in its upper region (**Fig. 11.1**). However, some authorities have questioned the continuity of the SMAS in the temporal region. Gosain et al³ reported that the SMAS terminates within 1 cm below the zygomatic arch and is not continuous with the temporoparietal fascia (superficial temporal fascia). Intraoperatively, the area over the zygomatic arch has a complicated structure. The superficial temporal artery passing from the deep plane to the superficial temporal fascia layer and the temporal branch of the facial nerve also passes from the deep layer to the inferior surface of the superficial temporal fascia. The SMAS is also difficult to dissect as a uniform layer. It is quite thick in the parotid–masseteric

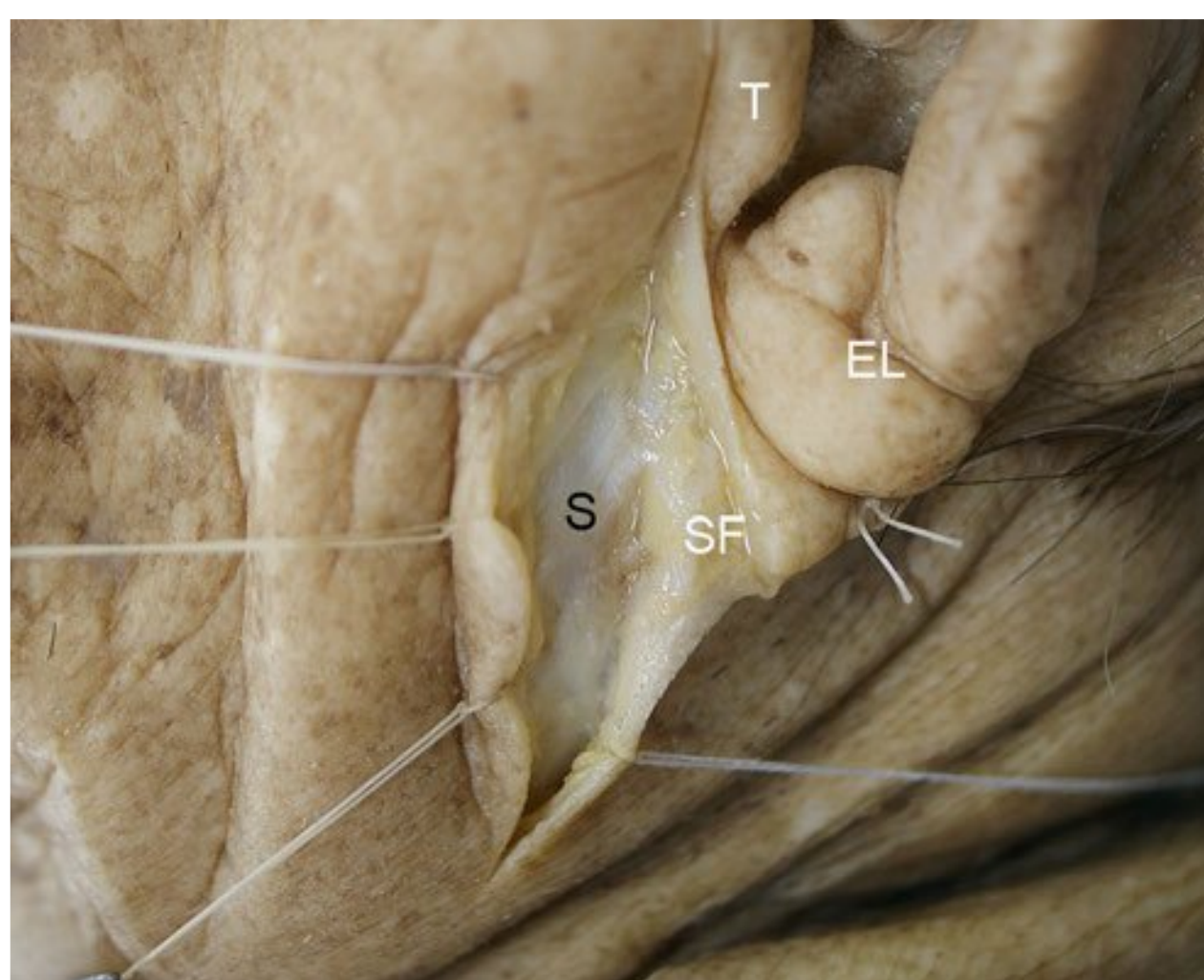
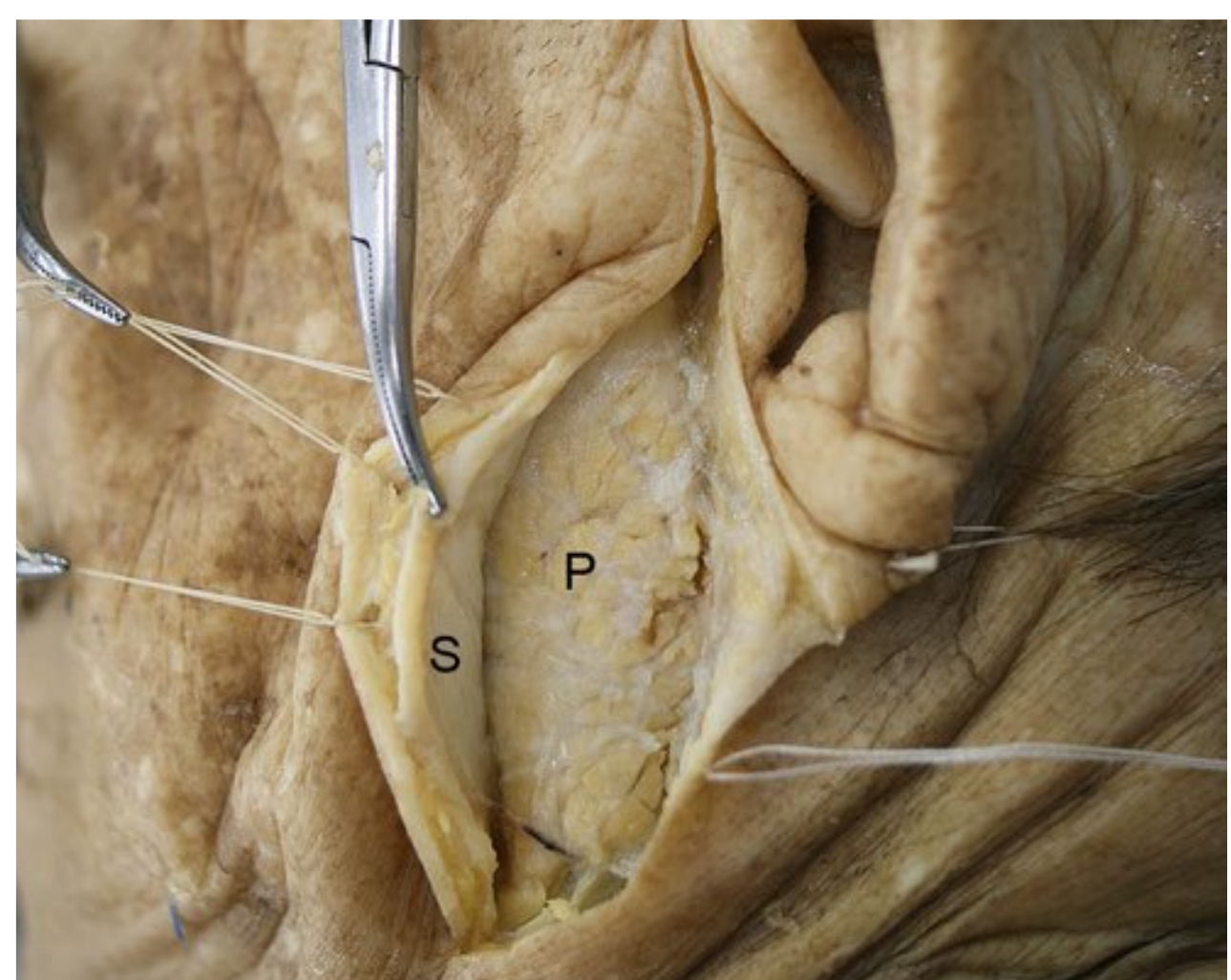
**a**

Fig. 11.1 Cadaveric dissection of the superficial musculoponeurotic system (SMAS) in the parotid region. **(a)** The SMAS is seen as a white fibrous layer under the subcutaneous fat. EL, Earlobe; T, tragus; S, SF,

**b**

subcutaneous fat. **(b)** The SMAS is elevated with Kocher forceps. The parotid gland is observed in the sub-SMAS layer. P, Parotid gland; S, SMAS.

and zygomatic areas and is easily dissected in this region under gross visualization. Beyond the anterior border of the masseter muscle, however, the SMAS becomes quite thin and almost invisible, making it quite difficult to dissect, raising questions about the continuity of the SMAS. Gardetto et al⁴ stated that the SMAS cannot be detected in any facial region other than the parotid region. Jost and Levet⁵ questioned whether the SMAS actually continues to the orbicularis oculi muscle from an embryologic point of view. The orbicularis oculi originates from the sphincter colli profundus; however, the platysma muscle, which lies on the same plane as does the SMAS, originates from a different layer (i.e., the platysma layer). Thus, confusion results from the histologic differences among the soft tissue layers of the lateral and central facial regions. Ghassemi et al⁶ claimed that the SMAS can be histologically classified as type 1 or type 2. Type 1 SMAS describes the common architecture of the posterior part of the face and is observed in the forehead, parotid region, zygomatic region, infraorbital region, and lateral aspect of the nasolabial fold. The subdermal structure comprises a meshwork of fibrous septa enveloping lobules of fat cells. Type 2 SMAS is found in the upper and lower lips, and the subdermal tissue comprises a meshwork of intermingled collagen, elastic fibers, and muscle fibers.

With respect to the relationship of the SMAS with mimetic muscles, Mitz and Peyronie² reported that the SMAS invests in and extends into the external part of the superficial facial muscles involving the risorius, frontalis, platysma, and orbicularis oculi muscles. Stuzin et al⁷ reported that the SMAS invests in the zygomaticus major and zygomaticus minor, in addition to the muscles described by Mitz and Peyronie.² The mimetic muscle layer is three-dimensional, and each of its muscles is located at a different depth from the surface. According to embryologic hypothesis, these facial muscles originate from three layers: the sphincter colli superficialis, sphincter colli profundus, and platysma, the last of which is located between the two sphincters. The sphincter colli profundus differentiates and be-

comes the buccinators, orbicularis oris, levator anguli oris, levator labii superioris, depressor anguli oris, and similar muscles. The platysma becomes other facial muscles, and the sphincter colli superficialis degenerates in many mammals. Freilinger et al⁸ reported the three-dimensional structure of the mimetic muscles as comprising four layers: layer 1, depressor anguli oris, zygomaticus minor, and orbicularis oculi; layer 2, depressor labii inferioris, risorius, platysma, zygomaticus major, and levator labii superioris alaeque nasi; layer 3, orbicularis oris and levator labii superioris; and layer 4, mentalis, levator anguli oris, and buccinator. The SMAS is presumed to have a close relationship with the two superficial layers of the mimetic muscles as described by Freilinger et al.⁸ According to Freilinger et al, however, some muscles are superficial to the SMAS (e.g., the platysma). Thus, the descriptions of the SMAS are presumed to be based more on clinical theory than strictly on embryologic theory.

There are many opinions about the embryologic origin of the SMAS.^{2,9} For example, some researchers have reported that the superficial fascia (tela subcutanea), which is a loose fibrous layer located just under the skin, is also observed in other parts of the body.² Others have described fibrous degeneration of the platysma,⁵ a distinct fibromuscular layer comprising the platysma and parotid fascia,¹⁰ a musculoponeurotic layer continuous with the platysma,⁶ and an evolutionary form of the panniculus carnosus.¹¹ Some reports state that the SMAS contains muscle fibers,^{2,8} which indicates the embryologic origin of the SMAS layer. One anatomical textbook also shows that the platysma sometimes extends farther upward than usual, in some cases as high as the zygoma.¹² Such a markedly upward-extending platysma is considered to represent remaining muscle fibers along the platysma layer. Another possibility is that a primitive muscle remains in the SMAS layer.¹³ Lei et al¹⁴ termed the muscle that spreads over the parotid gland *the transverse nuchae muscle* and assumed that this muscle is the SMAS muscle fiber described by Mitz and Peyronie.² This muscle was found in about 5% of our dissections.

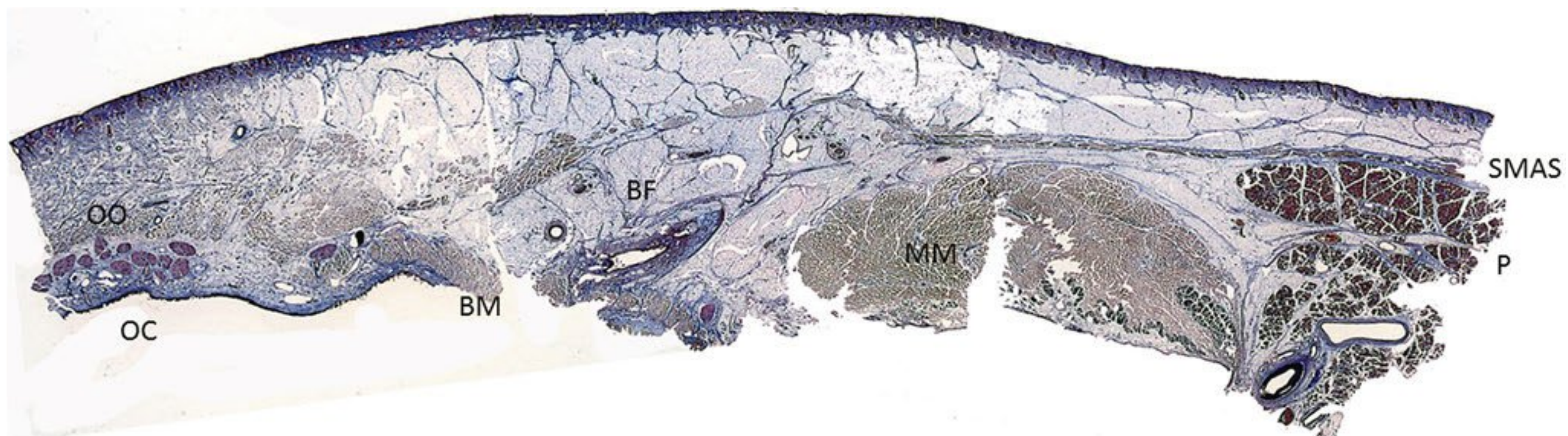


Fig. 11.2 Cross-section from the parotid gland to the upper lip (composite photograph of three preparation specimens; Masson trichrome stain, $\times 1$). BF, Buccal fat pad; BM, buccinator muscle; MM, masseter muscle; OC, oral cavity; OO, orbicularis oris muscle; P, parotid gland; SMAS, superficial musculoaponeurotic system.

Histologic Findings of the SMAS

Parotid Area to Cheek Region

The SMAS is a thick membranous tissue that lies on the parotid gland and extends anteriorly, maintaining almost the same thickness until reaching the anterior border of the masseter (Fig. 11.2). Some branched muscular fibers of the platysma are present within the SMAS layer. The subcutaneous fat tissue layer is relatively thin in this area. The fibrous septa within this layer basically run parallel to the SMAS and delineate long, oval-shaped fat tissue in the horizontal plane. The SMAS becomes dramatically thinner beyond the anterior border of the masseter as it enters the cheek area; it can be barely traced by the position of split peripheral part of the platysma. The thick fat tissue superficial to the SMAS layer is the malar fat pad. This fat tissue contains fibrous septa that run perpendicular to the SMAS toward the dermis and separate the fat tissue into long ovals in the vertical plane. The fat tissue observed anterior to the masseter is the buccal fat pad, which fills the masticatory space.

Temporal Region

In the temporal region, the SMAS meets the superficial temporal fascia (Fig. 11.3). The superficial temporal fascia usually comprises fibrous tissue without muscle; however, it sometimes contains visible degenerative facial muscles such as the superior auricular muscle and temporoparietal muscle. The SMAS becomes somewhat ambiguous between these two fasciae, around the region of the zygomatic arch. Toward the temporal region, the SMAS layer separates into fibers containing fat tissue, no longer constituting a sheet of membrane. This finding is in contrast to the idea that the SMAS is continuous. The fibers gradually converge as they course upward. The subcutaneous fat layer above the SMAS also becomes thinner toward the head.

Lower Eyelid

It is generally recognized that the SMAS runs superficial to the zygomaticus major and minor and continues to the orbicularis oculi; however, it is difficult to confirm that the SMAS constitutes one continuous sheet in this area (Fig. 11.4). The thick fat

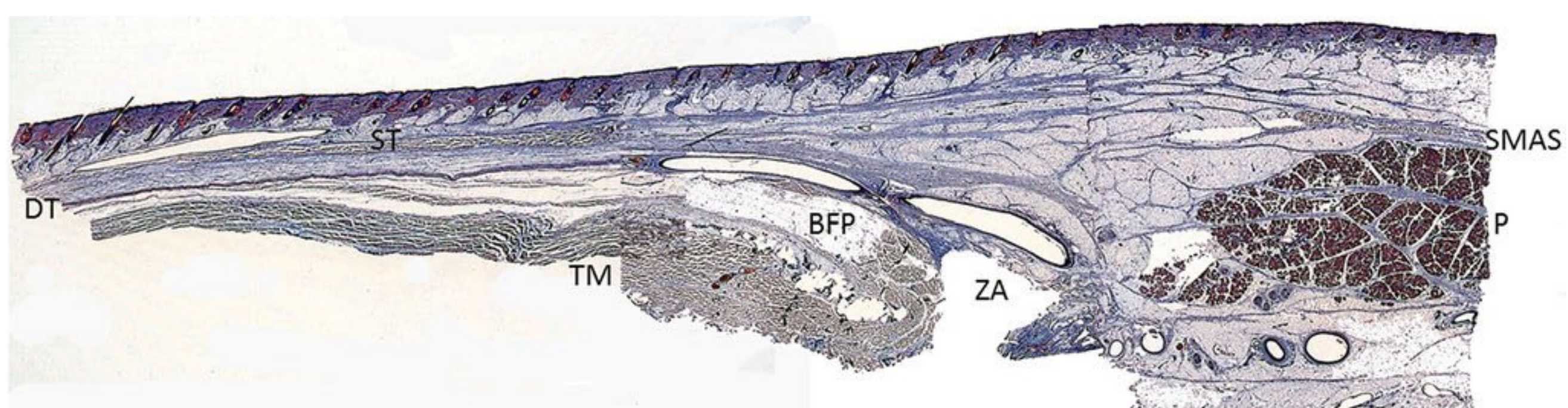


Fig. 11.3 Cross section from the parotid gland to the temporal region (composite photograph of three preparation specimens, Masson trichrome stain, $\times 1$). BF, Buccal fat pad; DT, deep temporal fascia;

P, parotid gland; SMAS, superficial musculoaponeurotic system; ST, superficial temporal fascia (in this case, the temporoparietal muscle); TM, temporalis muscle; ZA, zygomatic arch (removed).

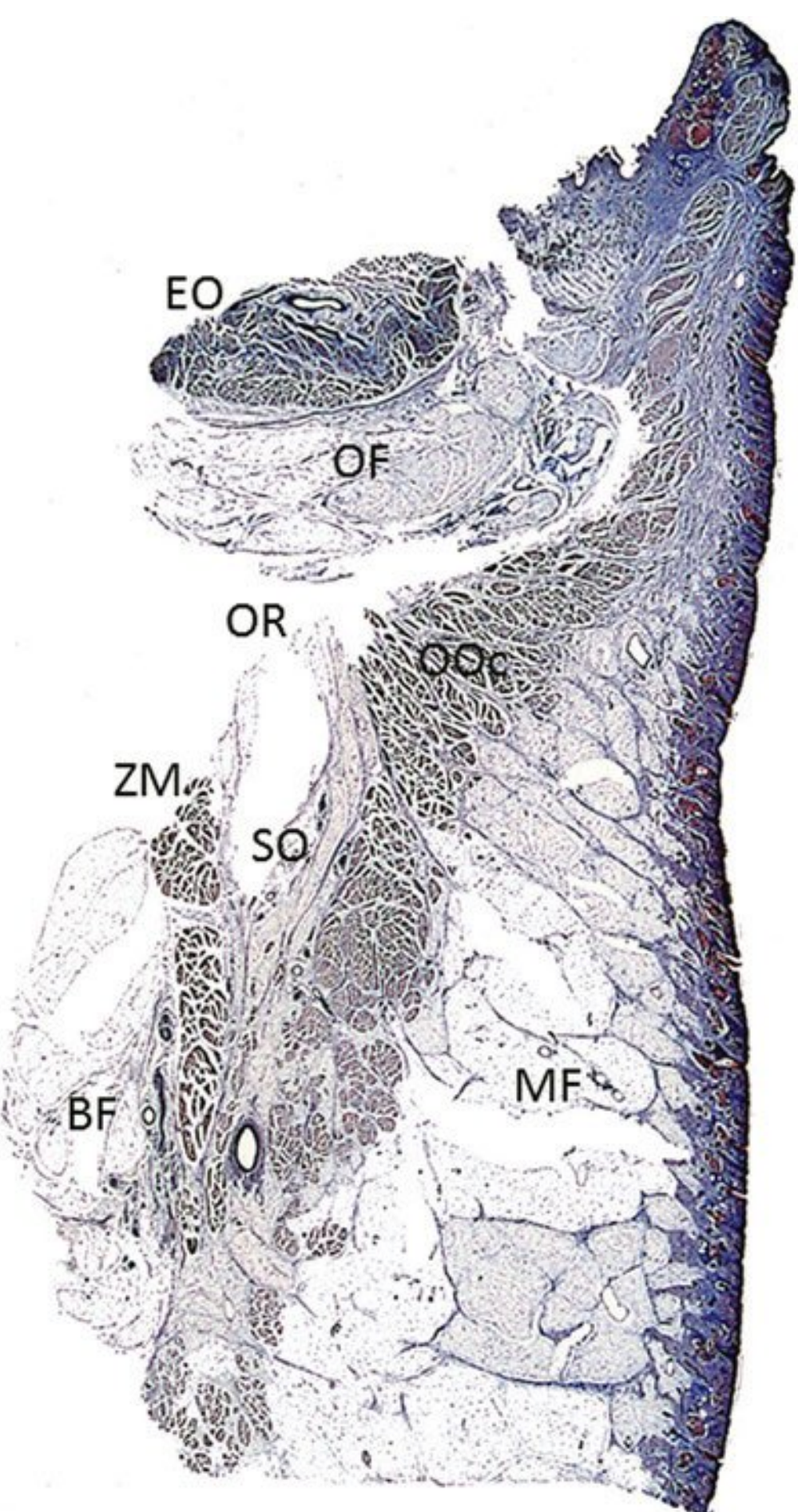


Fig. 11.4 Cross-section of lower eyelid (Masson trichrome stain, $\times 1$). EO, extraocular muscle; MF, malar fat pad; OF, orbital fat; OOc, orbicularis oculi muscle; SO, suborbicularis oculi fat pad; ZM, zygomatic muscles.

tissue overlying the SMAS layer is the malar fat pad. It is thick in the middle region of the cheek and ends at the orbital rim. The fat pad is vertically long and oval in shape, and its fibrous septa are strongly connected as they course toward the dermis. The fat tissue beneath the orbicularis oculi is the suborbicularis oculi fat pad.

Facial Soft Tissue Layer Deep To the SMAS (Mimetic Muscle Layer and Deep Tissue Layer)

Many structures important to facial function are located in the tissue layer deep to the SMAS, including the mimetic muscles, facial nerve, parotid gland, muscles of mastication, and others. When performing surgical procedures involving the sub-SMAS plane, accurate anatomical knowledge is required to prevent damage to these structures. The main structures encountered

on the floor of the lateral face during sub-SMAS dissection are the parotid gland and the masseter muscles (**Fig. 11.5a**). The parotid masseteric fascia envelops these structures. A part of the buccal fat pad exposed at the anterior masseteric muscle also constitutes the floor of the plane. In the anterior region of the face, the deep layer of the mimetic muscles includes structures such as the levator labii superioris, levator anguli oris, and buccinator muscles (**Fig. 11.5b**). The most important structures in the sub-SMAS plane are the peripheral branches of the facial nerve. The facial nerve runs through the parotid gland after emerging from the external skull base via the stylomastoid foramen, and the branches of the nerve run along the fascia after emerging from the superior, anterior, and inferior borders of the parotid gland. The peripheral branches of the facial nerve (the temporal, zygomatic, buccal, marginal mandibular, and cervical branches, especially the zygomatic and buccal branches) run along the basal floor. In contrast, the temporal, marginal mandibular, and cervical branches rise up to the SMAS plane from the base. These branches innervate the SMAS muscles, mainly the frontalis muscle, depressor anguli oris, platysma, and some others. The sub-SMAS space also contains some fiber bundles that support the facial skin. These fibers from a structure called the retaining ligament, which divides the sub-SMAS space into small compartments. The next section of this chapter describes the main retaining ligaments of the face and the sub-SMAS spaces related to the ligaments.

Mimetic Muscles and Facial Nerve

The details of the mimetic muscles and facial nerve are addressed in other chapters (Chapters 9 and 12).

Parotid Masseteric Fascia

The parotid masseteric fascia is a deep fascia that envelops the parotid gland and masseter muscle. This fascia also covers the parotid duct, the peripheral branches of the facial nerve, and the surface of the buccal fat pad. In its more anterior part, the fascia extends to the deep layer, reaching the elevator muscles of the upper lip. It continues to the deep cervical fascia inferiorly beyond the margin of mandible. Finally, it continues to the temporal fascia (deep temporal fascia) superiorly over the zygomatic arch.⁷

Retaining Ligaments of the Face

Some fibrous structures arising from the basal floor are observed in the sub-SMAS plane. These structures connect to the dermis and play a role in anchoring the facial skin, resisting gravity, and preventing drooping of the facial soft tissue. Loosening of this system causes aging changes of the facial appearance. This anchoring system is based on the retaining ligaments. McGregor first reported the retaining ligament of the face, termed the zygomatic ligament or McGregor's patch. Furnas subsequently summarized the retaining ligaments in 1989¹⁵ and described four retaining ligaments: the zygomatic (McGregor's patch), mandibular, platysma–auricular, and anterior platysma

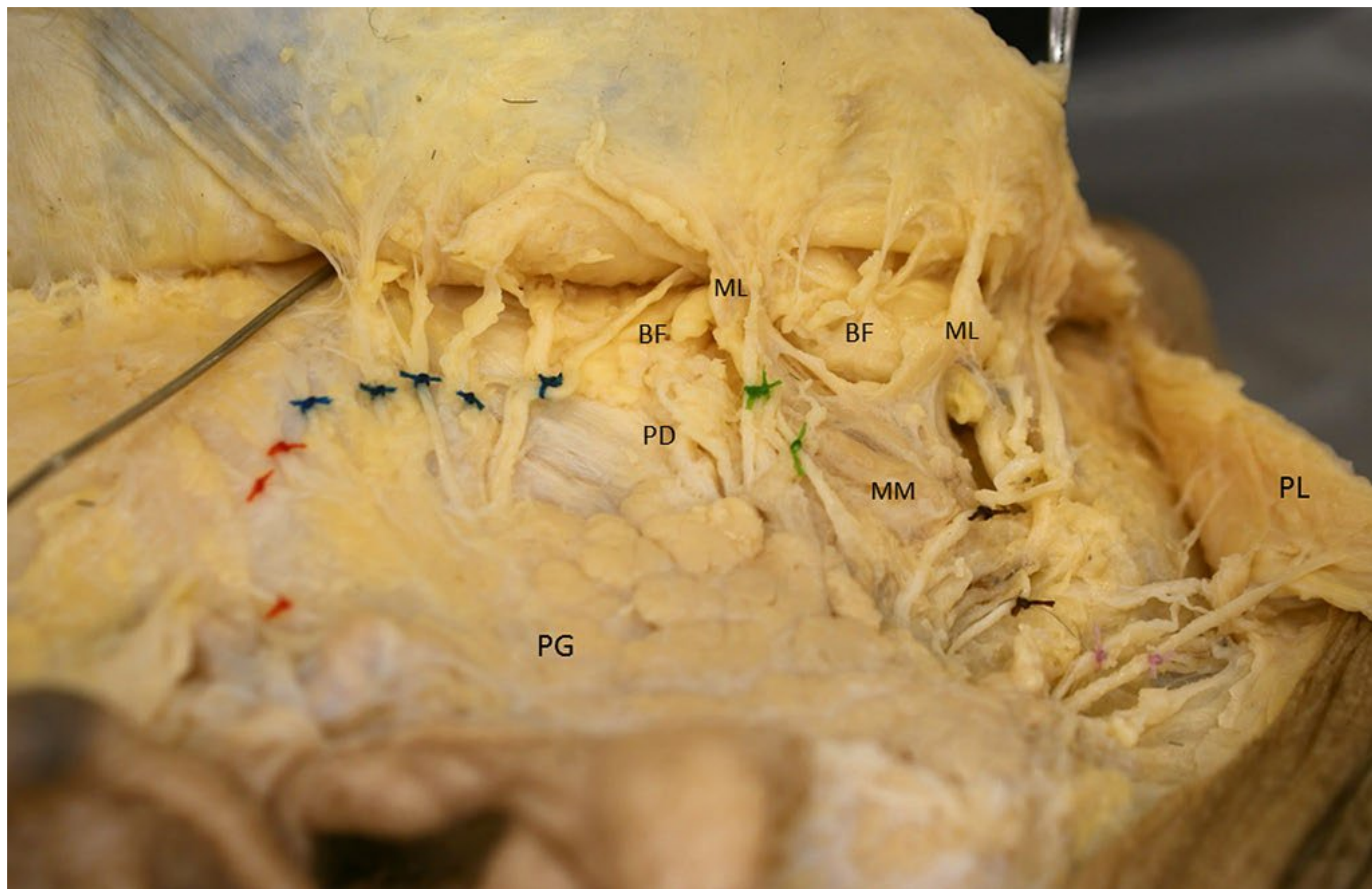
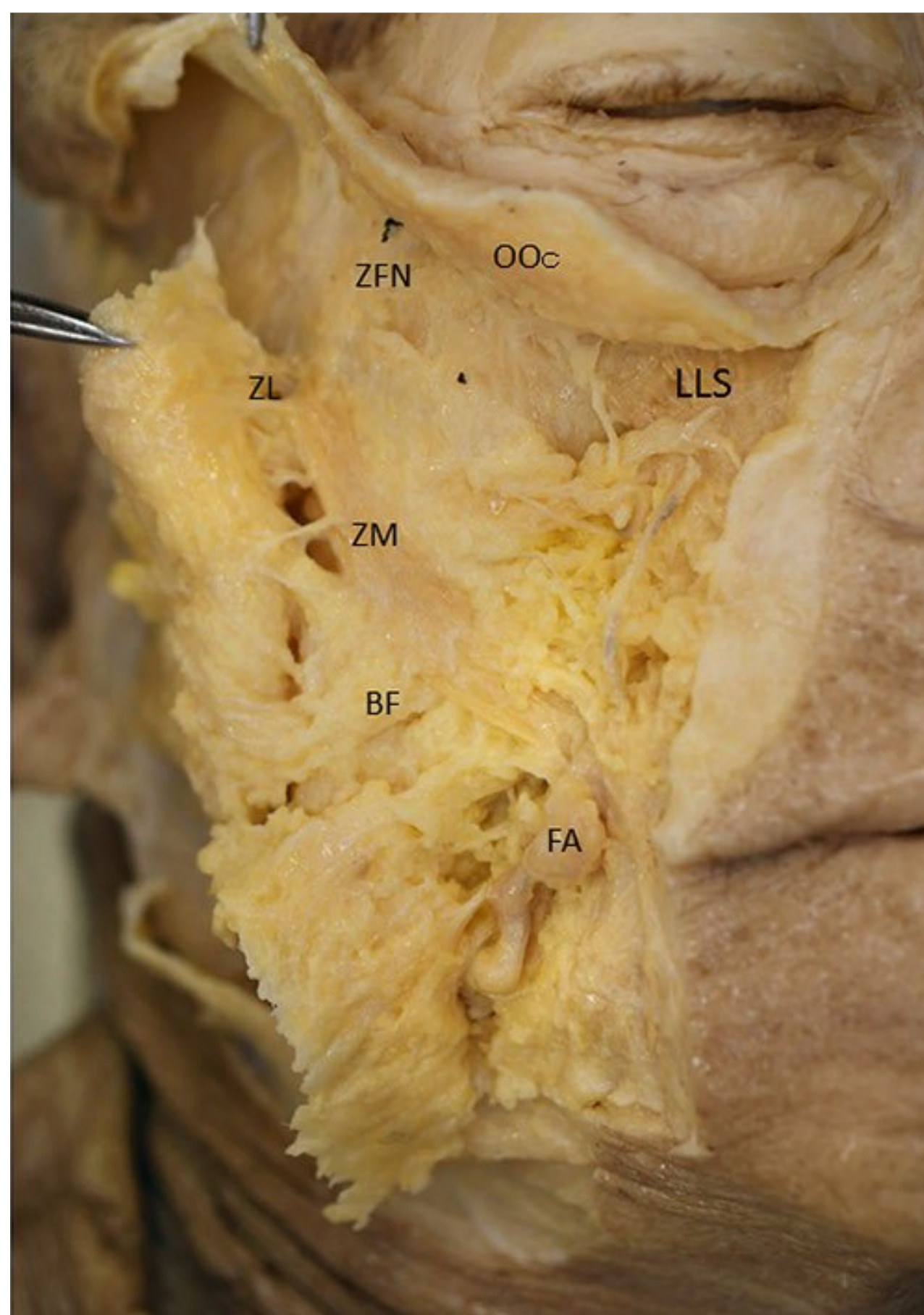
**a****b**

Fig. 11.5 Sub-superficial musculoaponeurotic system (SMAS) plane dissection. **(a)** Lateral part. Right lateral view of the right side of the face. The left side of the picture is the cranial aspect, and the right side is the caudal aspect. The area superior to the zygomatic arch was dissected from the more superficial layer to keep the temporal branch on the basal floor. The platysma was cut along the mandibular border. The branches of the facial nerve were marked as follows: temporal branches, orange string knot; zygomatic branches, dark blue; buccal branches, green; marginal mandibular branches, dark brown; and cervical branches, purple. A bar was inserted into the prezygomatic space. **(b)** Medial part. Frontal view of the right side of the face. BF, Buccal fat pad; FA, facial artery; LLS, levator labii superioris muscle; ML, masseteric ligament; MM, masseteric muscle; OOC, orbicularis oculi muscle; PD, parotid duct; PL, platysma; ZFN, zygomaticofacial nerve; ZL, zygomatic ligament; ZM, zygomaticus major muscle.

ligaments. These four ligaments can be classified into two types based on the tissues from which the ligaments arise. The zygomatic ligament and the mandibular ligament arise from the facial skeleton and insert into the dermis, whereas the platysma–auricular ligament and anterior platysma ligament connect the platysma and dermis. Stuzin et al⁷ also described two types of retaining ligaments, depending on whether they originate from the bone or from other structures. The ligament arising from the bone, which is compatible with the zygomatic and mandibular ligaments described by Furnas,¹⁵ was classified as a true osteocutaneous ligament. Other ligaments provide coalescence between the deep fascia and superficial fascia. The parotid cutaneous and masseteric cutaneous ligaments are also categorized in this group. Moreover, Moss et al¹⁶ described three type of retaining ligaments: true ligaments, adhesions, and septa. True ligaments are almost identical to the so-called true osteocutaneous ligament described by Stuzin,⁷ which arises from either the deep fascia or the periosteum, pierces the SMAS, and distributes the attachment of the ligament to the dermis by spreading like a branching tree. It is located mainly on the medial midface and lower face, and the zygomatic ligament and masseteric ligament are included in this category. Septa are fibrous walls passing between the deep fascia and the SMAS (superficial fascia) and do not adhere to the dermis. This category includes the inferior temporal septum, the superior temporal septum, and the periorbital septum. Finally, adhesions are low-density areas of fibrous or fibrofatty connections between the deep fascia (or pericranium) and the superficial fascia. They also connect the basal tissue and SMAS and do not adhere to the dermis. Adhesions are usually observed in the temporal and forehead regions, excluding the preauricular and parotid regions. Temporal and supraorbital ligamentous adhesions are included in this category.

Forehead and Temporal Region

A retaining ligament in the forehead and temporal region was first reported in detail by Moss et al (Fig. 11.6, Table 11.1).¹⁶ It includes one adhesion and two septa extending radially in the lateral direction. As previously mentioned, all these structures connect the basal tissue and the SMAS.

Temporal Ligamentous Adhesion

The temporal ligamentous adhesion is located at the lateral part of the supraorbital rim, medial to the anterior end of the temporal line. It is triangular shaped; the base of the triangle lies on a parallel line approximately 10 mm from the supraorbital rim and is approximately 15 mm in length, and the apex lies on the temporal line and is 20 mm in height. Three other ligaments in the forehead and the temporal region converge at this point: the superior temporal septum, inferior temporal septum, and supraorbital adhesion.¹⁶ The superior temporal septum continues to the superior apex of the triangular adhesion, and the inferior temporal septum continues to the lateral apex of the base. The supraorbital adhesion is located along the supraorbital rim me-

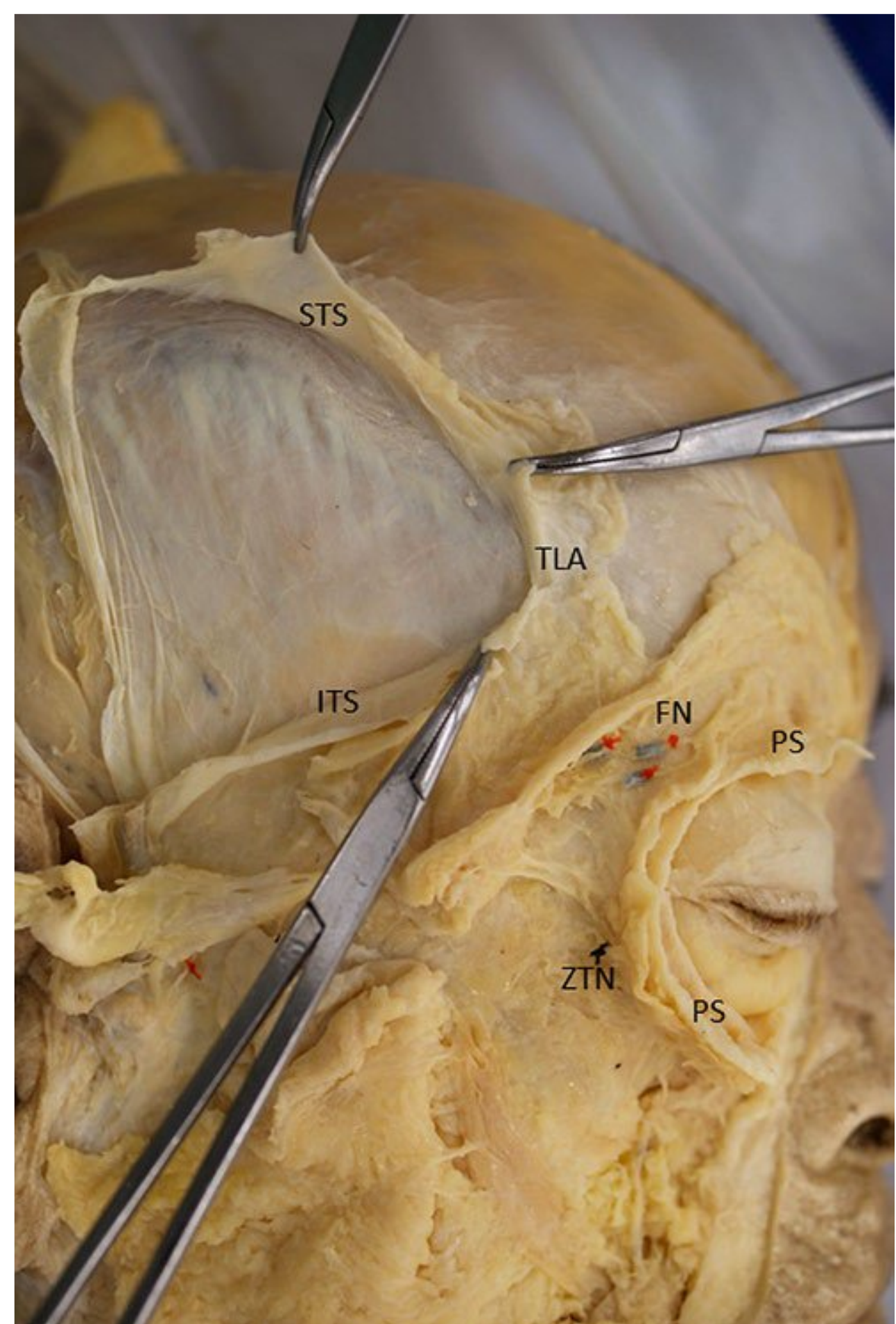


Fig. 11.6 Temporal region. Lateral view of the right side of the face. FN, temporal branches of the facial nerve; ITS, inferior temporal septum; PS, periorbital septum; STS, superior temporal septum; TLA, temporal ligamentous adhesion; ZTN, zygomaticotemporal nerve.

dial to the temporal ligamentous adhesion and continues to the medial apex of the triangle.

Superior Temporal Septum

This superior temporal septum starts from the temporal ligamentous adhesion and runs superiorly and laterally along the superior temporal line. It forms the connection between the periosteum and the transitional zone between the superficial temporal fascia and the galea aponeurotica.¹⁶

Inferior Temporal Septum

The inferior temporal septum starts from the lateral point of the base of the temporal ligamentous adhesion and runs inferiorly and laterally. It is located on an oblique line connecting the temporal ligamentous adhesion and external acoustic meatus. In the vertical section, it arises from the deep temporal fascia

Table 11.1 Retaining ligaments of the forehead and temporal region

Retaining ligament	Location	Type
Temporal ligamentous adhesion	Lateral part of supraorbital rim, medial to the anterior end of the temporal line	Adhesion between the pericranium and the superficial fascia
Supraorbital ligamentous adhesion	Supraorbital rim, medial to the temporal ligamentous adhesion	Adhesion between the pericranium and the superficial fascia
Superior temporal septum	On the superior temporal line	Septum, connecting between the periosteum and superficial fascia (superficial temporal fascia and galea aponeurotica)
Inferior temporal septum	On the line connecting between the temporal ligamentous adhesion and external acoustic meatus	Septum connecting between the deep temporal fascia and superficial temporal fascia

and inserts into the deepest layers of the superficial temporal fascia over the line. The temporal branches of the facial nerve run below the septum.¹⁶

Supraorbital Ligamentous Adhesion

The supraorbital ligamentous adhesion arises from the frontal bone above the orbital rim and extends in two directions to the corrugator supercilii muscle and temporal ligament.¹⁶

Periorbital Region (Tear Trough and Orbicularis Retaining Ligament, Periorbital Septum)

The ligaments in the periorbital region course along the orbital rim, covering almost the entire circumference of the orbit (**Table 11.2**). This ligamentous complex is the first reported true osteocutaneous ligament in the lower eyelid and was described by Wong in 2012.¹⁷ The tear trough–orbicularis retaining ligaments comprise the tear trough ligament, which is located medially, and the orbicularis ligament, which is located laterally. The tear trough ligament arises from the inferior orbital rim of the maxilla and connects the boundary of the palpebral and

orbital parts of the orbicularis oculi. The medial part of this ligament is located at the level of the medial canthal tendon, immediately inferior to the anterior lacrimal crest. It ends around the medial pupil line and continues laterally to the two orbicularis retaining ligaments. The orbicularis retaining ligament continues to the lateral orbital thickening at the level of the lateral canthus and the lateral brow thickening at the superior lateral angle of the orbital rim, finally ending at the origin of the corrugator supercilii at the superior medial part of the orbital rim.

Middle and Lower Facial Region

Beginning with McGregor's description of the zygomatic ligament, the retaining ligaments in the middle and lower facial regions have been reported in detail by many researchers (**Fig. 11.7, Table 11.3**). In this region, the zygomatic ligament and mandibular ligament are so-called true osteocutaneous ligaments that arise from the periosteum and insert into the dermis. With respect to other ligaments, the masseteric cutaneous ligament forms the coalescence between the deep fascia and the superficial fascia; the fibers of this ligament do not reach the dermis. The platysma auricular ligament is an adhesion only located in the superficial layer, and it connects the platysma and the dermis. In this area, many branches of the facial nerve run

Table 11.2 Retaining ligaments of the periorbital region

Retaining ligament	Location	Type
Tear-trough Ligament	Inferior orbital rim from the medial canthal tendon to medial pupil line	Osteocutaneous ligament
Orbicularis retaining ligament	Continuing to the tear-trough ligament Two ligaments run parallel on the inferior orbital rim and end at the lateral canthus	Osteocutaneous ligament
Lateral orbital thickening	Lateral canthus	Osteocutaneous ligament
Lateral brow thickening	Superior lateral angle of the orbital rim and inferior to the temporal ligamentous adhesion The ligament continues to the medial part of the orbital rim along the superior orbital rim	Osteocutaneous ligament



Fig. 11.7 Prezygomatic space. ILS, levator labii superioris; ORN, orbicularis retaining ligament; Zb, zygomatic branch of the facial nerve; ZFN, zygomaticofacial nerve; ZL, zygomatic ligament; ZM, zygomatic major muscle.

Table 11.3 Retaining ligaments of the middle and lower facial region

Retaining ligament	Location	Type
Zygomatic ligament (McGregor's patch)	Usually two bundles About 4.5 cm from the tragus Inferior border of the anterior end of zygomatic arch and behind the insertion of the zygomatic minor	Osteocutaneous ligament
Mandibular ligament	Mandibular bone along a line that is 1cm above the mandibular border and which extends along the anterior third of the mandibular body Immediately in front of the masseter muscle's anterior border.	Osteocutaneous ligament
Masseteric cutaneous ligament	Serous of fibers arising along the anterior border of the masseter muscle	Coalescence between the deep fascia and the SMAS
Platysma cutaneous ligament	Middle and anterior cheek	Aponeurotic connection between the platysma and the dermis
Platysma auricular ligament	Inferior auricular region	Connection between the posterior border of the platysma and the dermis of the inferior auricular region

along the basal floor of the sub-SMAS plane, and some branches run in the vicinity of the ligaments.

Perforating vessels and cutaneous nerves also run with the ligament. Accurate intraoperative identification of these accompanying structures is very important to prevent complications.

Zygomatic Ligament

The zygomatic ligament is a representative true osteocutaneous ligament. It arises from the bone or periosteum and inserts into the dermis, exhibiting treelike spreading. The origin of this ligament is located around the inferior border of the anterior end of the zygomatic arch, behind the insertion of the *zygomaticus minor* muscle, and about 4.5 cm anteriorly from the tragus.

Two ligamentous bundles are usually present; both are similar in size, measuring approximately 3.0 mm wide, 0.5 mm thick, and 6.0 to 8.0 mm long.¹⁵ One of the upper rami of the zygomatic branch of the facial nerve and a branch of the transverse facial artery usually lie directly beneath this ligament.^{15,18} The zygomatic ligament pierces the malar fat pad as it courses toward the overlying dermis and plays a role in supporting the fat pad. As the ligament loosens with aging, the malar fat pad descends and the nasolabial crease deepens. The space on the zygoma anterior to the zygomatic ligament is termed the prezy-

gomatic space. The superior boundary of this space is the orbicularis retaining ligament, and the roof of the space is the orbicularis oculi muscle. The prezygomatic space is filled with the suborbicularis oculi fat pad and provides mobility to the orbicularis oculi muscle during facial expression. The zygomaticotemporal nerve, which is a cutaneous nerve of the face, runs upward toward the dermis, and part of the zygomatic branch of the facial nerve to the orbicularis oculi muscle runs along the roof side of the space.

Mandibular Ligament

Like the zygomatic ligament, the mandibular ligament is also categorized as a true osteocutaneous ligament (Fig. 11.8). Fornas¹⁵ reported that the mandibular ligament originates from the mandibular bone along a line that lies approximately 1 cm above the mandibular border and extends along the anterior third of the mandibular body. The mandibular ligament usually appears as a linear series of parallel fibers. A sensory nerve and cutaneous artery usually accompany and run with the ligaments. Mendelson et al¹⁹ reported that the mandibular ligament is located immediately in front of the anterior border of the masseter muscle; this border is curved and extends anteriorly toward the lower edge of the mandible. The mandibular ligament

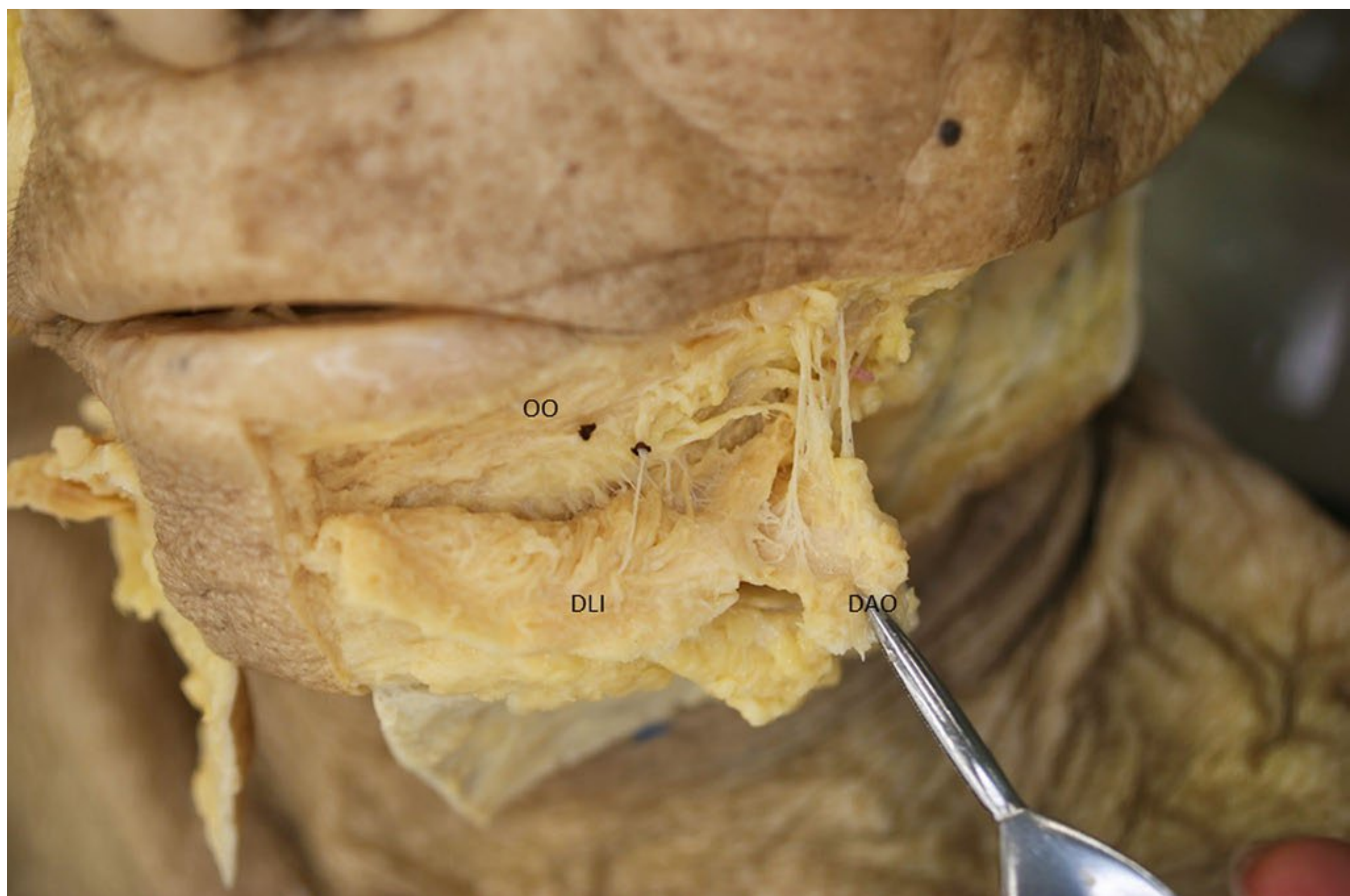


Fig. 11.8 Mandibular area. Frontal view of the left mandibular area. The depressor anguli oris muscle and depressor labii inferioris are elevated. Linear adhesions parallel to the mandibular border are ob-

served. DAO, depressor anguli oris muscle; DLI, depressor labii inferioris, OO, orbicularis oris muscle.

maintains the lateral facial fat in the correct position. Loosening of the ligament with aging causes the fat tissue to droop, forming the facial jowl.

Masseteric Cutaneous Ligament

Stuzin et al⁷ stated that a series of fibers arises along the entire anterior border of the masseter muscle superiorly from the malar region and courses inferiorly to the mandibular border. These fibers play a role in supporting the soft tissues of the medial cheek region. This ligament is categorized as *Stuzin's second type* (coalescence between the deep fascia and the SMAS). The zygomatic branch of the facial nerve runs in close proximity to the masseteric cutaneous ligament.¹⁸ The space located posterior to the masseteric cutaneous ligament is termed the *pre-masseter space*. This space is located between the masseter and platysma and is delineated posteriorly by the posterior border of the masseter and inferiorly by the mandibular border. With

age, the fat tissue in this space bulges onto the mandibular ligament and forms the jowls.¹⁹

Platysma Cutaneous Ligament

Furnas¹⁵ also reported that an aponeurotic connection between the anterior platysma and skin of the middle and anterior cheek is sometimes seen. The incidence of this ligament may not be constant. Ozdemir et al¹⁸ observed this ligament in only a few cases.

Platysma Auricular Ligament

Furnas¹⁵ described the platysma auricular ligament as follows. The posterior border of the platysma recedes into an intricate fascial condensation that often attaches intimately to the overlying skin. This structure provides firm anchorage between the platysma and the dermis of the inferior auricular region.

References

1. Nakajima H, Imanishi N, Minabe T, Kishi K, Aiso S. Anatomical study of subcutaneous adipofascial tissue: a concept of the protective adipofascial system (PAFS) and lubricant adipofascial system (LAFFS). *Scand J Plast Reconstr Surg Hand Surg* 2004;38(5):261–266 [PubMed](#)
2. Mitz V, Peyronie M. The superficial musculo-aponeurotic system (SMAS) in the parotid and cheek area. *Plast Reconstr Surg* 1976; 58(1):80–88 [PubMed](#)
3. Gosain AK, Yousif NJ, Madiedo G, Larson DL, Matloub HS, Sanger JR. Surgical anatomy of the SMAS: a reinvestigation. *Plast Reconstr Surg* 1993;92(7):1254–1265 [PubMed](#)
4. Gardetto A, Dabernig J, Rainer C, Piegger J, Piza-Katzer H, Fritsch H. Does a superficial musculoaponeurotic system exist in the face and neck? An anatomical study by the tissue plastination technique. *Plast Reconstr Surg* 2003;111(2):664–672, discussion 673–675 [PubMed](#)
5. Jost G, Levet Y. Parotid fascia and face lifting: a critical evaluation of the SMAS concept. *Plast Reconstr Surg* 1984;74(1):42–51 [PubMed](#)
6. Ghassemi A, Prescher A, Riediger D, Axer H. Anatomy of the SMAS revisited. *Aesthetic Plast Surg* 2003;27(4):258–264 [PubMed](#)
7. Stuzin JM, Baker TJ, Gordon HL. The relationship of the superficial and deep facial fascias: relevance to rhytidectomy and aging. *Plast Reconstr Surg* 1992;89(3):441–451 [PubMed](#)
8. Freilinger G, Gruber H, Happak W, Pechmann U. Surgical anatomy of the mimic muscle system and the facial nerve: importance for reconstructive and aesthetic surgery. *Plast Reconstr Surg* 1987; 80(5):686–690 [PubMed](#)
9. Ferreira LM, Hochman B, Locali RF, Rosa-Oliveira LM. A stratigraphic approach to the superficial musculoaponeurotic system and its anatomic correlation with the superficial fascia. *Aesthetic Plast Surg* 2006;30(5):549–552 [PubMed](#)
10. Thaller SR, Kim S, Patterson H, Wildman M, Daniller A. The submuscular aponeurotic system (SMAS): a histologic and comparative anatomy evaluation. *Plast Reconstr Surg* 1990;86(4):690–696 [PubMed](#)
11. Fodor PB. From the panniculus carnosum (PC) to the superficial fascia system (SFS). *Aesthetic Plast Surg* 1993;17(3):179–181 [PubMed](#)
12. Bergman RA, Thompson SA, Afifi AK, Saadeh FA. Compendium of human anatomic variation: text, atlas, and world literature. Baltimore: Urban & Schwarzenberg; 1988:30.
13. Wilhelm BJ, Mowlavi A, Neumeister MW. The safe face lift with bony anatomic landmarks to elevate the SMAS. *Plast Reconstr Surg* 2003;111(5):1723–1726 [PubMed](#)
14. Lei T, Cui L, Zhang YZ, et al. Anatomy of the transversus nuchae muscle and its relationship with the superficial musculoaponeurotic system. *Plast Reconstr Surg* 2010;126(3):1058–1062 [PubMed](#)
15. Furnas DW. The retaining ligaments of the cheek. *Plast Reconstr Surg* 1989;83(1):11–16 [PubMed](#)
16. Moss CJ, Mendelson BC, Taylor GI. Surgical anatomy of the ligamentous attachments in the temple and periorbital regions. *Plast Reconstr Surg* 2000;105(4):1475–1490, discussion 1491–1498 [PubMed](#)
17. Wong CH, Hsieh MKH, Mendelson B. The tear trough ligament: anatomical basis for the tear trough deformity. *Plast Reconstr Surg* 2012;129(6):1392–1402 [PubMed](#)
18. Ozdemir R, Kilinç H, Unlü RE, Uysal AC, Sensöz O, Baran CN. Anatomicohistologic study of the retaining ligaments of the face and use in face lift: retaining ligament correction and SMAS plication. *Plast Reconstr Surg* 2002;110(4):1134–1149 [PubMed](#)
19. Mendelson BC, Freeman ME, Wu W, Huggins RJ. Surgical anatomy of the lower face: the premasseter space, the jowl, and the labiomandibular fold. *Aesthetic Plast Surg* 2008;32(2):185–195 [PubMed](#)

12 Mimetic Muscles

Hee-Jin Kim

Layers of the Face

Basic facial soft tissues are composed of five layers: (1) skin, (2) subcutaneous layer, (3) superficial musculoaponeurotic system (SMAS), (4) retaining ligaments and spaces, and (5) periosteum and deep fascia (Fig. 12.1). Except for the auricles and nose alae supported by the cartilage under the skin, facial skin glides over the loose areolar connective tissue layer. Facial skin contains numerous sweat and sebaceous glands.

Superficial fascia or subcutaneous connective tissue contains unequal amounts of fat tissue, and these fat tissues make the facial contour smooth between the skin and underlying facial musculatures. In some areas, the fat tissues are broadly distributed. The buccal fat pad forms the bulge over the cheek and continues to the scalp behind the orbit. Facial vessels, trigeminal nerve branches, facial nerve branches, and the muscles of facial expression are contained within the subcutaneous tissue.

The superficial musculoaponeurotic system (SMAS) is the superficial fascial structure composed of muscle fibers and superficial facial fascia. This musculofascial unit is manipulated during facial cosmetic surgery, especially rhytidectomy, and the SMAS extends from the platysma to the galea aponeurotica and is continuous with the temporoparietal fascia and galea. It connects to the dermis through vertical septa.

Facial Expression Muscles and their Actions

Facial muscles are attached to the facial skeleton or membranous superficial fascia beneath the skin (Fig. 12.2). The topography of the facial muscles varies between males and females, as well as between individuals of the same sex. It is important to define muscle shapes, their associations with the skin, and their relative functionality to explain the unique expressions people can make. The face is divided into several distinct areas: (1) forehead and temporal region, (2) periorbital region covered by the eyelid, (3) external nose, (4) anterior cheek region (upper lip elevators), (5) perioral region, and (6) chin region and superficial neck.

Generally, the facial muscles are found within the superficial fascia or subcutaneous tissue layer of the face. These muscles are involved in two different roles: (1) control of the opening of the orifices as dilators or sphincters and (2) in the formation of various facial expressions by moving the overlying facial skin. Most of the facial expression muscles originate from the bones of the face or fascia and are inserted into the facial skin. Therefore, facial skin by the contraction of the facial muscle produces the various expressions, such as sadness, anger, joy, fear, disgust, and surprise.

Forehead and Temporal Region

The occipitofrontalis muscle (OFM) is the widest and largest constituent of the complex of muscles underlying the upper face and occipital area, covering from the highest nuchal line to the eyebrows, but the intensity of contractions along that width can differ substantially from person to person. The frontal belly of the OFM is the frontal portion of this muscle, and it arises from the galea aponeurotica and is inserted into the frontal skin above the eyebrow. During anxiety or surprise, this muscle contracts and produces the transverse wrinkles of the forehead.

The OFM is roughly rectangular and has bilateral symmetry; its muscle fibers are approximately vertically oriented and attached to the superficial fascia of the skin in the region where it meets the muscles above the glabella and brow ridges. Its attachment is broader and has longer fibers than the occipitalis. The OFM lies at a uniform depth beneath the skin of the forehead (3–5 mm on average), although that depth can differ considerably (2–7 mm) between individuals and is 1 mm greater on average in men than in women. The OFM does not attach to

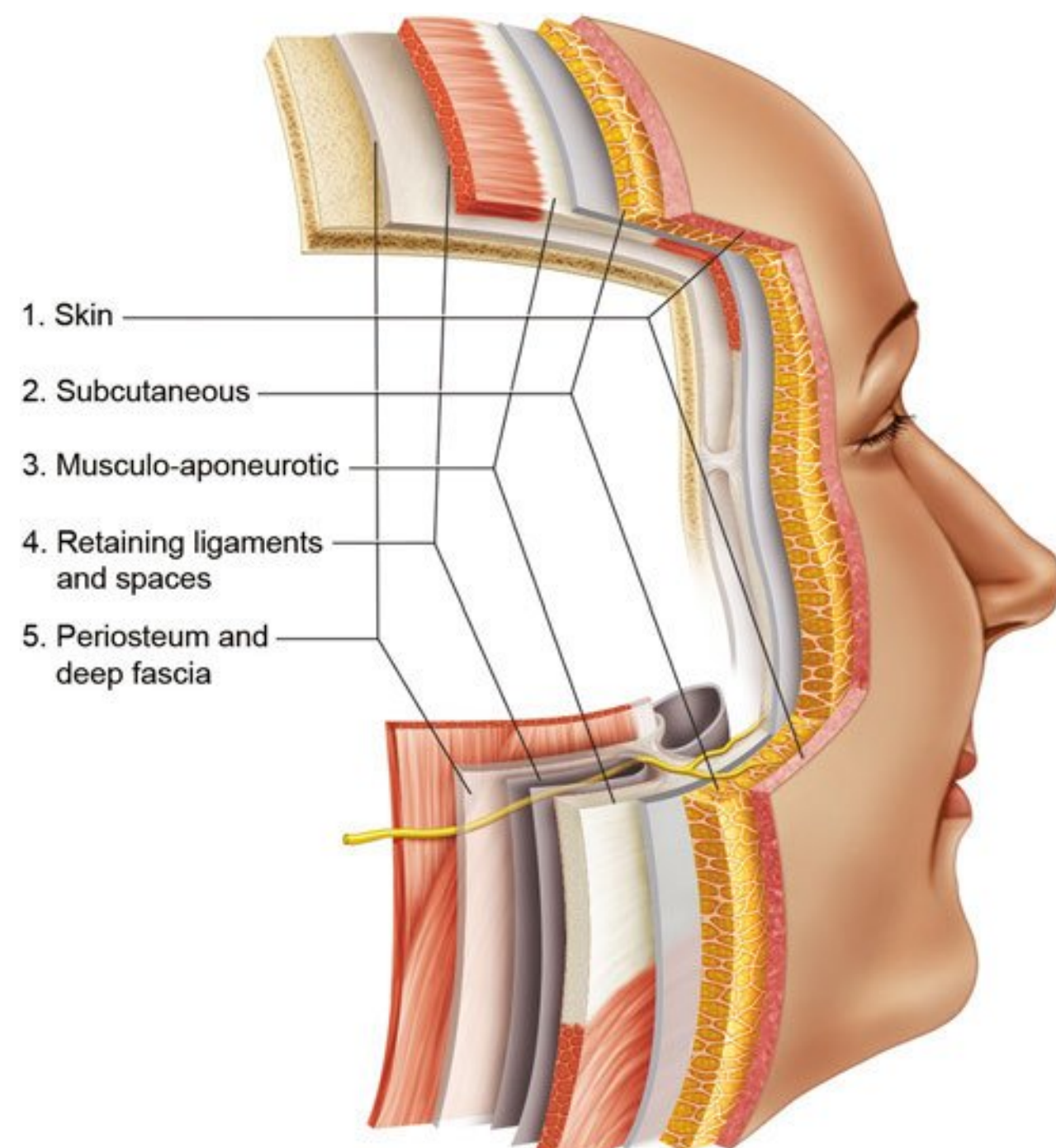


Fig. 12.1 Layers of the face. Facial soft tissues are composed of five layers: (1) skin, (2) subcutaneous layer, (3) superficial musculoaponeurotic system (SMAS), (4) retaining ligaments and spaces, and (5) periosteum and deep fascia.

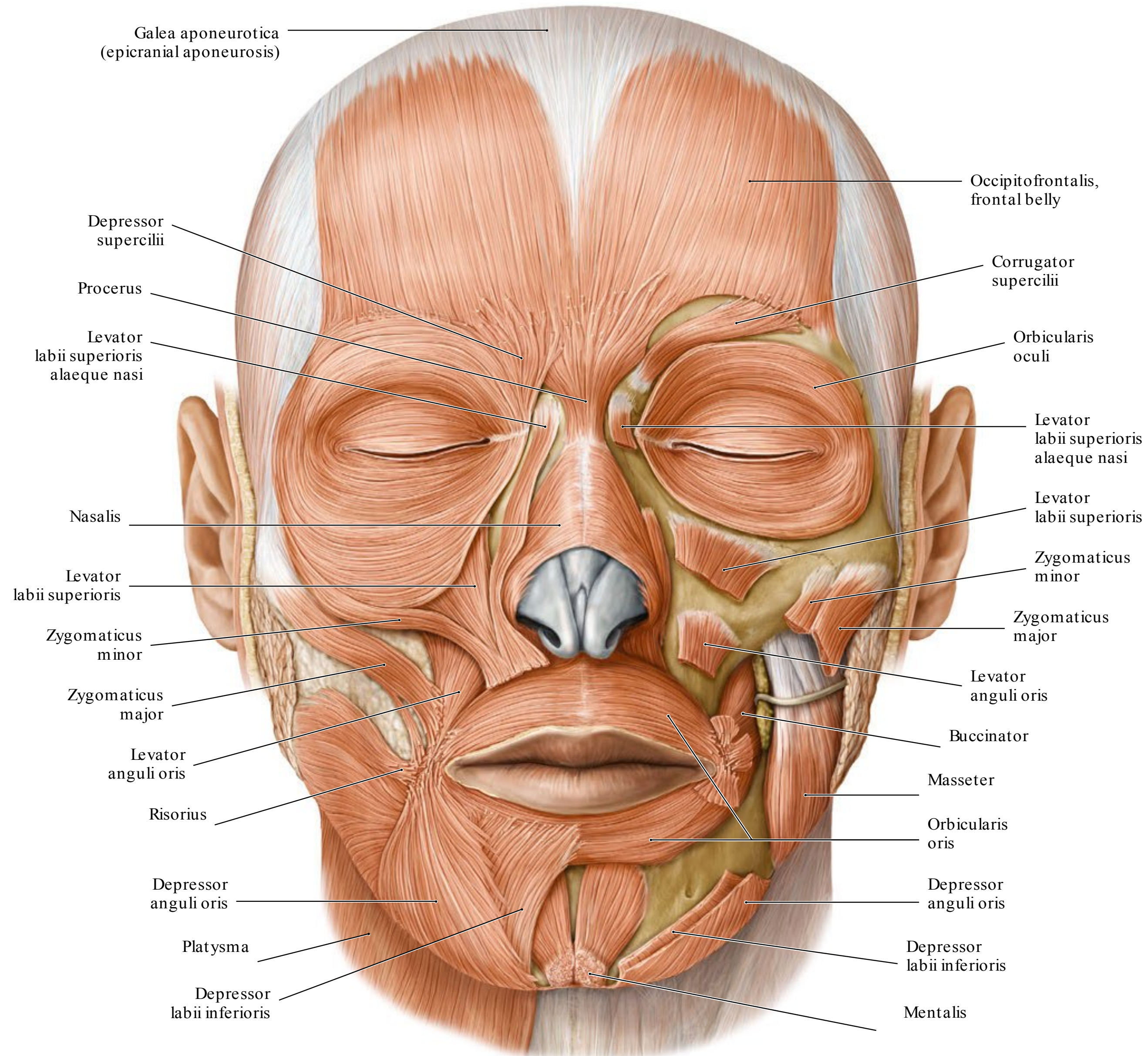


Fig. 12.2 Facial muscles. (a) Anterior view. The superficial layer of the muscle is shown on the right half of the face, and the deep layer is shown on the left half.

a bony structure. Instead, its medial fibers continue along procerus, intermediate fibers along the corrugator supercilii (CS) and orbicularis oculi (OOc), and lateral fibers along the OOc over the zygomatic process (Fig. 12.3). The temporoparietalis is located between OFM and the anterior and superior auricular muscles, and its development and shape vary.

Periorbital Region

The shape of the eye is clearly framed by the moving muscles surrounding it, which thus determine the basic facial expression. The OOc muscle is located around the orbit and into the

eyelids, anterior temporal region, infraorbital cheek, and superciliary region. The OOc is a broad, flat, elliptical muscle composed of three portions: (1) an orbital portion that concentrically encircles the orbit, including the depressor supercilii; (2) a palpebral portion, with finer and paler muscle fibers than the orbital part, that sweeps across the eyelids anterior to the orbital septum and arises from the medial palpebral ligament; and (3) a lacrimal portion that arises from the upper part of the lacrimal crest and passes laterally behind the nasolacrimal sac (Fig. 12.4).

The main function of the OOc is to mediate eye closure. The OOc has many neighboring muscles: the corrugator supercilii muscle (CSM), procerus, frontal belly of the OFM, zygomaticus major (ZMj), and zygomaticus minor (ZMi) muscles) and various

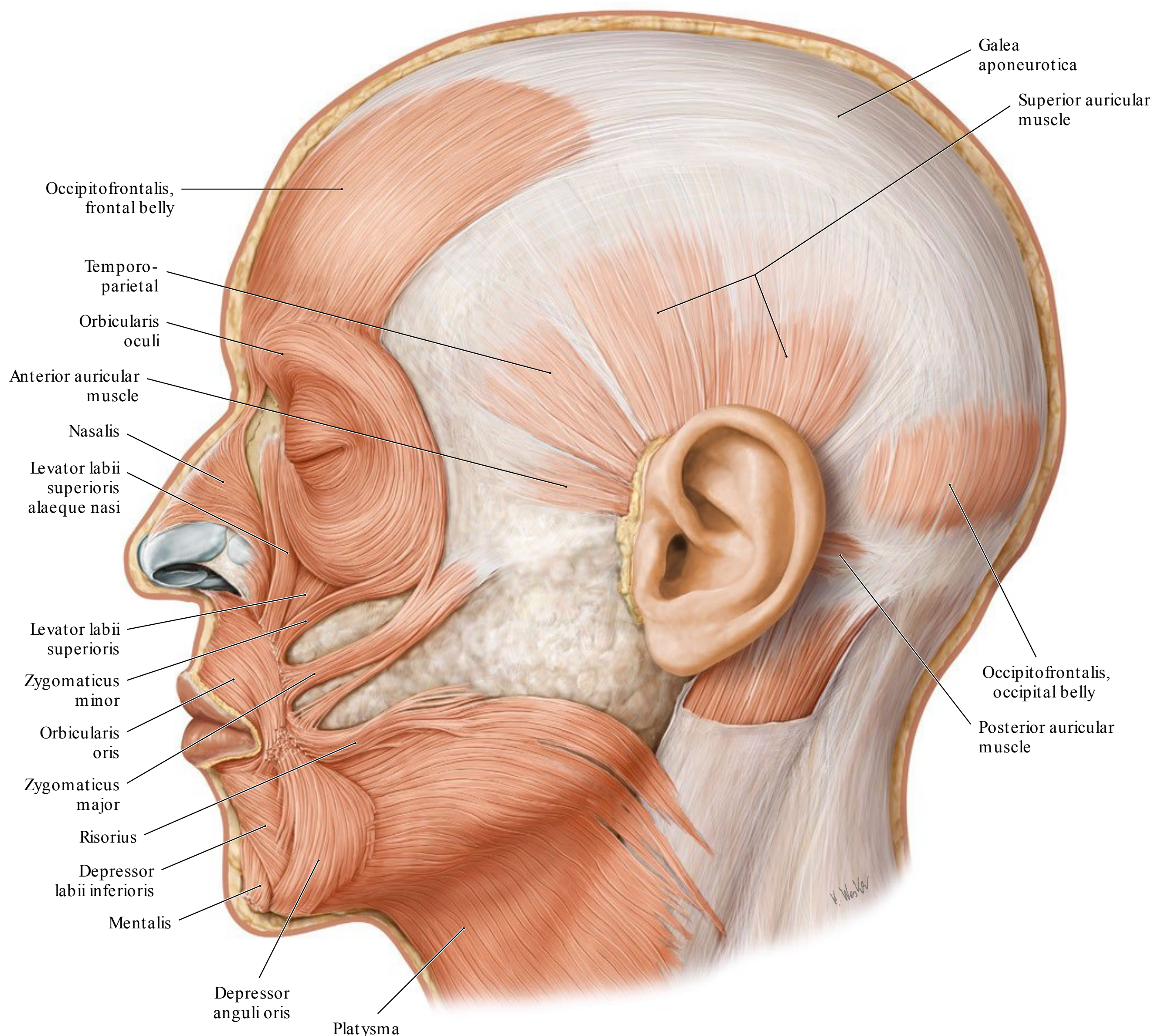


Fig. 12.2 (continued) (b) Left lateral view. (Reproduced from THIEME Atlas of Anatomy, Head and Neuroanatomy. © Thieme 2010, Illustrations by Karl Wesker.)

direct and indirect muscular connections between the OOC and the surrounding musculature; these may participate in the formation of various facial expressions. A lateral muscular band (malaris muscle) can be observed in 54.1% of Asians. It originates from the superficial temporal fascia and terminates in three different regions: at the zygomatic arch (27.9%), at the cheek region (18%), and at the angle of the mouth (8.2%). It plays a role in facial animation and dimple formation. Medial muscular bands of the orbital portion of OOC are found in 65.6% of Asians. This muscular band helps to prevent further drooping of the OOC. On the other hand, there are many muscular connections between the OOC and ZMi in 88.5% of the cases; this particular anatomical feature may play a specific role in facial expression.

The CSM originates from the periosteum on the frontal bone and merges into the frontal belly of the occipitofrontalis muscle (Fb). The CSM consists of distinct two bellies: transverse and oblique. The origin of the transverse belly of the CSM is more superior and lateral than the origin of the oblique belly, and most are attached into the Fb and the superolateral orbital part of the OOC. The transverse belly is located more deeply and is more horizontal than the oblique belly. The transverse belly is more or less triangular in shape with its inferomedial part as the apex. The oblique belly is classified into two different types: narrow vertical or broad triangular types.¹ The CSM with the OFM cause wrinkling of the skin at the glabella (**Fig. 12.5**).

The depressor supercilii (DS) is a fan or triangular shaped muscle that originates from the frontal process of the maxilla

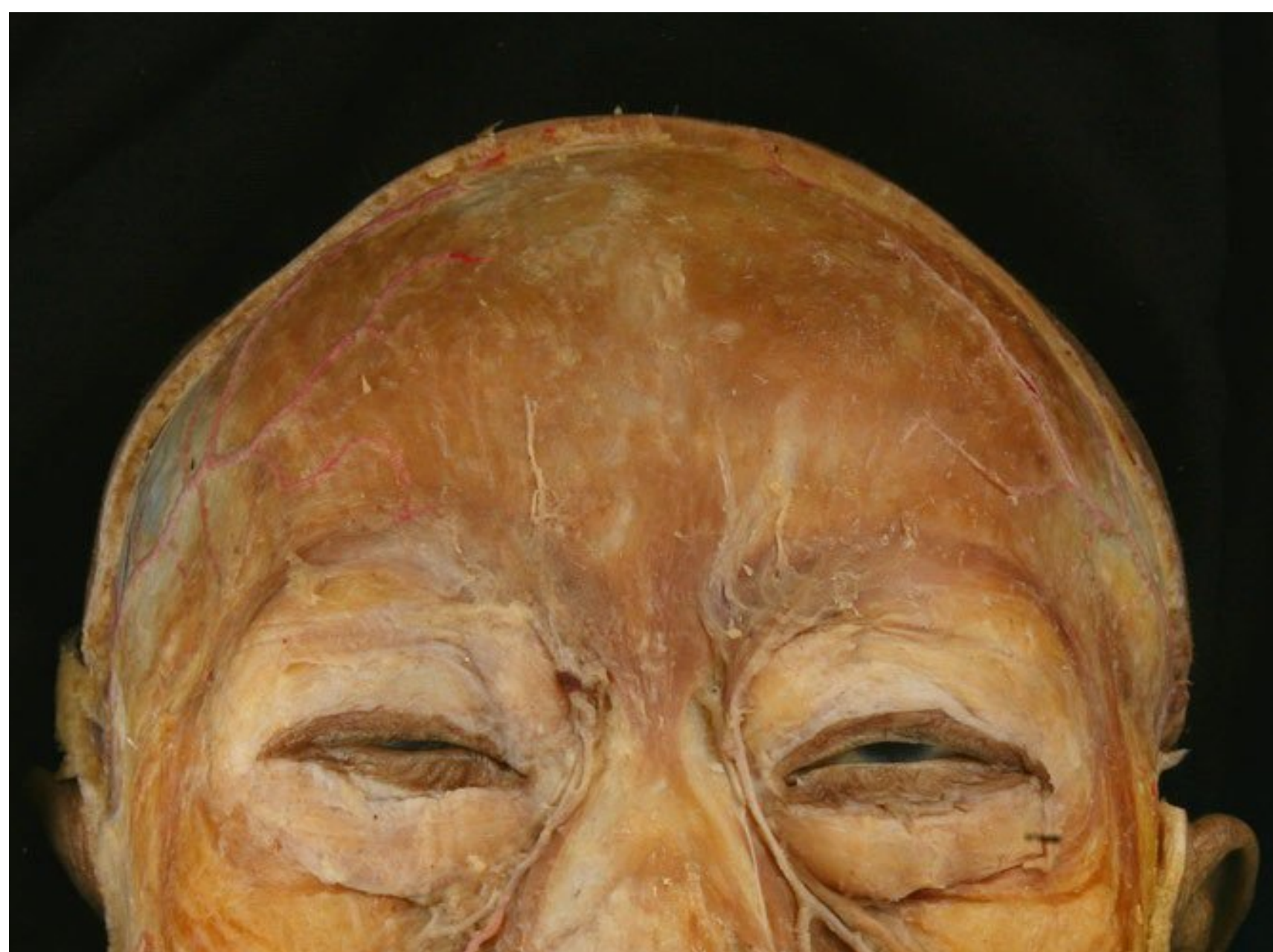


Fig. 12.3 Frontalis. The frontal belly of the occipitofrontalis muscle is the anterior portion of this muscle, and it arises from the galea aponeurotica and is inserted into the frontal skin above the eyebrow.



Fig. 12.4 Orbicularis oculi muscle (left side of the face). The orbicularis oculi muscle is located around the orbit and into the eyelids, anterior temporal region, infraorbital cheek and superciliary region.

and the nasal portion of the frontal bone 1 cm above the medial palpebral ligament. At the glabella, DS mixes with fibers of the CS is intermingled with the medial fibers of the OOC. Some muscular fibers of the DS originate from the lacrimal sac, and it plays a role in movement of the eyebrow.

External Nose Region

The nose is a dynamic structure; nasal musculature moves the nasal cartilages and plays an important role in nasal physiology. The transverse part of the nasalis, originating from the maxilla, is thin, flat, and has a triangular shape. It is located deep in the alar part and ascends to the dorsum of the nose. The transverse part of the nasalis, which is C-shaped, surrounds the posterior nasal aperture and ascends anteriorly toward the dorsum of the nose (Fig. 12.6). This transverse part lies between the lateral nasal cartilage and the greater alar cartilage and receives some muscle fibers from the superficial layer of levator labii superioris alaqueae nasi muscle (LLSAN).

The procerus muscle originates from the fascia covering the dorsum of the nose and inserts superiorly into the skin of the glabella. The contraction of procerus makes the transverse wrinkles on the radix of the nose.

The alar part of nasalis originates with the transverse part of the nasalis from the maxilla and inserts into the alar facial crease and the adjacent deep surface of the external skin of the alar lobule.

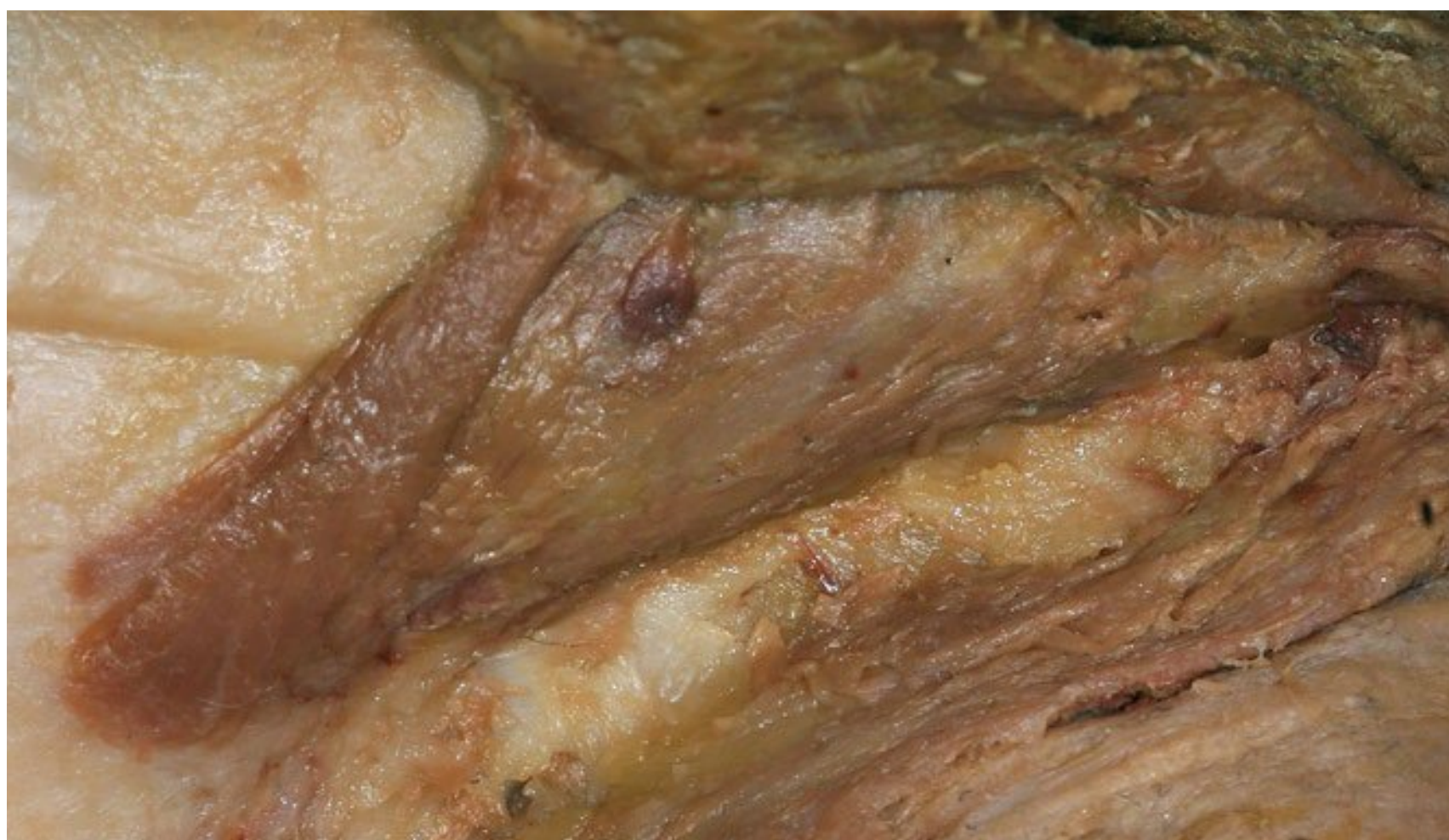


Fig. 12.5 Corrugator supercilii muscle. The corrugator supercilii muscle originates from the periosteum on the frontal bone and merges into the frontal belly of the occipitofrontalis muscle.

The dilator naris vestibularis muscle is located between the external and vestibular skin of the alar lobule.² Its muscle fibers radiate along the dome-shaped nasal vestibule. The dilator naris anterior muscle originates from the frontal surfaces of the lateral half of the lateral crus and the accessory alar cartilage adjacent to the lateral crus.

The depressor septi muscle is located in the deep aspect of the lip, continues to the maxillary incisive fossa, and inserts to the mobile portion of the nasal septum. It participates in enlarging the naris by pulling down the tip of the nose.

Anterior Cheek Region (Upper Lip Elevators)

The appearance of the lip framework is determined by the activity of various facial muscles, such as the levator labii superioris (LLS), the LLSAN, and the ZMi/ZMj (Fig. 12.7). Among these, the LLS, the LLSAN, and the ZMi determine the amount of lip elevation that occurs during smiling or sadness.

The LLS originates from the orbital rim of the maxilla and zygomatic bone above the infraorbital foramen and inserts into the upper lip area. The LLS is rectangular in 83% and trapezoid in 7%.³ Its medial fibers are attached to the deep surface of the alar facial crease between the lateral slip of LLSAN and ZMi and are mainly intermingled with the alar part of the nasalis. Some of the deeper muscle fibers of the LLS extend to the vestibular skin of the nasal lobule.

The LLSAN originates from the frontal process of the maxilla and inserts into the upper lip and the ala of the nose. The LLSAN is divided into medial and lateral slips and then is divided into two layers, which are superficial and deep to the levator labii

superioris muscle (LLS), respectively. The medial slip is inserted into the alar cartilage, and the lateral slip continues to the lateral part of the upper lip, then to the LLS and the orbicularis oris (OOr). The superficial layer of LLSAN descends on the LLS, and the deep layer is located deep to the LLS. The deep layer of



Fig. 12.6 Nasalis (right side of the face).



Fig. 12.7 Upper lip elevators (left side). The levator labii superioris (LLS), the levator labii superioris alaeque nasi (LLSAN), and the zygomaticus minor (ZMi) have a role in lip elevation that occurs during smiling or sadness.

LLSAN originates from the superficial layer of LLSAN and the frontal process of the maxilla. It inserts between the levator anguli oris and the OOr muscles. The transverse part of the nasalis originates from the maxilla and ascends passing posterior to the superficial layer of LLSAN (65%), or it originates as two muscle bellies from the maxilla and the upper half of the alar facial crease (35%).⁴

The ZMi originates from the zygomatic bone behind the zygomaticomaxillary suture and inserts into the skin and the upper lip. It is separated superiorly by a narrow triangle-shaped space from the LLS, and it blends with the muscle inferiorly. Besides the bony origin of the ZMi, the lateral belly of the orbital part of the OOr blends with the ZMi in 88.5% of cases. In addition, ZMi attaches into both the upper lip and the ala of the nose in 28% of cases.

The LLSAN and ZMi cover the insertion of the LLS partially or entirely, and these three muscles converge on the area lateral to the ala of the nose. The levator muscles of the upper lip pass through the OOr and participate in the formation of the nasolabial fold.

Perioral Region

In the perioral region, the muscles for facial expression are arranged in four layers based on their origins (**Fig. 12.8**). The individual muscles are arranged in the superficial (first, second, and third) layer and the deepest (fourth) layer, and it has been documented that the ZMj is located in the superficial layer. The deepest, fourth layer is composed of the levator anguli oris, mentalis, and buccinator muscles.

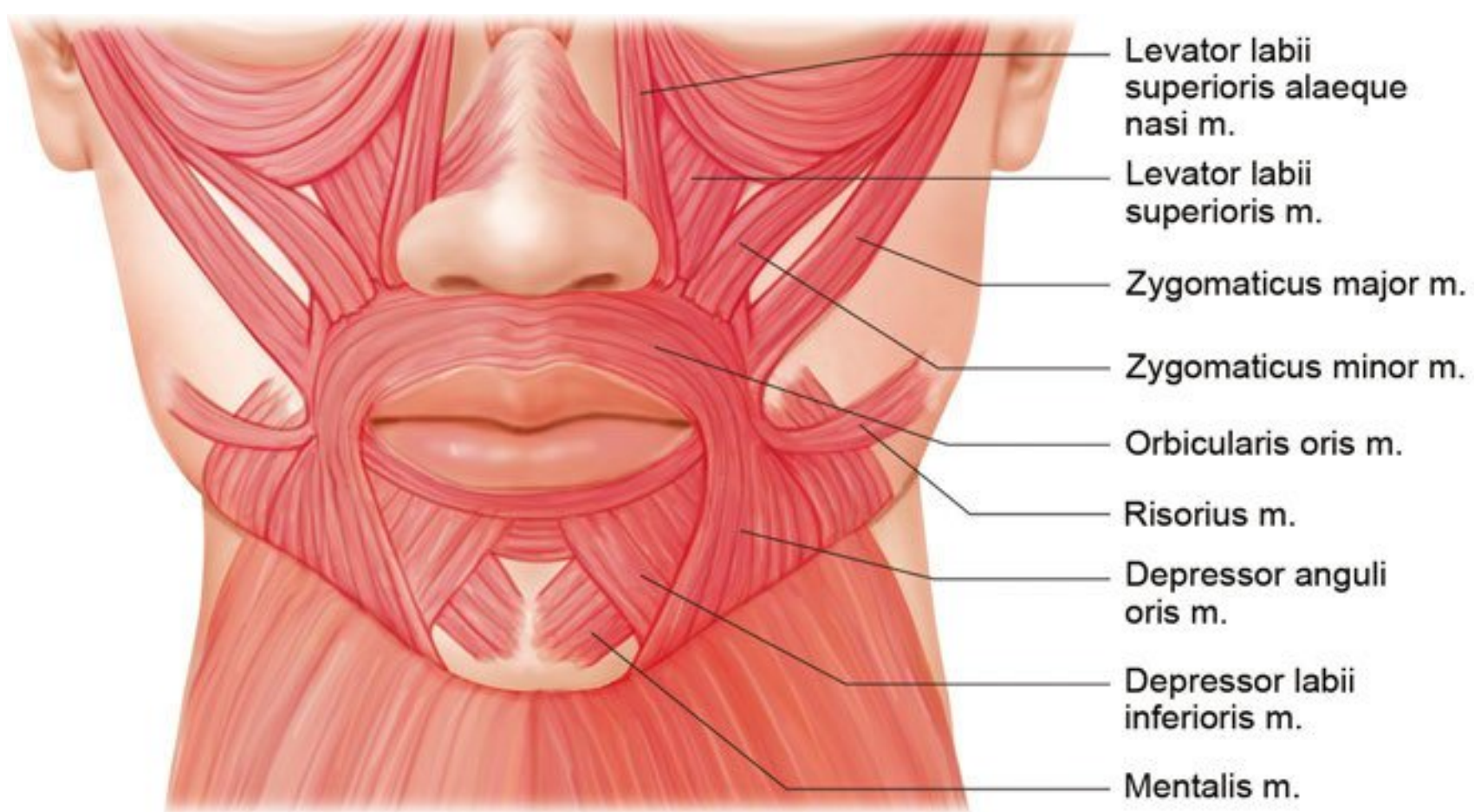
As a constrictor of the mouth, the OOr encircles the mouth and is located within the upper and lower lips. Most muscle fibers originate from the other facial muscles converging to the mouth. A part of intrinsic muscle fibers arise from the labial alveolar bone covering the upper and lower incisors. This muscle acts in closing the mouth and protrusion of the lips in the manner of a sphincter. The OOr divides into four quadrants, which further divide into a pars peripheralis and a pars marginalis. Pars peripheralis is a lateral stem attached to the labial side. Most originate from the modiolus itself, but some continue from the other modiolar muscles. Pars marginalis is narrow and is connected to the red lip margin. It is involved with speech and production of musical tones. Its medial fibers interface with the contralateral pars marginalis and attaches to the dermis of the lip.

The levator anguli oris muscle (LAO) originates from the canal nine fossa below the infraorbital foramen and inserts into the modiolus. This muscle intermingles with the OOr, ZMj, and DAO and inserts to the modiolus, thereby raising the corner of the mouth. Infraorbital vessels and a nervous plexus lie between the LAO and LLS.

The depressor anguli oris muscle (DAO) is a triangular muscle on the most superficial layer of the perioral muscles originating from the external oblique line of the mandible. Its continuation forms an oblique line below and lateral to the depressor labii inferioris muscle, and it converges into a narrow fasciculus that blends at the modiolus with the OOr and risorius muscles. Some of its fibers continue below the mental tubercle and cross the midline. Consequently, it interlaces with its contralateral mate creating the transversus menti muscle. The medial border of the DAO overlaps with DLI and its lateral border is adjacent to the risorius, ZMj, and platysma muscles.

The depressor labii inferioris (DLI) originates from the lower part of the oblique line of the mandible between the symphysis menti and the mental foramen and inserts into the lower lip with the paired muscle from the opposite site and with OOr. DLI passes upwards and medially into the skin and mucosa of the lower lip.

The ZMj originates from the facial surface of the zygomatic bone. This muscle descends inferomedially, blends with the OOr, and terminates at the modiolus. The insertion patterns of the zygomaticus major are variable, and the existence of distinct muscle fibers of the ZMj passing deep to the LAO is not always observed. A bifid ZMj, one type of ZMj, separates into two portions, and the LAO passes between the two heads. The ZMa inserts around the modiolar region, and the muscle fibers are interlaced with the buccinator, LAO, and OOr. Even though all these muscles converge and are interdigitated in the modiolar

**Fig. 12.8** Perioral region.

region, knowledge of the relationship between the deep muscle band of the ZMj and the buccinator is crucial in the understanding of facial animation. In every case, the main insertion of the deep muscle band of the ZMj is at the anterior margin of the buccinator and its fascia. This anatomical relationship provides the synchronous pulling of the anterior region of the buccinator with the corresponding buccal mucosa outward and upward to create a smile. The outward movement of the anterior margin of the buccinator and the contraction of the lip elevators naturally compress the cheek fat mass above the nasolabial fold, and this cheek mass becomes quite prominent. These muscle actions also widen the nasal width because of the expansion of the midface contour, followed by the muscle pulling upward and laterally.

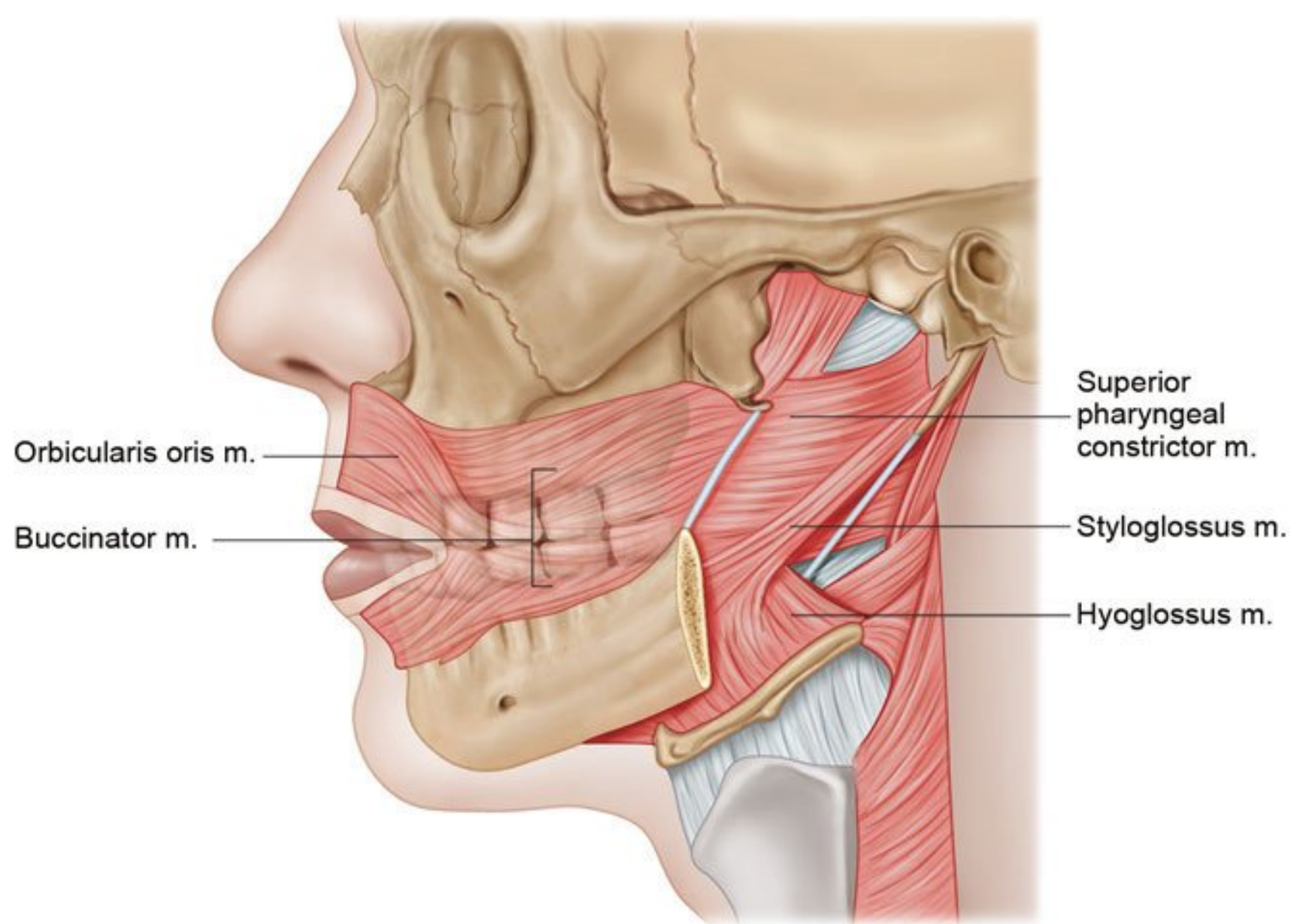
The risorius is a thin and slender muscle and is usually located 20 to 50 mm lateral to the cheilion and 0 to 15 mm below the intercheilion horizontal line. Most risorius muscle fibers originate from the SMAS and some fibers from the parotid fascia or masseteric fascia. In some cases, this muscle receives the upper muscle fibers of platysma. It terminates in the modiolus region and acts by pulling the corner of the mouth when smiling. Risorius can be categorized into three common types: zygomaticus risorius, platysma risorius, and triangularis risorius.⁵ It also inserts into the modiolus in three distinct layers in relation to the DAO: superficial, flush, and deep (**Fig. 12.9**).

The buccinator originates from three regions: pterygomandibular raphe, maxillary, and mandibular alveolar processes. It is located between the maxilla and the mandible. The buccinator is rectangular and has four bands: (1) a band originating from the maxilla, (2) a band from the anterior margin of the pterygomandibular raphe, (3) a band extending from the mandible, and (4) an additional inferior band also extending from the mandible. The buccinator is reinforced by the incisivus labii inferioris (ILI).⁶ A few fibers spring from a fine tendinous band that bridges between the maxilla and the pterygoid hamulus (**Fig. 12.10**).

Chin Region and Superficial Neck

The mentalis muscle (MT) is the only elevator of the lower lip and the chin, and it provides the major vertical support for the lower lip. The absence of this muscular function would result in the lower central incisors being visible at rest. Resection of the MT may cause the patient to drool and may affect denture stability. MT is cone-shaped; the apex of this muscle originates from the incisive fossa of the mandible. The medial fibers of both

**Fig. 12.9** Risorius (left side).

Fig. 12.10 Buccinator.

MTs descend anteromedially and cross over together, forming a dome-shaped chin prominence. The lateral fibers of the MT descend mostly inferomedially. The upper fibers are short and horizontal, whereas the lower fibers are long and descend inferomedially or vertically.⁷ MT contraction causes the skin over the mentum to wrinkle. The upper fibers of the MT intermingle with the inferior margin of the OOr. In addition, the originating muscle fibers of the ILI intermingle with the upper lateral MT (**Fig. 12.11**).

The platysma attaches to the lower border of the mandible and consists of two types of fibers. A flattened bundle passes superomedially to the lateral border of the DAO, and others continue deep into DAO and reappear at its medial border. Lack of decussation creates a cervical defect, resulting in a reduction in elasticity of the cervical skin and platysma with ageing, which gives rise to the so-called turkey gobble neck. Platysmal fibers do not merely decussate and interlace from each side,

but sometimes one side of the muscle overlaps and covers the other side.⁸

Modiolus

The modiolus is a fibromuscular structure that decussates between the OOr muscle and the labial retractors, ending at the lateral border of the cheilion (**Fig. 12.12**).⁹ It extends 20 mm above and below a horizontal line through the buccal angle. It is strongly associated with facial expression, beauty, aging, and formation of the nasolabial fold. The modiolus is a dense, compact, and mobile muscular mass located at the lateral border of the corner of the mouth and is formed by a convergence of muscle fibers from the zygomaticus major, levator labii superioris, depressor labii inferioris, DAO, risorius, OOr, buccinators, and LAO muscles. The formation of subtle and detailed facial ex-

**Fig. 12.11** Mentalis muscle.



Fig. 12.12 Modiolus (left side). The modiolus is a fibromuscular structure that decussates between the orbicularis oris muscle and the labial retractors ending at the lateral border of the cheilion.

pressions of the inferior face, such as those reflecting determination, satisfaction, smiling, purposeful action, and sadness, are possible by contracting these muscles, which terminate at the

modiolus. A tendinous tissue nodule in the modiolus is found in about 20% of cases. The facial artery passes approximately 1 mm lateral to the lateral border of the modiolus.

References

1. Yang HM, Kim HJ. Anatomical study of the corrugator supercilii muscle and its clinical implication with botulinum toxin A injection. *Surg Radiol Anat* 2013;35(9):817–821 [PubMed](#)
2. Hur MS, Hu KS, Youn KH, Song WC, Abe S, Kim HJ. New anatomical profile of the nasal musculature: dilator naris vestibularis, dilator naris anterior, and alar part of the nasalis. *Clin Anat* 2011;24(2):162–167 [PubMed](#)
3. Hur MS, Youn KH, Hu KS, et al. New anatomic considerations on the levator labii superioris related with the nasal ala. *J Craniofac Surg* 2010;21(1):258–260 [PubMed](#)
4. Hur MS, Hu KS, Park JT, Youn KH, Kim HJ. New anatomical insight of the levator labii superioris alaeque nasi and the transverse part of the nasalis. *Surg Radiol Anat* 2010;32(8):753–756 [PubMed](#)
5. Kim HS, Pae C, Bae KS, et al. An anatomical study of the risorius in Asians and its insertion at the modiolus. *Surg Radiol Anat* 2015;37:147–151 [PubMed](#)
6. Hur MS, Hu KS, Kwak HH, Lee KS, Kim HJ. Inferior bundle (fourth band) of the buccinator and the incisivus labii inferioris muscle. *J Craniofac Surg* 2011;22(1):289–292 [PubMed](#)
7. Hur MS, Kim HJ, Choi BY, Hu KS, Kim HJ, Lee KS. Morphology of the mentalis muscle and its relationship with the orbicularis oris and incisivus labii inferioris muscles. *J Craniofac Surg* 2013;24(2):602–604 [PubMed](#)
8. Kim HJ, Hu KS, Kang MK, Hwang K, Chung IH. Decussation patterns of the platysma in Koreans. *Br J Plast Surg* 2001;54(5):400–402 [PubMed](#)
9. Yu SK, Lee MH, Kim HS, Park JT, Kim HJ, Kim HJ. Histomorphologic approach for the modiolus with reference to reconstructive and aesthetic surgery. *J Craniofac Surg* 2013;24(4):1414–1417 [PubMed](#)

13 Orbital Anatomy

Swapna Vemuri and Jeremiah P. Tao

Clinical Anatomy

The orbit is conical and has a volume of about 30 cm³. The anterior orbital rim has horizontal and vertical diameters of 4.0 cm and 3.5 cm, respectively; however, the orbital dimension widens posteriorly, with a maximum diameter 1 cm posterior to the rim. The distance from the anterior orbital rim to the apex is approximately 4.5 to 5 cm along the medial orbital wall, whereas the distance from the lateral orbital rim to the superior orbital fissure is about 4 cm.^{1,2}

The medial orbital walls are parallel to each other and approximately 2.5 cm apart. The lateral wall forms a 45-degree angle with the ipsilateral medial wall. The two lateral walls form a 90-degree angle (Fig. 13.1).

Orbital Bones

Orbital Rim

The orbital rim is composed of the frontal, zygomatic, and maxillary bones that adjoin at suture lines (frontozygomatic, zygomaticomaxillary, and frontomaxillary, respectively). The lateral and superior rims are the strongest. The orbital rim creates the anterior lacrimal crest and then spirals posteriorly to end at the posterior lacrimal crest. The lacrimal sac fossa is found between the two crests (Fig. 13.2a).

Orbital Walls

Seven orbital bones compose the four walls of the orbit (Fig. 13.2a).

Orbital Roof

The orbital roof, which is the floor of the anterior cranial fossa, consists of the frontal and lesser wing of sphenoid bones. The supraorbital notch or foramen, through which the supraorbital nerve (CN V₁) and vessels travel, divides the medial one-third and lateral two-thirds of the superior orbital rim. The lacrimal gland is found laterally in the lacrimal gland fossa.

Lateral Orbital Wall

The lateral orbital wall, separated from the roof by the superior orbital fissure, consists of the zygomatic and greater wing of the sphenoid bones (Fig. 13.2b). The zygomaticofacial and zygomaticotemporal canals transmit vessels and zygomatic nerve branches. Occasionally, a meningo-orbital foramen is identified

lateral to the superior orbital fissure and transmits a branch of the middle meningeal artery.^{3,4} Whitnall's tubercle is a protuberance on the inner aspect of the lateral orbital rim approximately 4 mm posterior to the rim and 10 mm inferior to the frontozygomatic suture. The lateral canthal tendon, lateral horn of the levator aponeurosis, Lockwood's ligament, and check ligament of the lateral rectus muscle attach to the tubercle.

Orbital Floor

The orbital floor, separated from the lateral wall by the inferior orbital fissure, consists of the zygomatic, maxillary, and palatine bones. The floor forms the roof of the maxillary sinus. The infraorbital groove or canal, through which the infraorbital nerve (CN V₂ branch) and artery travel, divides the floor. The infraorbital nerve and artery then exit through the infraorbital foramen, which is approximately 1 cm inferior to the orbital rim on the anterior maxillary bone face (Fig. 13.2c).

Medial Orbital Wall

The medial orbital wall consists of the maxillary, lacrimal, ethmoid, and sphenoid bones. The anterior and posterior ethmoidal foramina, with ethmoidal vessels passing through, are found on the medial wall along the frontoethmoidal suture. Along the medial wall, the distance between the anterior lacrimal crest, anterior ethmoidal foramen, posterior ethmoidal foramen, and orbital apex is approximately 24 mm, 12 mm, 6 mm, respectively (Fig. 13.2d).

Additional Fissures, Canals, and Foramina and Contents

The superior orbital fissure (SOF) is located between the greater and lesser wings of sphenoid. The annulus of Zinn, a tendinous ring at the orbital apex formed by the extraocular rectus muscles, divides the SOF. The annulus also encircles the optic foramen, which is medial to the SOF. Above the annulus, the lacrimal and frontal nerves (CN V₁ branches), trochlear nerve (CN IV), and superior ophthalmic vein pass through the SOF. The superior and inferior branches of the oculomotor nerve (CN III), abducens nerve (CN VI), and nasociliary nerve (CN V₁) pass through the annulus. The inferior ophthalmic vein may pass below the annulus (Fig. 13.3).

The optic foramen is located medial to the SOF in the lesser wing of the sphenoid and separated by a bony optic strut. It extends posteriorly as the optic canal that has an approximate diameter of 6 mm and a length of 10 mm. The optic nerve and ophthalmic artery pass through the optic canal.

The inferior orbital fissure (IOF) is located inferior to the SOF between the greater wing of sphenoid (lateral orbital wall) and

Fig. 13.1 Orbital dimensions and volumes.

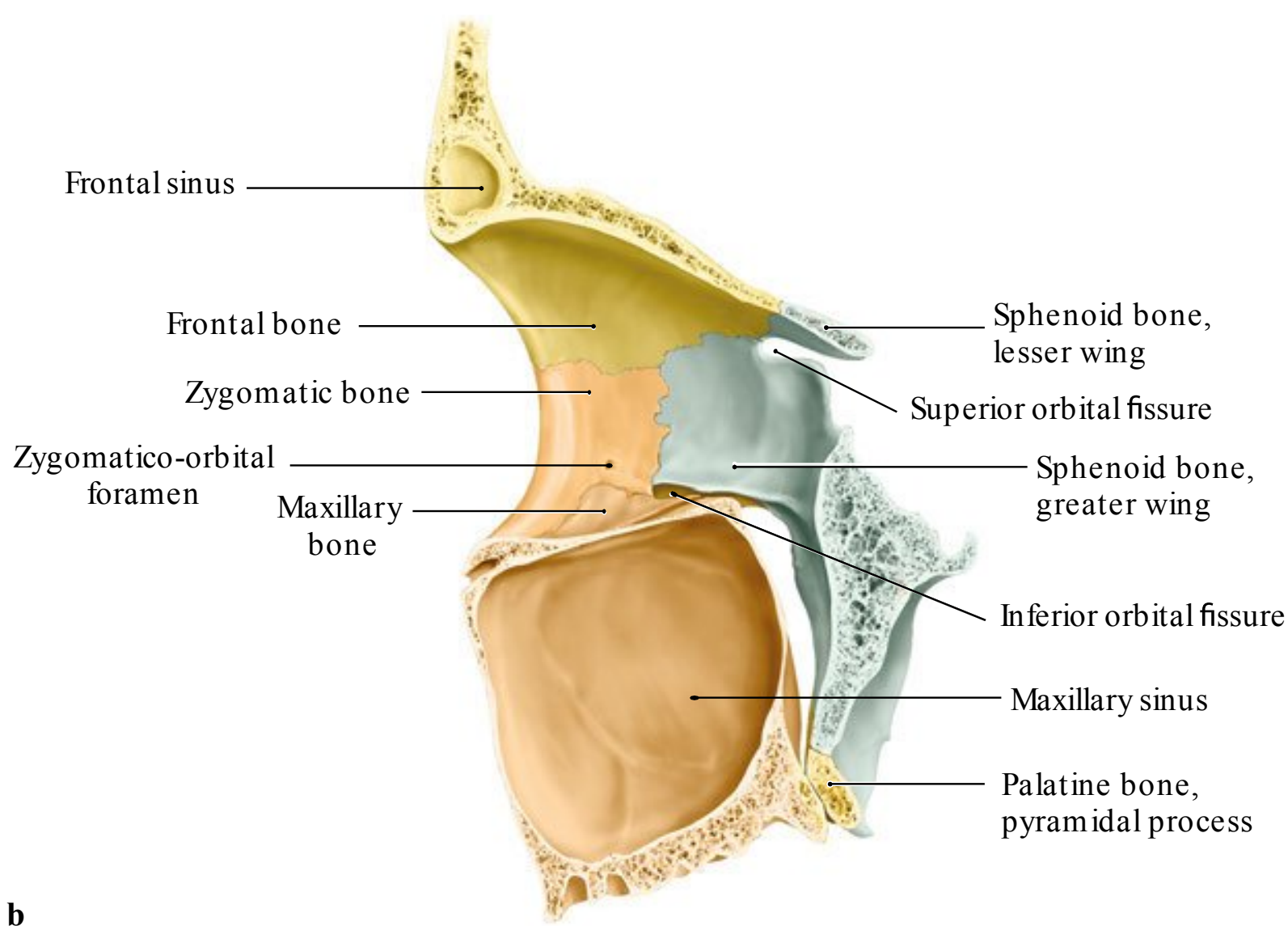
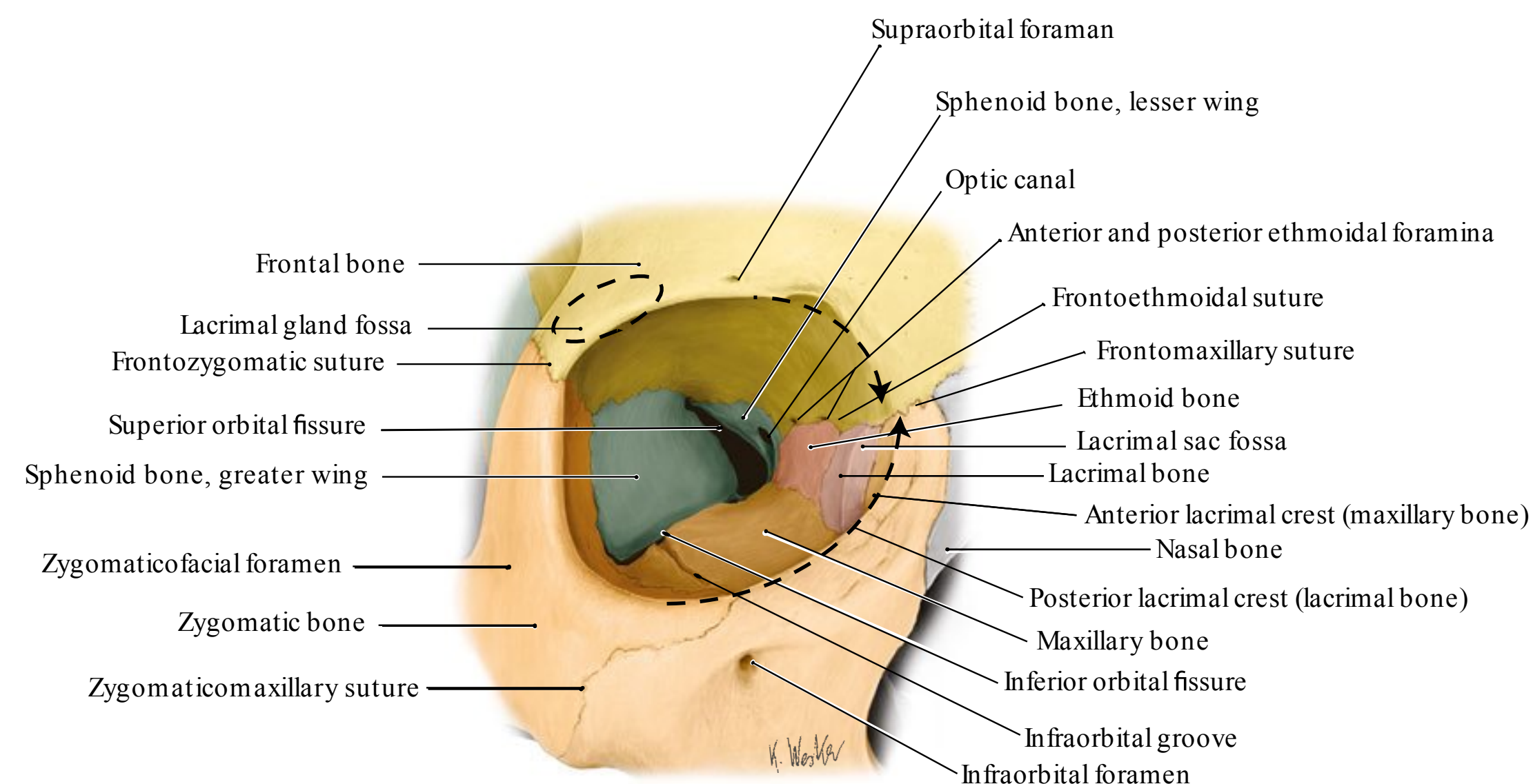
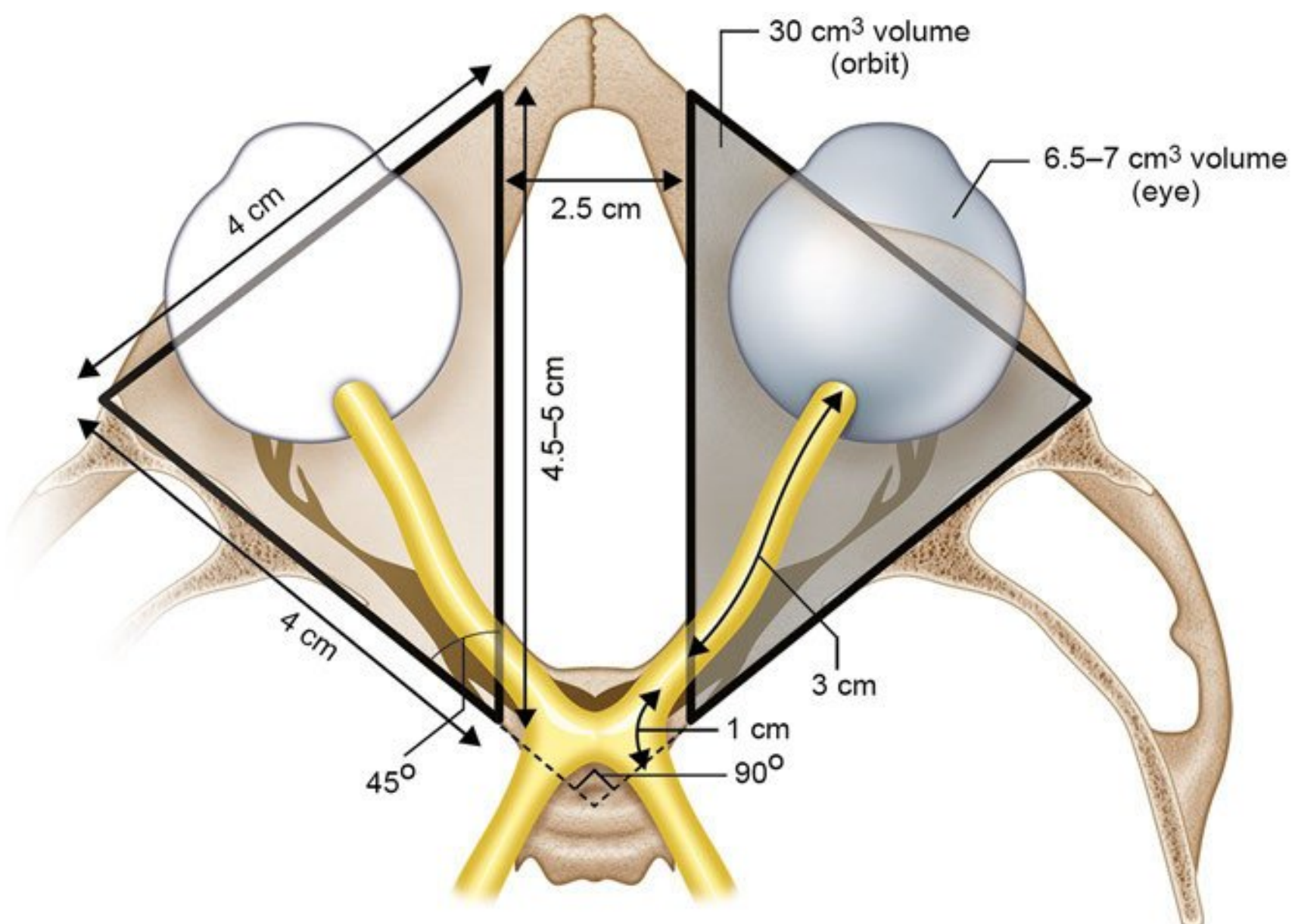


Fig. 13.2 (a) Orbital bones, sutures, foramina, and fissures. Anterior view. The orbital rim is composed of the frontal, zygomatic, and maxillary bones that adjoin at suture lines (frontozygomatic, zygomaticomaxillary, and frontomaxillary, respectively). (b) Lateral wall, right orbit. The lateral orbital wall, separated from the roof by the superior orbital fissure, consists of the zygomatic and greater wing of sphenoid bones. (continued on page 122)

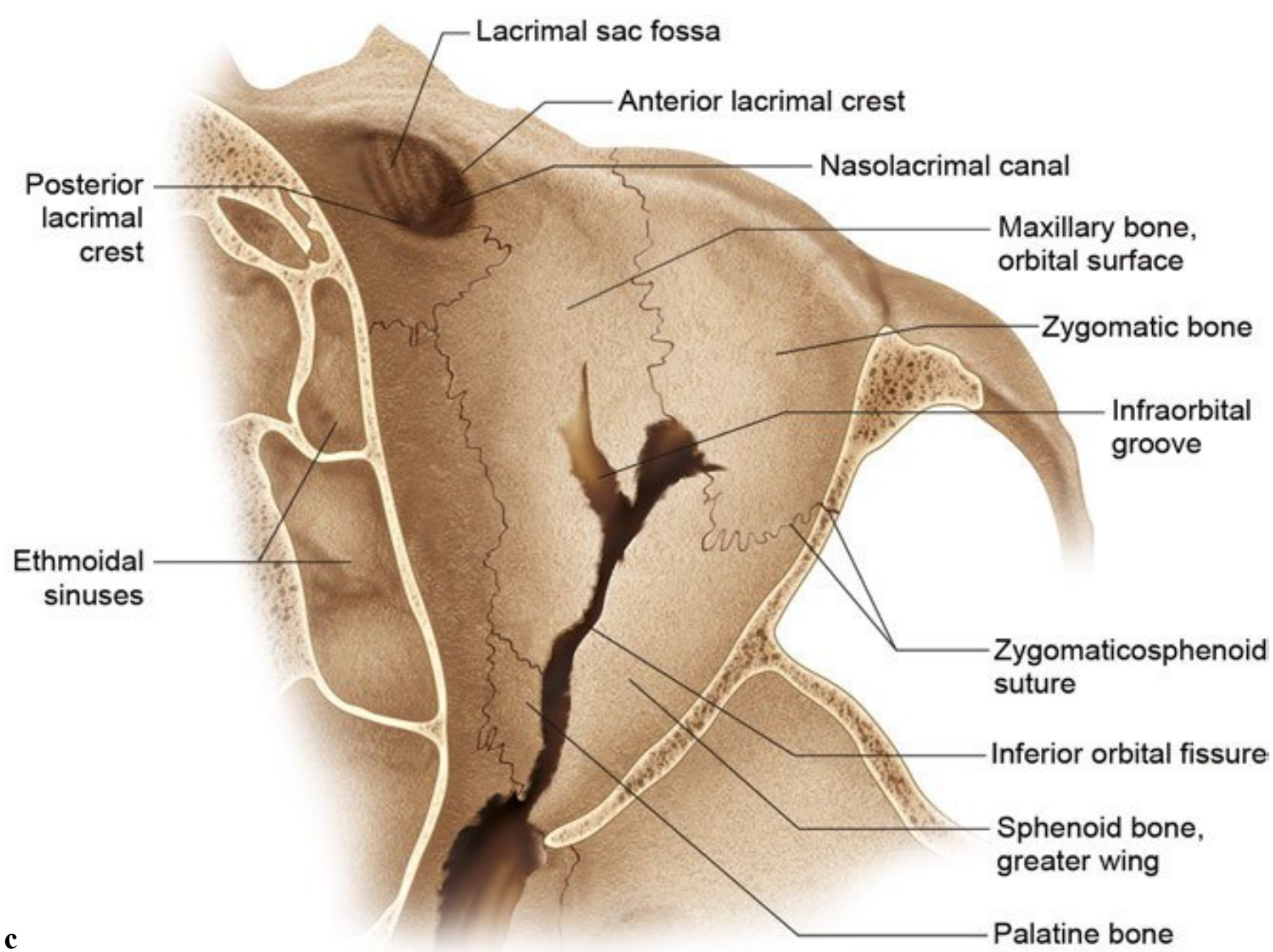
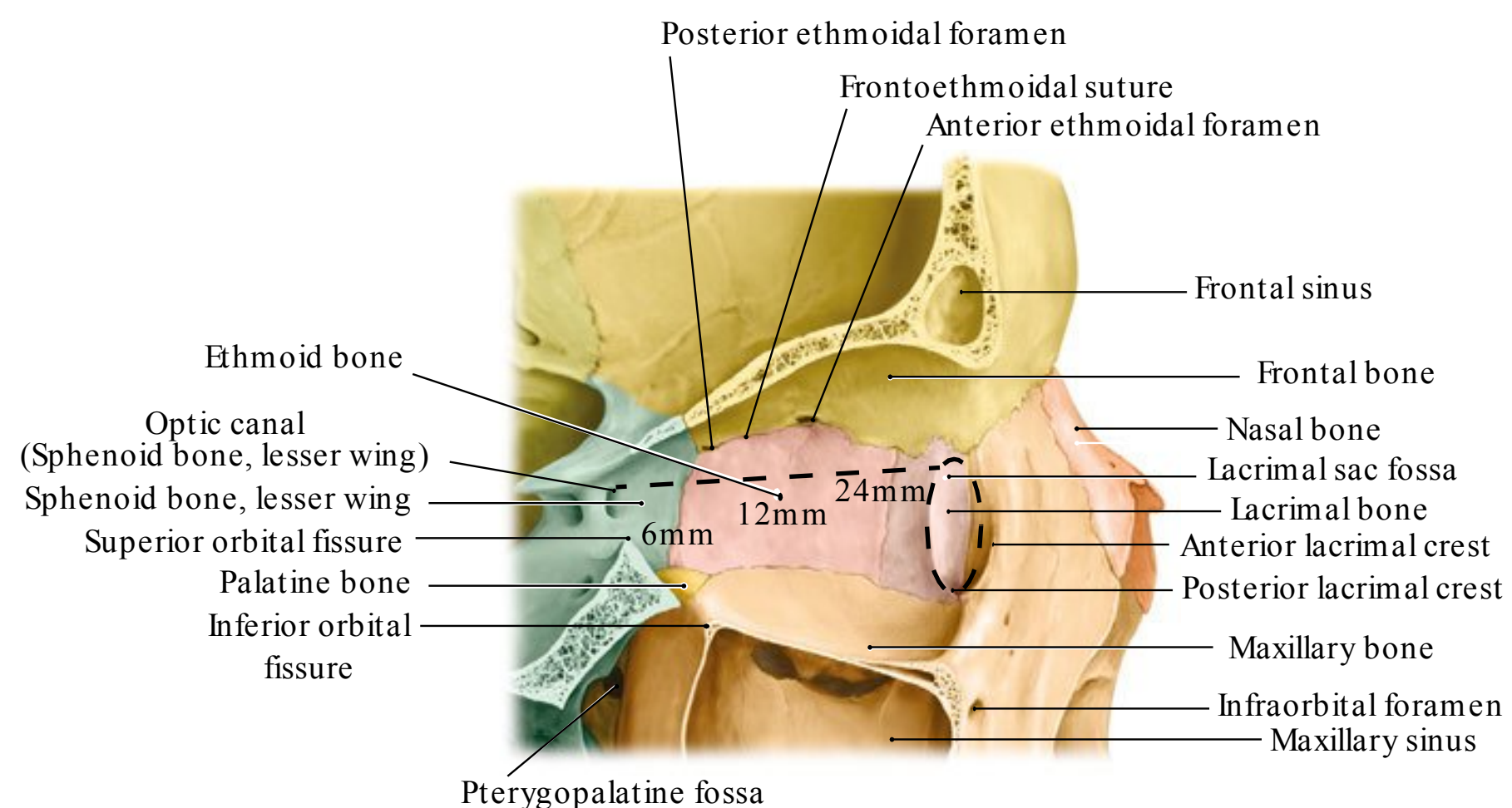


Fig. 13.2 (continued) (c) Orbital floor, right orbit. The orbital floor, separated from the lateral wall by the inferior orbital fissure, consists of the zygomatic, maxillary, and palatine bones. **(d)** Medial wall, right orbit. The medial orbital wall consists of the maxillary, lacrimal, ethmoid, and sphenoid bones. (Modified from THIEME Atlas of Anatomy, Head and Neuroanatomy. © Thieme 2010, Illustrations by Karl Wesker.)



palatine and maxillary bones (orbital floor). The infraorbital and zygomatic nerves (CN V₂), infraorbital artery, inferior ophthalmic vein, and pterygopalatine ganglion autonomic branches pass through the IOF.

pass through Tenon's fascia to insert onto the globe. Muscular fascial sheaths are found surrounding each extraocular muscle with projections to the orbital walls, known as check ligaments. The fascial sheath in the anterior orbit is also found in between each muscle to create the intermuscular septum.

Periorbita and Fascial Tissues

Perosteum covers the orbital bones and is known as periorbita along the orbital walls (Fig. 13.4). It is loosely adherent over the walls but tightly adherent at suture lines, the orbital rim where it forms the arcus marginalis, foramina, and fissures. The orbital septum originates from the arcus marginalis. At the optic canal, periorbita is continuous with the dural sheath of the optic nerve.

Orbital fascia is complexly organized.⁵ Tenon's capsule, a fibrous membrane, extends from the posterior globe and fuses with conjunctiva anteriorly at the limbus. Fibrous septa extend from Tenon's to divide lobules of orbital fat. Extraocular muscles

Surgical Annotation

Orbital Surgical Spaces and Approaches

The organization of orbital fascia and structures compartmentalizes the orbit. From deep to superficial, the surgical spaces of the orbit include the following: intraconal, sub-Tenon's, extraocular muscles, extraconal, subperiosteal, and extraorbital (Fig. 13.5). The appropriate orbital surgical approach is determined

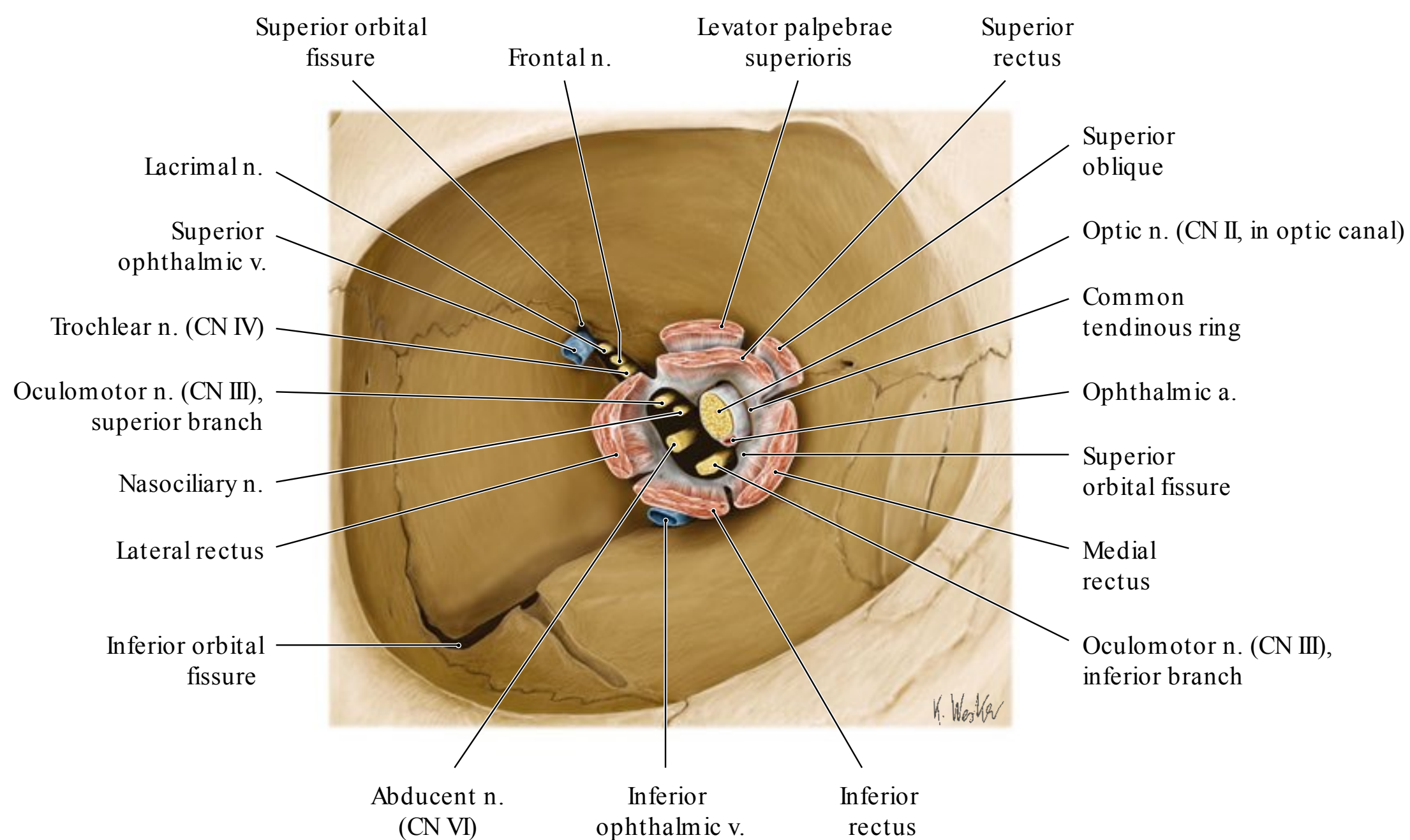


Fig. 13.3 Structures of the orbital apex including muscle origin, annulus of Zinn, fissures, and contents. Right orbit, anterior view, with most of the orbital contents removed. (Reproduced from THIEME Atlas of Anatomy, Head and Neuroanatomy. © Thieme 2010, Illustration by Karl Wesker.)

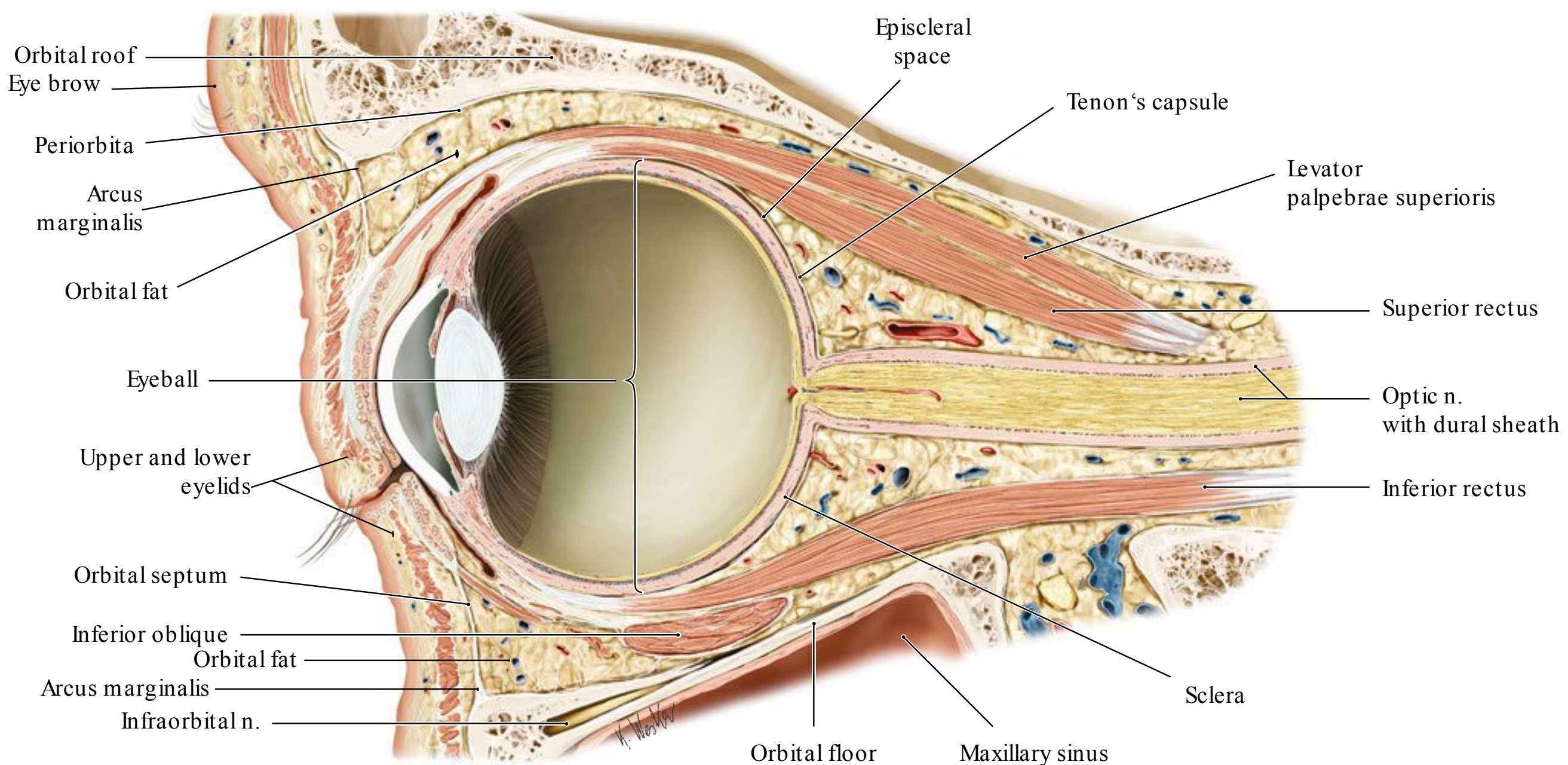


Fig. 13.4 Sagittal view of right orbit demonstrating periorbita, fascia, and relationship of extraorbital and intraorbital structures. Periorbita covers the orbital bones. It is loosely adherent over the walls but tightly

adherent at suture lines. (Modified from THIEME Atlas of Anatomy, Head and Neuroanatomy. © Thieme 2010, Illustration by Karl Wesker.)

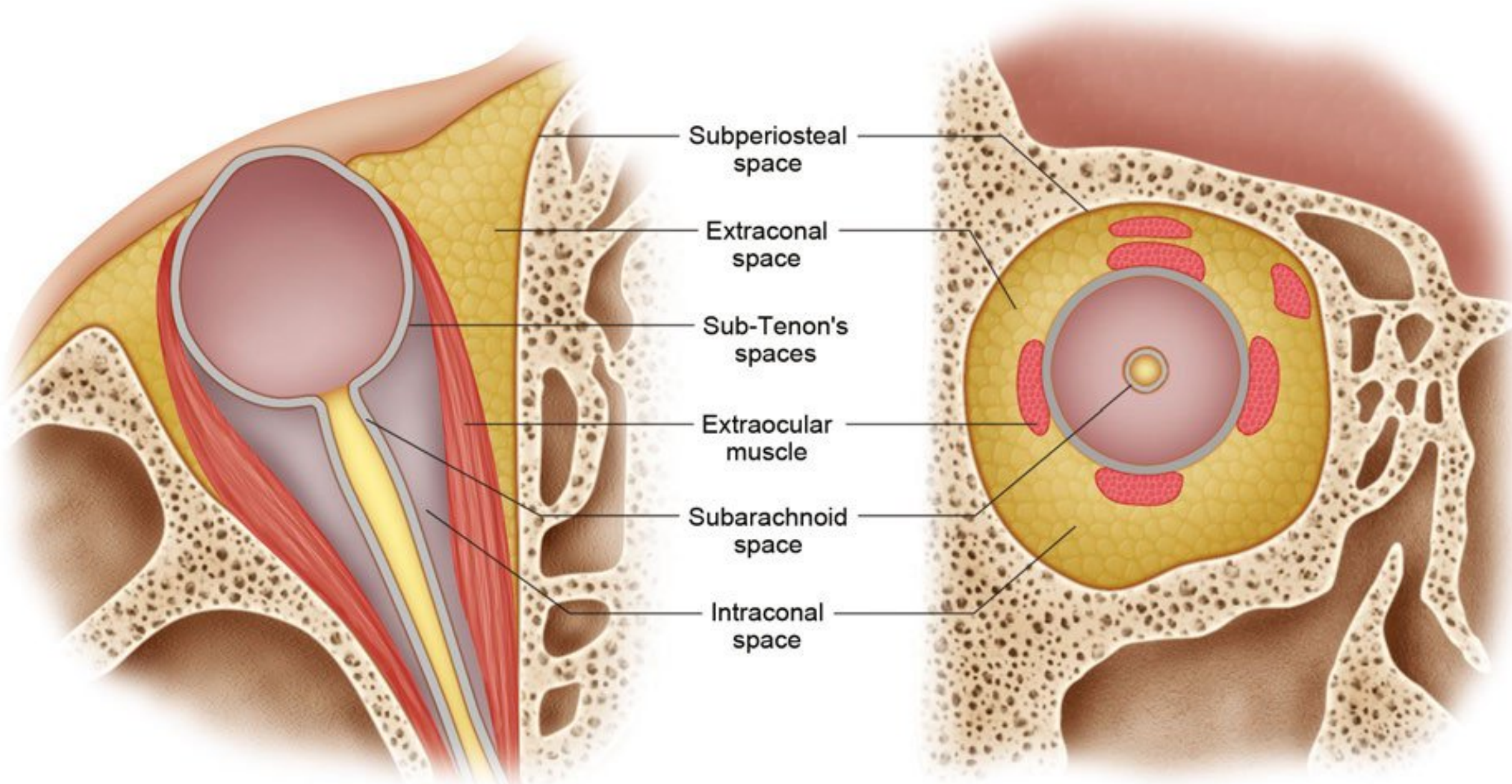


Fig. 13.5 Axial and coronal views of right orbit demonstrating surgical spaces. From deep to superficial, the surgical spaces of the orbit include the following: intraconal, sub-Tenon's, extraocular muscles, extraconal, subperiosteal, and extraorbital.

by the location of pathology with regards to surgical space, depth in orbit relative to the globe equator, and location relative to optic nerve.

Anatomical Considerations during Orbital Surgery

Orbital Wall Surgery

Due to the tight space and numerous vital structures in this region, orbital surgery poses significant risks. A thorough understanding of orbital anatomy is essential for safe surgery.

Orbital Floor

The most commonly fractured orbital wall is the floor. The inferomedial wall (medial to the infraorbital canal) is particularly susceptible. During orbital floor surgery (i.e., fracture repair or bone decompression), the safest dissection plane is subperiosteal. The authors prefer a transconjunctival approach combined with lateral canthotomy and inferior cantholysis; however, transcutaneous approaches are alternative options. The following are important considerations, once in the orbit:

- Anteromedially, the inferior oblique muscle originates on the maxillary bone just behind the inferior orbital rim and lateral to the lacrimal sac fossa. Dissection near the antero-medial floor can result in its unintentional disruption along with damage to the lacrimal sac.
- The infraorbital nerve travels in the infraorbital groove along the central floor and should be visualized and preserved. Damage to the nerve results in bother some infraorbital hypoesthesia. Elevation of periosteum over the canal may in-

duce small to medium size arterial bleeding. Electrocautery to these vessels should be performed cautiously and with a minimal energy technique.

- Lateral to the infraorbital groove, along the posterior floor, the contents of the infraorbital fissure can be found entering the fissure and should not be confused with entrapped orbital soft tissues.
- The postero-medial floor has a relatively steep supero-medial incline. This can result in difficulty visualizing the postero-medial ledge of a floor fracture from the head-of-bed surgeon perspective. Entering the maxillary sinus and following its roof anteriorly may aid in the identification of the posterior ledge.
- The posterior wall of the maxillary sinus is an excellent landmark for the orbit apex. Intraorbital dissection posterior to this depth is risky and is usually not necessary.

Medial Orbital Wall

The following are important considerations for orbit medial wall surgery (fracture repair or decompression):

- The medial canthal tendon inserts onto the anterior and posterior lacrimal crest with the lacrimal sac located in the lacrimal sac fossa. The cutaneous approach to the medial orbit offers a panoramic view of the medial orbit, however medial canthal tendon disinsertion is necessary and a canthopexy suture is placed to forestall telecanthus.^{6,7}
- The transcaruncular approach avoids a cutaneous incision with preservation of the medial canthal tendon while offering good access to the medial wall.⁸ The leading periosteal edge for subperiosteal dissection must begin at the posterior lacrimal crest with care not to violate the lacrimal sac. Herniation of surrounding orbital fat and a tighter surgical space

are disadvantages of this approach compared to the transcutaneous approach.

- Periosteal elevation should begin on the thicker frontal bone maxillary process. A subperiosteal plane is more difficult to achieve on the thin ethmoid bone that fractures easily with manipulation.
- The anterior and posterior ethmoidal foramina mark the level of the fovea ethmoidalis, the roof of the ethmoid sinus. This is the superior extent of medial orbital decompression as there is risk of disrupting the cribriform plate and entering the anterior cranial fossa with a resultant cerebrospinal fluid (CSF) leak or intracranial hemorrhage.
- The anterior and posterior ethmoidal arteries pose a risk of orbital hemorrhage if lacerated.
- Dissection greater than a 4 cm depth from the orbital rim along the medial wall risks damage to the optic nerve.

Lateral Orbital Wall

The anterior lateral orbital wall is strong; however, the posterior border of the deep lateral orbital wall is thin.^{2,9} When performing lateral wall surgery (i.e., zygomaticomaxillary complex fracture repair or decompression) the following should be considered:

- The distance along the lateral wall from the orbital rim to the SOF is about 4 cm.

References

1. Lemke BN, Lucarelli MJ. Anatomy of ocular adnexa and orbit. In: Smith BC, editor. Ophthalmic Plastic and Reconstructive Surgery. 2nd ed. St. Louis, MO: CV Mosby; 1997:3–78
2. Whitnall SE. The Anatomy of the Human Orbit and Accessory Organs of Vision. New York: Oxford University Press; 1932:1–252
3. Mysorekar VR, Nandedkar AN. The groove in the lateral wall of the human orbit. J Anat 1987;151:255–257 [PubMed](#)
4. Kwiatkowski J, Wysocki J, Nitek S. The morphology and morphometry of the so-called “meningo-orbital foramen” in humans. Folia Morphol (Warsz) 2003;62(4):323–325 [PubMed](#)
5. Koornneef L. Details of the orbital connective tissue system in the adult. In: Koornneef L, ed. Spatial Aspects of Orbital Musculo-Fibrous Tissue in Man: A new anatomical and histological approach. Amsterdam: Swets and Zeitlinger; 1977
6. Nunery WR, Tao JP, Johl S. Nylon foil “wraparound” repair of combined orbital floor and medial wall fractures. Ophthal Plast Reconstr Surg 2008;24(4):271–275 [PubMed](#)
7. Timoney PJ, Sokol JA, Hauck MJ, Lee HB, Nunery WR. Transcutaneous medial canthal tendon incision to the medial orbit. Ophthal Plast Reconstr Surg 2012;28(2):140–144 [PubMed](#)
8. Shorr N, Baylis HI, Goldberg RA, Perry JD. Transcaruncular approach to the medial orbit and orbital apex. Ophthalmology 2000; 107(8):1459–1463 [PubMed](#)
9. Kakizaki H, Nakano T, Asamoto K, Iwaki M. Posterior border of the deep lateral orbital wall—appearance, width, and distance from the orbital rim. Ophthal Plast Reconstr Surg 2008;24(4):262–265 [PubMed](#)
10. Goldberg RA, Kim AJ, Kerivan KM. The lacrimal keyhole, orbital door jamb, and basin of the inferior orbital fissure. Three areas of deep bone in the lateral orbit. Arch Ophthalmol 1998;116(12):1618–1624 [PubMed](#)

14 Orbital Soft Tissues

Swapna Vemuri and Jeremiah P. Tao

Extraocular Muscles and Innervation

The six extraocular muscles (medial, lateral, superior and inferior recti, and superior and inferior oblique muscles) move the globe. With the exception of the inferior oblique muscle, which originates on the anteromedial orbital floor, all the extraocular muscles originate at the orbital apex (**Fig. 14.1a**). The rectus muscles originate at the fibrous annulus of Zinn. These muscles course anteriorly, penetrate Tenon's capsule, and insert onto the anterior aspect of the globe, forming the spiral of Tillaux (**Fig. 14.1b**). The rectus muscles form the muscle cone and delineate the intraconal and extraconal spaces.

The levator palpebrae superioris muscle originates on the lesser wing of sphenoid superior to the annulus. The superior oblique muscle also originates on the lesser wing of sphenoid medial to the levator muscle origin, continues anteriorly through the trochlea, then courses posterolaterally under the superior rectus muscle to insert onto the globe. The inferior oblique originates on the maxillary bone lateral to the lacrimal sac fossa, continues posterolaterally under the inferior rectus, and inserts onto the globe posterior to the macula.

The extraocular muscles are innervated by cranial nerves (CN) III (oculomotor), IV (trochlear), and VI (abducens). CN III divides into superior and inferior branches in the cavernous sinus before entering the orbit. The superior branch innervates the levator and superior rectus muscles. The inferior branch innervates the medial rectus, inferior rectus, and inferior oblique muscles. CN IV innervates the superior oblique muscle. CN VI innervates the lateral rectus muscle. Cranial nerves III and VI enter the orbit through the superior orbital fissure, travel through the intraconal space, and innervate the rectus muscles at the posterior one-third and anterior two-thirds junction. The blood supply for the rectus muscles arises from muscular anterior ciliary artery branches of the ophthalmic artery, lacrimal artery, and infraorbital artery. The inferior division of CN III to the inferior oblique travels lateral to the inferior rectus to innervate the muscle on the posterior surface. A parasympathetic branch to the ciliary ganglion travels with this inferior oblique muscle branch. CN IV travels extraconally to innervate the superior oblique on the superior surface at the posterior third of the muscle.

Optic Nerve

The optic nerve (CN II) can be divided into intraocular, intraorbital, intracanalicular, and intracranial segments measuring approximately 1 mm, 25 to 30 mm, 10 mm, and 10 mm long, respectively. The intraorbital optic nerve exits the posterior as-

pect of the globe and increases in diameter as it extends posteriorly through the orbit. Its intraorbital length is greater than the distance from the posterior globe to the optic canal (18 mm), allowing for eye movement and a safety margin in the event of proptosis. The optic nerve, with a 4-mm diameter and surrounded by the meninges (pia, arachnoid, and dura mater), then enters the optic foramen, which is 6.5 mm in diameter. Dura fuses with the annulus of Zinn and the optic canal periosteum, resulting in immobilization of the optic nerve. The optic nerve courses through the optic canal, which is about 10 mm long, and continues intracranially until it reaches the optic chiasm. Surgical management of intraconal pathology requires a keen understanding of the optic nerve course.

Orbital Nerves

In addition to the cranial nerves previously described, sensory, motor, and autonomic nerves supply the orbit.

Sensory Innervation

The ophthalmic (V_1) and maxillary (V_2) divisions of the trigeminal nerve (CN V) provide sensory innervation to the orbital and periorbital regions (**Fig. 14.2**).

Ophthalmic Nerve

The ophthalmic nerve (CN V_1) divides into the frontal and lacrimal nerves, which enter the orbit above the annulus of Zinn, and the nasociliary nerve, which enters through the annulus. The frontal nerve divides further; the supratrochlear nerve innervates the medial upper lid, glabellar region, and medial conjunctiva, and the supraorbital nerve innervates the medial forehead. The lacrimal nerve innervates the lateral upper lid, lacrimal gland, and lateral conjunctiva. The nasociliary nerve crosses the optic nerve superiorly from lateral to medial and courses between the superior oblique and medial rectus muscles before further dividing. Anterior and posterior ethmoidal nerves innervate the middle and inferior turbinates, nasal septum, lateral nasal wall, and tip of the nose (terminal infratrochlear nerve). Ciliary nerves provide sensory innervation to the ciliary body, iris, and cornea along with sympathetic innervation to the dilator pupillae muscle.

Ciliary Ganglion

The ciliary ganglion, which is located lateral to the optic nerve and medial to the lateral rectus muscle, is about 1.5 cm posterior

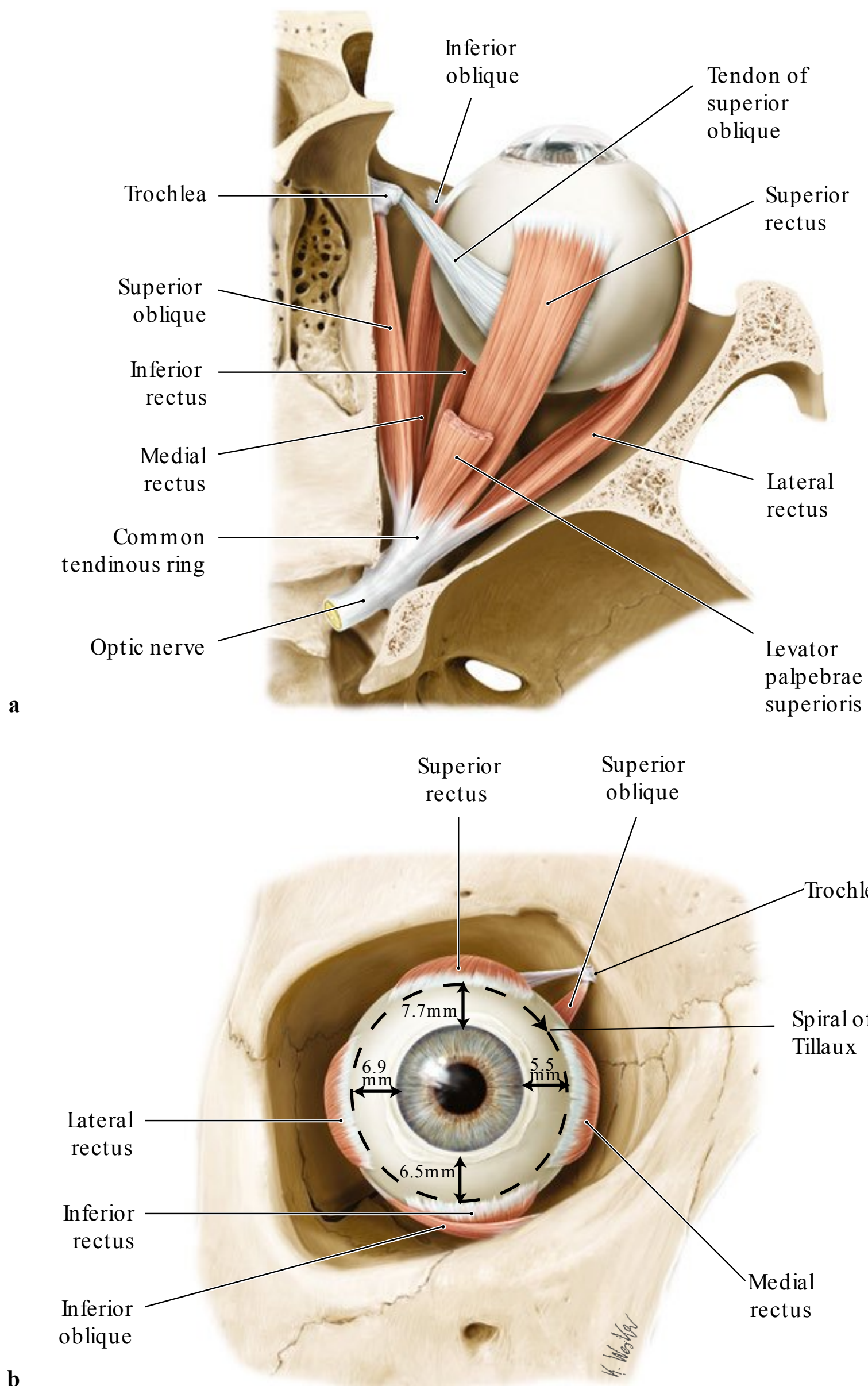


Fig. 14.1 Extraocular muscles, right eye. **(a)** Superior view. **(b)** Anterior view. Muscle insertions onto the anterior aspect of the globe beginning with the medial rectus and ending with the superior rectus create the spiral of Tillaux. The distance between the muscle insertion and limbus are indicated. (Modified from THIEME Atlas of Anatomy, Head and Neuroanatomy. © Thieme 2010, Illustrations by Karl Wesker.)

to the globe. Sensory (V_1) and sympathetic fibers pass through without synapsing, whereas parasympathetic fibers synapse in the ganglion. The ganglion can be encountered during lateral orbital intraconal surgery.

Maxillary Nerve

The maxillary nerve ($CN\ V_2$) divides into the infraorbital, zygomatic, nasal branches, palatine, superior alveolar, and pharyngeal nerves. After leaving the trigeminal ganglion, the maxillary nerve enters the foramen rotundum into the pterygopalatine fossa. The nerve enters the inferior orbital fissure to continue through the infraorbital groove and canal to exit anteriorly through the infraorbital foramen as the infraorbital nerve. The infraorbital nerve divides into the inferior palpebral branch, nasal branch, and superior labial branch to supply the inferior eyelid, lateral

nose, and upper lip, respectively. The zygomatic nerve divides in the inferior orbital fissure into the zygomaticofacial and zygomaticotemporal nerves to exit through the respective foramina and innervate the cheek and lateral forehead, respectively.

The infraorbital, zygomaticofacial, and zygomaticotemporal may be encountered during surgery of the midface. Care should be taken to preserve these sensory nerves; however, compromise to the zygomaticofacial and zygomaticotemporal nerves may be less consequential than infraorbital nerve damage that may result in symptomatic hypoesthesia.

Motor Innervation

Motor innervation to the facial muscles is supplied by the facial nerve ($CN\ VII$), which is described in further detail along with facial anatomy in other chapters. In the periorbital region, the

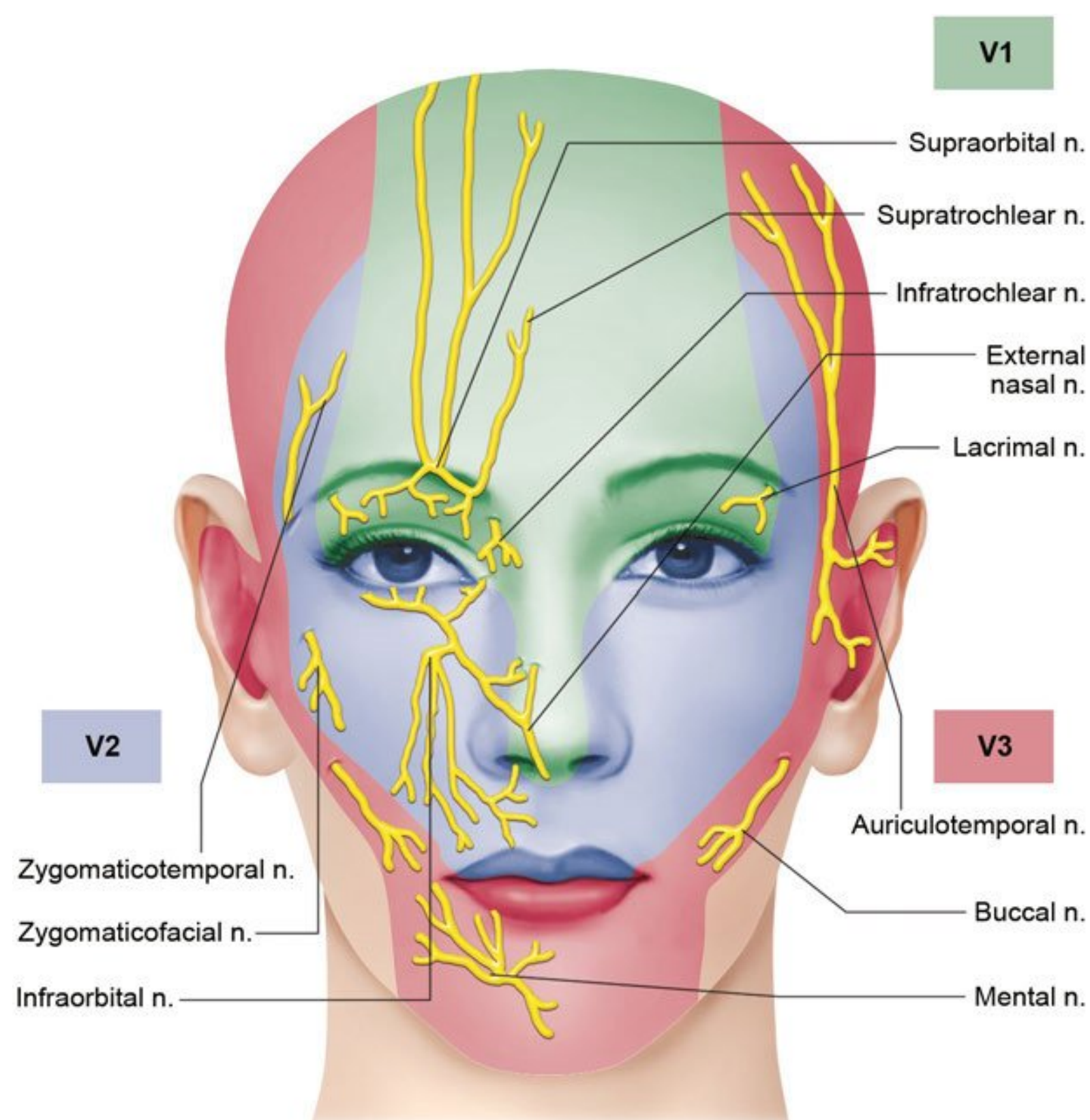


Fig. 14.2 Trigeminal nerve (CN V) cutaneous distribution. The ophthalmic (V1) and maxillary (V2) divisions of the trigeminal nerve (CN V) provide cutaneous innervation to the orbital and periorbital regions.

facial nerve lies in a deep plane as it emerges from the parotid gland (**Fig. 14.3**). The temporal branch courses superiorly and crosses over the zygomatic arch about midway between the lateral canthus and tragus. Dissection in the subperiosteal plane is safe in this region. Superior to the arch, the facial nerve lies beneath the superficial temporalis fascia, which is an extension of the superficial musculoponeurotic system (SMAS). To avoid damaging the facial nerve in this region, dissection should be performed deep to SMAS, just anterior to the deep temporalis fascia. In addition, a branch can be found along a line from approximately 1 cm inferior to the tragus to 1.5 cm superior to the lateral brow. Inferior to the arch, dissection superficial to SMAS and the parotid gland avoids the facial nerve.

Autonomic Innervation

The sympathetic nerves from the superior cervical ganglion enter the carotid canal as a plexus around the internal carotid artery (ICA). Sympathetics to the lacrimal gland leave the ICA to exit the petrous bone and eventually parallel the parasympathetic fibers to the lacrimal gland. The fibers to the dilator pupillae muscle leave the ICA in the cavernous sinus and travel with CN VI and then the nasociliary branch of V₁ before leaving the cavernous sinus. These fibers pass through the ciliary ganglion without synapsing, travel with the long ciliary nerves, and result in pupil dilation. The fibers to Müller muscle travel along ophthalmic artery branches to stimulate upper lid elevation.

Sympathetic innervation results in lower lid retraction via the inferior tarsal muscle and causes hidrosis.

Parasympathetic fibers from the Edinger-Westphal nucleus travel with the inferior division of the oculomotor nerve, synapse in the ciliary ganglion, and continue with the branch to the inferior oblique muscle. They enter the globe as posterior ciliary nerves and cause accommodation through ciliary muscle contraction and pupil constriction through the pupillary sphincter muscle. Parasympathetic fibers from the pterygopalatine ganglion travel through the inferior orbital fissure then with the lacrimal nerve to innervate the lacrimal gland.

Orbital Vessels

The periorbital and facial region receives blood supply from both the ICA and external carotid arteries, resulting in rich anastomoses and vascular supply (**Fig. 14.4**). In the cavernous sinus, the ICA gives off the ophthalmic artery, which then travels inferior to the optic nerve through the optic canal. The pial branch of the ophthalmic artery supplies the intracanalicular optic nerve. The central retinal artery branches off about 10 mm posterior to the globe. Additional branches include the lacrimal, supraorbital, ethmoidal, and extraocular muscle branches; long posterior ciliary arteries; and terminal branches (supratrochlear, medial palpebral, and dorsal nasal). The external carotid artery branches include the maxillary and facial artery. The an-

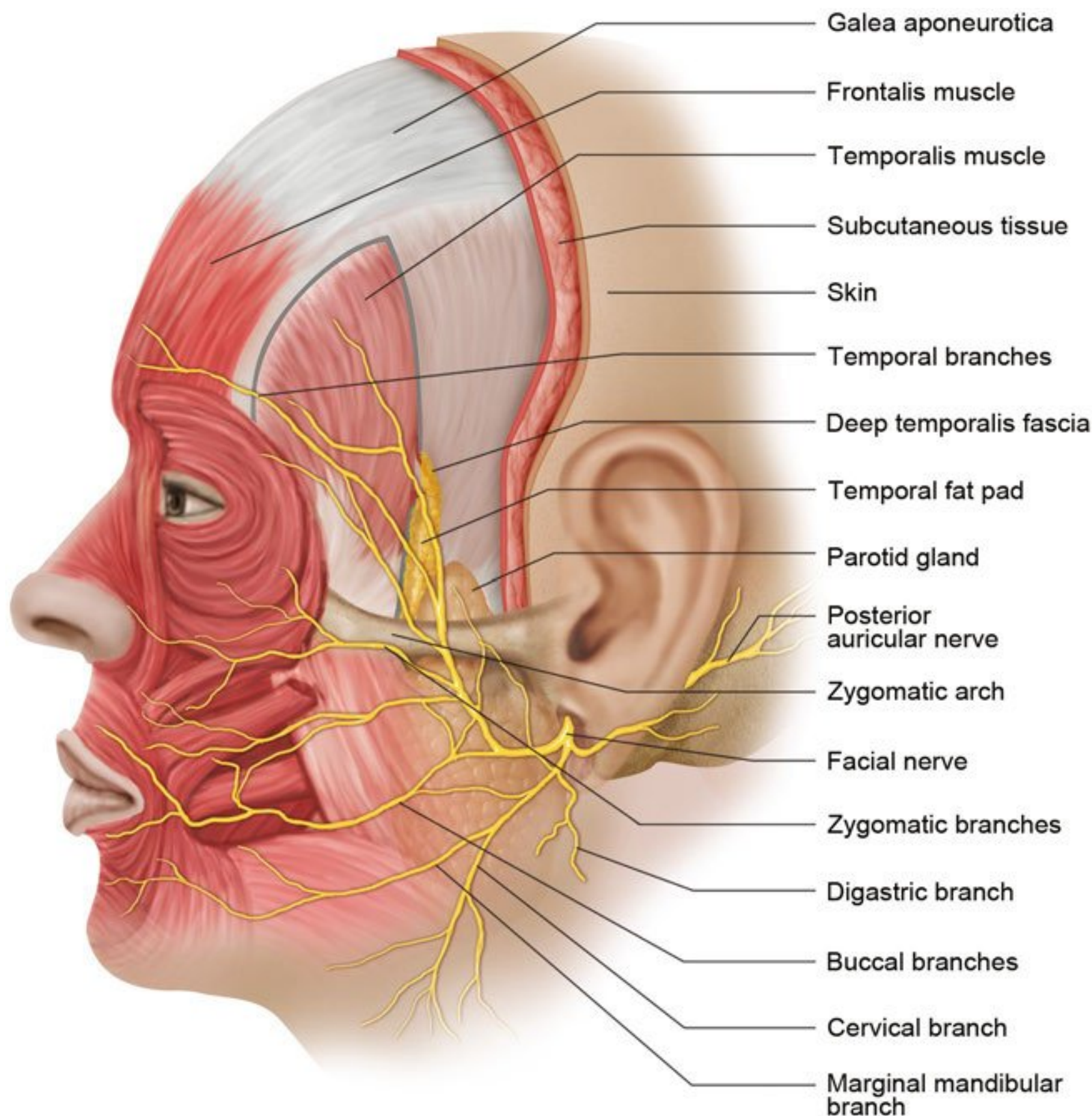


Fig. 14.3 Facial nerve (CN VII) distribution. Left lateral view of the face. Motor innervation to the facial muscles is supplied by the facial nerve (CN VII). In the periorbital region, the facial nerve lies in a deep plane as it emerges from the parotid gland.

angular artery, a branch of the facial artery, courses about 5 mm anterior to the medial canthal tendon (MCT) insertion and may be encountered along with the angular vein during dissection in this area. The superior ophthalmic vein provides orbital venous drainage. It courses from superomedially to laterally in the orbit as it enters the cavernous sinus.

Orbital Lymphatics

Lymphatics were previously thought to be absent in the orbit; however, recent studies challenge this notion.^{1,2}

Orbital Fat

Orbital fat surrounds the globe and orbital structures. Anteriorly, extraconal orbital fat is found in the postseptal plane in the upper and lower lids. The superior orbital fat is divided by the trochlea into the medial and central fat pads (**Fig. 14.5**).

The inferior orbital fat is divided into the medial, central, and lateral fat pads (**Fig. 14.5**). The inferior oblique muscle courses between the medial and central fat pads. The lateral and central fat pads are separated by the fascial arcuate expansion of the inferior oblique muscle.

Surgical Annotation: Precautions during Orbital Fat Pad Manipulation

During upper or lower lid blepharoplasty, debulking of the fat pads can result in insidious bleeding into the fat and subsequently retrobulbar. If hemostasis is not ensured before wound closure, an orbital compartment syndrome may result in vision compromise. Aggressive orbital fat pad removal in the upper and lower lids was once thought to improve cosmetic outcomes. Conservative excision and fat preservation, especially laterally, may be associated with improved aesthetic results and avoid hollowing.

Upper Eyelid

The orbital lobe of the lacrimal gland is found in the postseptal, or preaponeurotic, plane lateral to the orbital fat pads, and may be easily confused for orbital fat; therefore, careful dissection is required if the central fat pad is debulked during an upper lid blepharoplasty. The lacrimal gland appears more pink and lobulated and is more firm compared with the orbital fat.

Lower Eyelid

The inferior oblique muscle is encountered between the central and medial fat pads of the lower eyelid. During lower lid

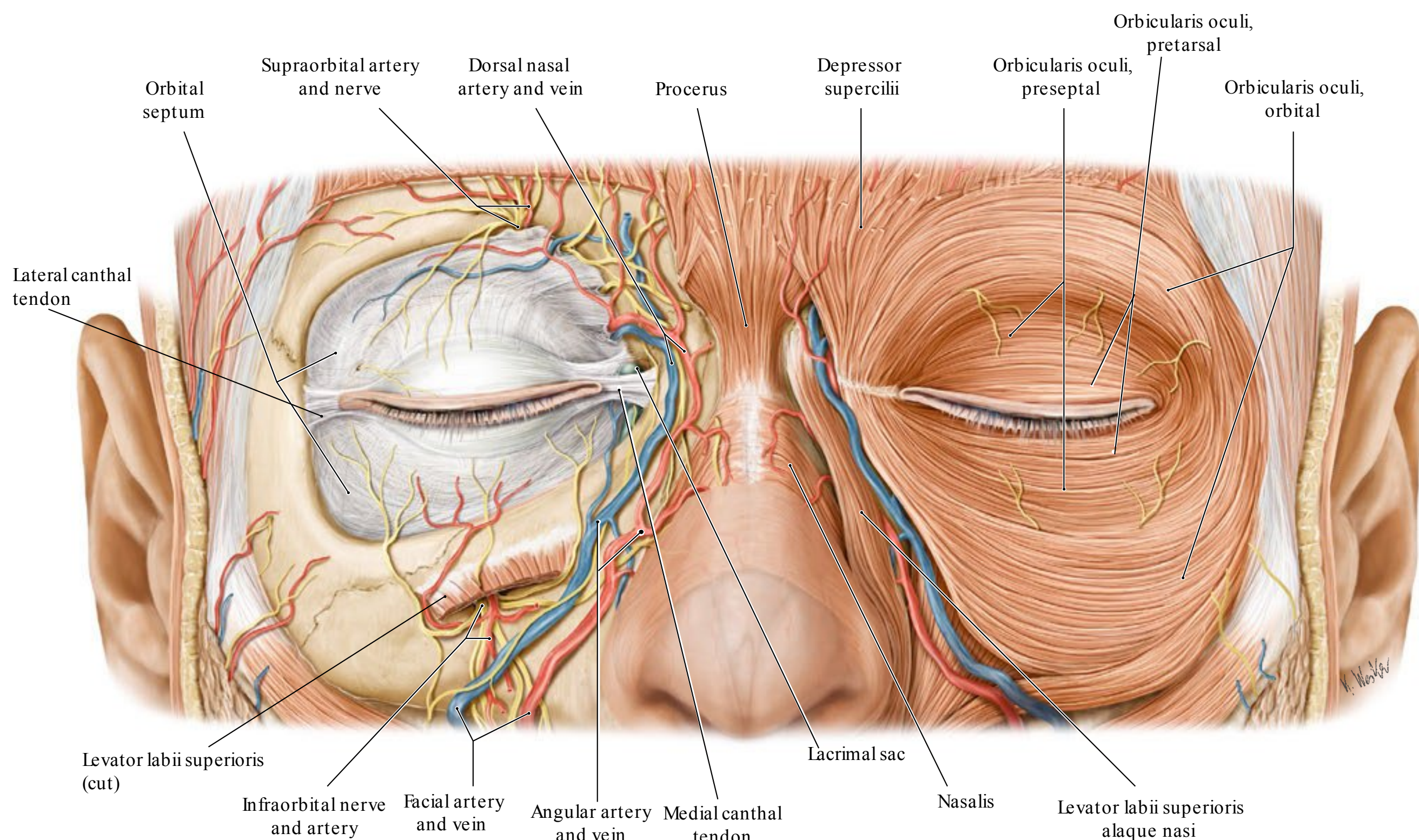


Fig. 14.4 Periorbital neurovascular structures. Right orbit: Orbicularis oculi muscle removed. The periorbital and facial region receives blood supply from both the internal and external carotid arteries resulting in

rich anastomoses and vascular supply. (Modified from THIEME Atlas of Anatomy, Head and Neuroanatomy. © Thieme 2010, Illustration by Karl Wesker.)

blepharoplasty and fat redistribution, the fat pads must be gently separated from their connective tissue attachments to the inferior oblique before translocation. A restrictive strabismus may otherwise result. Some surgical techniques involve direct visualization of the inferior oblique muscle and release from surrounding soft tissues.³

The lacrimal gland has been found to receive both sympathetic and parasympathetic innervation, and innervation from CN V and VII. The lacrimal nerve of CN V₁ carries sensory information from the gland and upper lid.

Lacrimal System

Lacrimal Gland

The lacrimal gland and accessory glands of Wolfring and Kraus produce the aqueous layer of the tear film. The lacrimal gland is thought to produce chiefly reflex tears and to contribute to basal tear secretion provided by the glands of Wolfring and Kraus located in the superior or inferior tarsal border and fornix, respectively. The lacrimal gland is located in the lacrimal gland fossa in the lateral aspect of the frontal bone. It consists of an orbital lobe, which is visible during an upper eyelid dissection, and a palpebral lobe, which can be visualized in the superolateral fornix by manually elevating the eyelid. The lateral horn of the levator aponeurosis separates the two lobes, with secretory ductules connecting them. To avoid damage to these ductules, an incisional lacrimal gland biopsy should be performed on the orbital lobe.

Nasolacrical System and Lacrimal Pump

The eyelids help pump tears produced by the lacrimal apparatus across the ocular surface to drain medially through the upper and lower lid 0.3 mm diameter puncta. The puncta are positioned opposed to the globe. With punctal eversion, tears are unable to drain appropriately, resulting in epiphora. Lateralization of the puncta suggests medial canthal tendon laxity or disruption.

After entering the puncta, tears travel 2 mm vertically to the ampulla of the canaliculi, then 8 mm horizontally through the canaliculi. In more than 90 percent of individuals, the superior and inferior canaliculi merge into a common canaliculus before draining into the nasolacrical sac.^{4,5}

The lacrimal sac measures about 12 mm vertically, extending about 3 to 5 mm superior to the MCT. It is located in the lacrimal sac fossa, which is created by the maxillary bone anteriorly and lacrimal bone posteriorly.

The lacrimal sac then opens into a nasolacrical duct, which courses posteriorly, laterally, and inferiorly for 18 mm in an os-

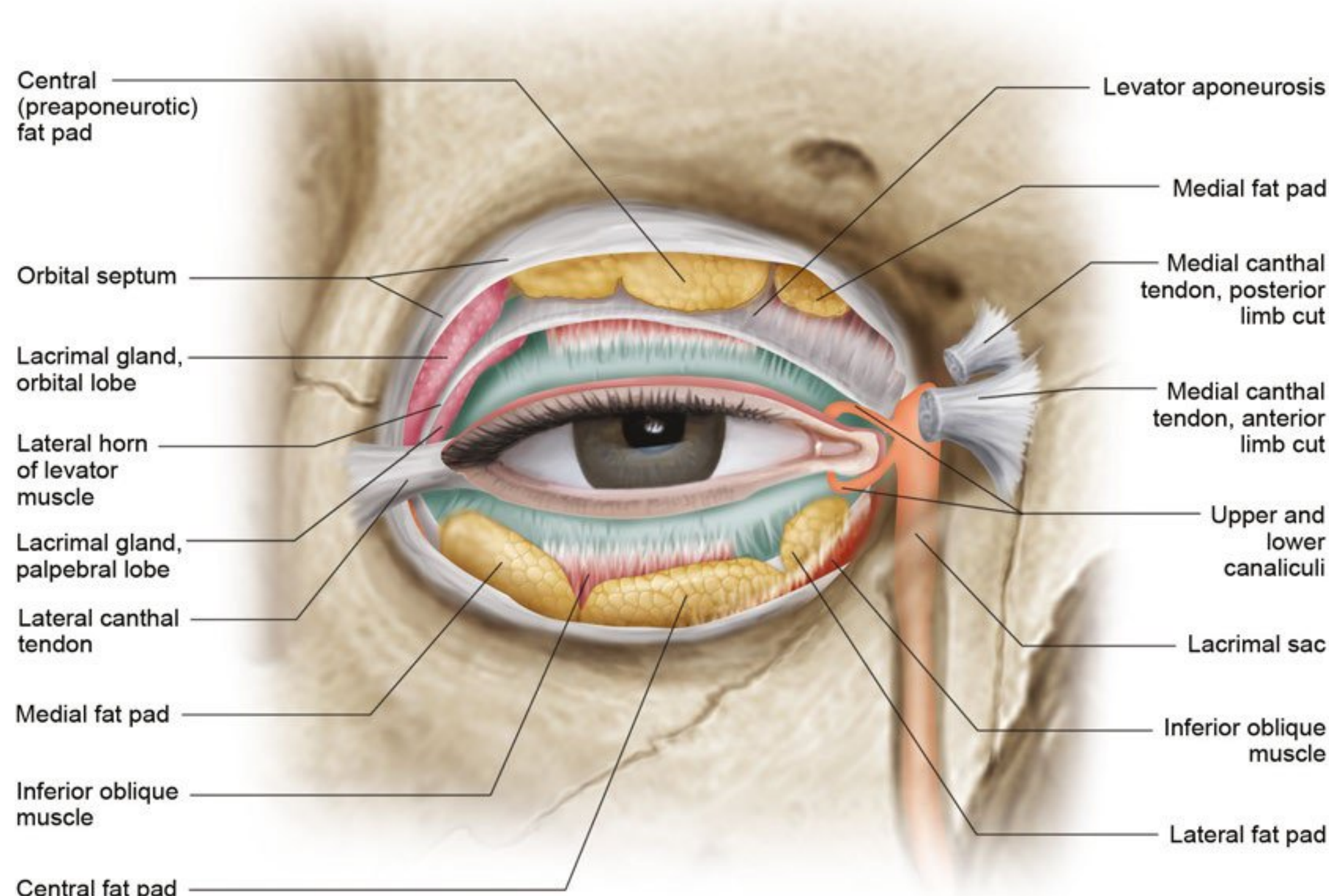


Fig. 14.5 Orbital fat pad distribution in relation to surrounding structures, right orbit. Orbital fat surrounds the globe and orbital structures. Anteriorly, extraconal orbital fat is found in the postseptal

plane in the upper and lower lids. The superior orbital fat is divided by the trochlea into the medial and central fat pads. The inferior orbital fat is divided into the medial, central, and lateral fat pads.

seous nasolacrimal canal. The duct opens beneath the inferior turbinate into the inferior meatus. The duct opening is about 25 mm posterior to the anterior naris (**Fig. 14.6**).

Various valves have also been described in the nasolacrimal system. The valve of Rosenmüller at the opening of the common canaliculus to the lacrimal sac prevents reflux of tears. The valve of Krause is found between the sac and duct. The valve of Hasner is located at the duct opening into the inferior meatus (**Fig. 14.6**).

Lid position and tone are important to allow for adequate lacrimal pump function. In addition, the organization of the structures around the nasolacrimal system contributes to appropriate tear drainage.

The pretarsal orbicularis muscle surrounds the canaliculi. Periorbital fascia and the thick anterior and thin posterior limbs of the MCT encircle the lacrimal sac. The anterior limb inserts onto the anterior lacrimal crest and the posterior limb inserts onto the posterior lacrimal crest (**Fig. 14.4**). The deep pretarsal orbicularis muscle, also called the Horner muscle, courses posterior to the lacrimal sac and posterior limb of the MCT to insert onto the posterior lacrimal crest.

During a transcaruncular approach to the medial orbit, blunt dissection along Horner's muscle allows identification of the posterior lacrimal crest. A periosteal incision and elevation gives access to the subperiosteal plane along the medial orbit.

Surgical Annotation: Anatomical Considerations during Nasolacrimal Surgery

Nasolacrimal Intubation

During canicular intubation, gentle introduction of a stent after the previously described anatomy prevents creation of false passageways. When retrieving a canicular intubation stent through the nose, a retrieving instrument introduced parallel to the floor of the nasal cavity, along the lateral nasal wall, and in a posterolateral direction helps locate the stent. Occasionally, the inferior turbinate may need to be fractured if it is too close to the lateral nasal wall.

Dacryocystorhinostomy

A dacryocystorhinostomy (DCR), whether external or endoscopic, involves fistulization of the lacrimal sac into the nasal cavity for management of nasolacrimal duct obstruction. The lacrimal sac is located in a fossa between the anterior lacrimal crest of the maxillary bone and the posterior lacrimal crest of the lacrimal bone. For an external DCR, after making a transcutaneous incision along the medial canthus, dissection

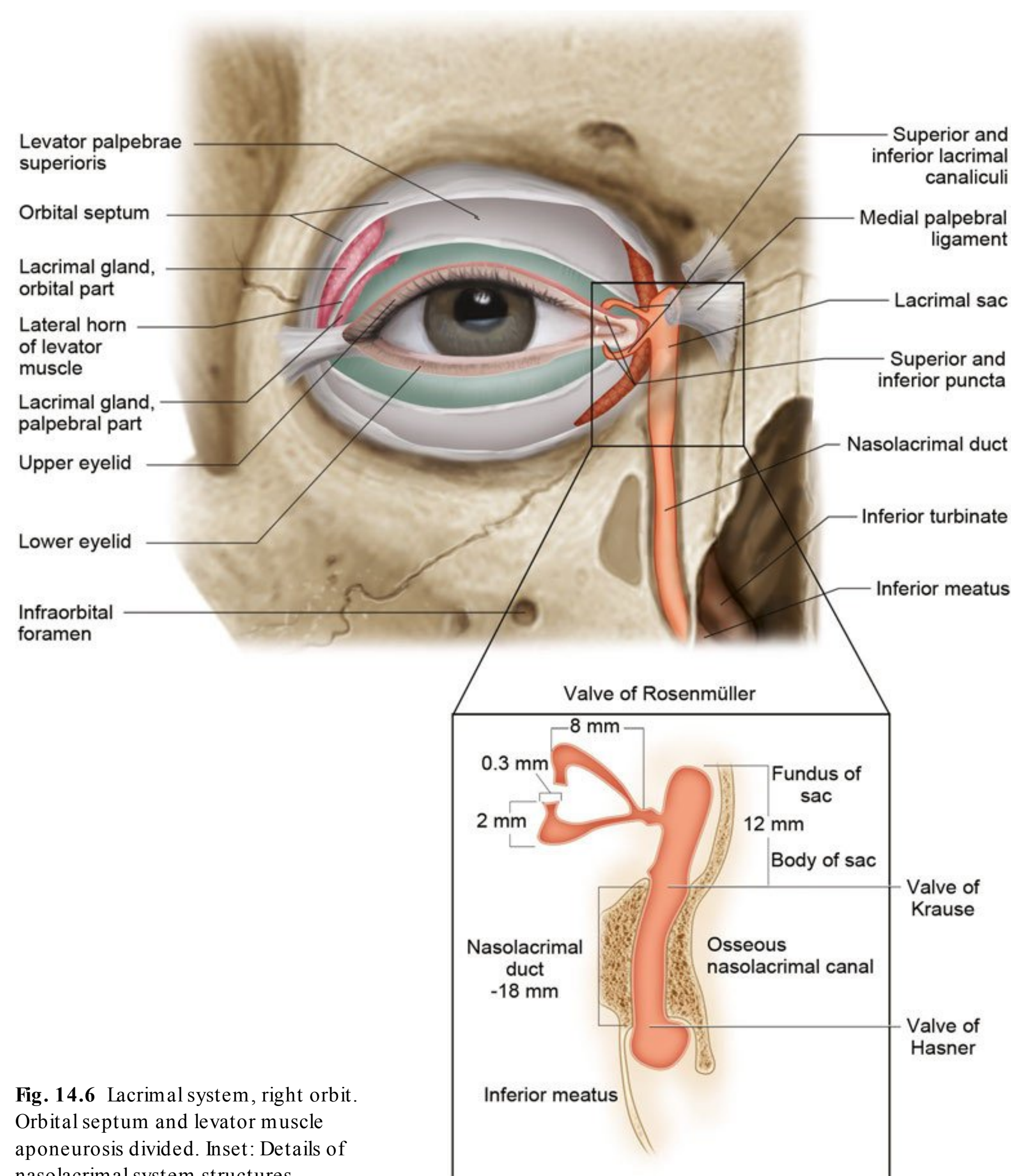


Fig. 14.6 Lacrimal system, right orbit. Orbital septum and levator muscle aponeurosis divided. Inset: Details of nasolacrimal system structures.

continues down to periosteum. The anterior lacrimal crest is exposed, the sac is elevated out of the fossa, and the posterior lacrimal crest is visualized. Although the anterior limb of the MCT may be intentionally disinserted, too posterior of a dissection may result in disinsertion of the posterior limb of the MCT at the posterior lacrimal crest and loss of lid apposition to the globe.

An osteotomy is created anterior to the middle meatus to enter the nasal cavity. In many individuals, ethmoidal air cells are present medial to the lacrimal sac fossa or at least extend anterior to the posterior lacrimal crest.^{6,7} The ethmoidal air cells may have to be removed for the new osteotomy to communi-

cate with the nasal cavity and not with the ethmoid sinus. A larger osteotomy and the absence of obstruction of the common internal ostium may increase the chance of a successful DCR.⁸ A distance of at least 5 mm has been suggested between the common internal ostium and osteotomy margin.⁹

If a patient has persistent epiphora despite a patent DCR, lacrimal sump syndrome should be considered.¹⁰ Inadequate drainage of tears that accumulate in an intact inferior lacrimal sac with possible bone remaining medially may result in this finding. This can be avoided by ensuring that the osteotomy and lacrimal sac marsupialization extend inferior to the proximal nasolacrimal duct.

References

1. Sherman DD, Gonnering RS, Wallow IHL, et al. Identification of orbital lymphatics: enzyme histochemical light microscopic and electron microscopic studies. *Ophthal Plast Reconstr Surg* 1993; 9(3):153–169 [PubMed](#)
2. Gausas RE, Gonnering RS, Lemke BN, Dortzbach RK, Sherman DD. Identification of human orbital lymphatics. *Ophthal Plast Reconstr Surg* 1999;15(4):252–259 [PubMed](#)
3. Massry G. “The inverse shoe shine sign” in transconjunctival lower blepharoplasty with fat repositioning. *Ophthal Plast Reconstr Surg* 2012;28(3):234–235 [PubMed](#)
4. Jones LT. An anatomical approach to problems of the eyelids and lacrimal apparatus. *Arch Ophthalmol* 1961;66:111–124 [PubMed](#)
5. Lemke BN. Lacrimal anatomy. *Adv Ophthalmic Plast Reconstr Surg* 1984;3:11–23
6. Whitnall SE. The relations of the lacrimal sac fossa to the ethmoidal cells. *Ophthalmic Res* 1911;30:321–325
7. Blaylock WK, Moore CA, Linberg JV. Anterior ethmoid anatomy facilitates dacryocystorhinostomy. *Arch Ophthalmol* 1990;108(12): 1774–1777 [PubMed](#)
8. Linberg JV, Anderson RL, Bumsted RM, Barreras R. Study of intranasal ostium external dacryocystorhinostomy. *Arch Ophthalmol* 1982;100(11):1758–1762 [PubMed](#)
9. Jones LT. The cure of epiphora due to canicular disorders, trauma and surgical failures on the lacrimal passages. *Trans Am Acad Ophthalmol Otolaryngol* 1962;66:506–524 [PubMed](#)
10. Jordan DR, McDonald H. Failed dacryocystorhinostomy: the sump syndrome. *Ophthalmic Surg* 1993;24(10):692–693 [PubMed](#)

Surface Anatomy

The eyelids provide globe protection, contribute to tear production, and distribute tears. The adjacent forehead and midface influence correct eyelid positioning. Understanding these relationships is essential in eyelid surgery.

The upper and lower eyelids, along with the upper and lower puncta, oppose the globe. The upper lid naturally rests 1 to 2 mm below the superior limbus and peaks 1 mm medial to the center of the pupil. The lower lid rests at the inferior limbus and peaks 1 mm lateral to the center of the pupil. Horizontal and vertical interpalpebral fissures are about 30 mm and 10 mm, respectively. The lateral canthal angle is about 2 mm higher than the medial canthal angle. The medial canthal angle is slightly rounded compared with the sharply peaked lateral canthal angle (Fig. 15.1).

The eyebrows set above the superior orbital rim but slightly lower at the rim in males. The brow usually peaks at the lateral limbus. The forehead extends from the hairline to the glabella and superior orbital rim. The midface extends from the lower lids tapering medially to the nasolabial folds to encompass a triangular area. Facial mimetic muscles, those contributing to facial expression, influence brow position, and also cause skin furrows, including in the forehead, periorbital region, and midface.

Eyelid Anatomy

Upper Eyelid Layers

The layers of the upper eyelid vary depending on the location in the eyelid (Fig. 15.2a). Anterior to the tarsus, the structures from anterior to posterior include skin, orbicularis oculi muscle, tarsus, and conjunctiva. A few millimeters above the tarsus, structures include skin, orbicularis, orbital septum, orbital fat, levator palpebrae superioris muscle, Müller muscle, and conjunctiva. The orbital septum fuses with the levator muscle about 2 to 5 mm superior to the tarsus in non-Asians and anterior to tarsus in Asians. Orbital fat descends inferiorly to fill the space between the septum and levator, which results in a fuller lid appearance.

Lower Eyelid Layers

The layers of the lower lid are similar to those of the upper except that the lid retractors consist of the capsulopalpebral fascia, analogous to the levator muscle, and the inferior tarsal muscle, analogous to Müller muscle (Fig. 15.2a).

Skin

The eyelid skin is the thinnest in the body. The lid also lacks subcutaneous tissue so the skin attaches directly to the underlying orbicularis muscle. In the upper lid, the levator muscle sends fascial attachments to the overlying orbicularis and skin to create an upper lid crease. The crease is about 10 mm or 8 to 9 mm above the lid margin in females and males, respectively. In Asians, it may be closer to the lid margin or absent. The upper lid skin is continuous with that of the thicker skin of the brow. The superior sulcus is located below the brow and tends to hollow with age.

Protractors

Orbicularis oculi muscle contraction results in eyelid closure. Its fibers are concentric around the eyelids. It is divided into the pretarsal, preseptal, and orbital regions (Fig. 15.3). The pretarsal and preseptal orbicularis are involved in involuntary blink, whereas the orbital portion is involved in voluntary lid closure. The orbicularis oculi contributes to the lacrimal pump.

The pretarsal orbicularis oculi divides into a superficial and deep head at the medial canthus. The superficial head fuses with the medial canthal tendon (Fig. 15.4). The deep head, also known as Horner's muscle, inserts onto the posterior lacrimal crest. Contraction pulls the lid medially and posteriorly against the globe. Laterally, the fibers from the upper and lower lids fuse into a common tendon and insert onto Whitnall's tubercle.

The preseptal orbicularis also divides into a superficial and deep head that insert onto the medial canthus. The superficial

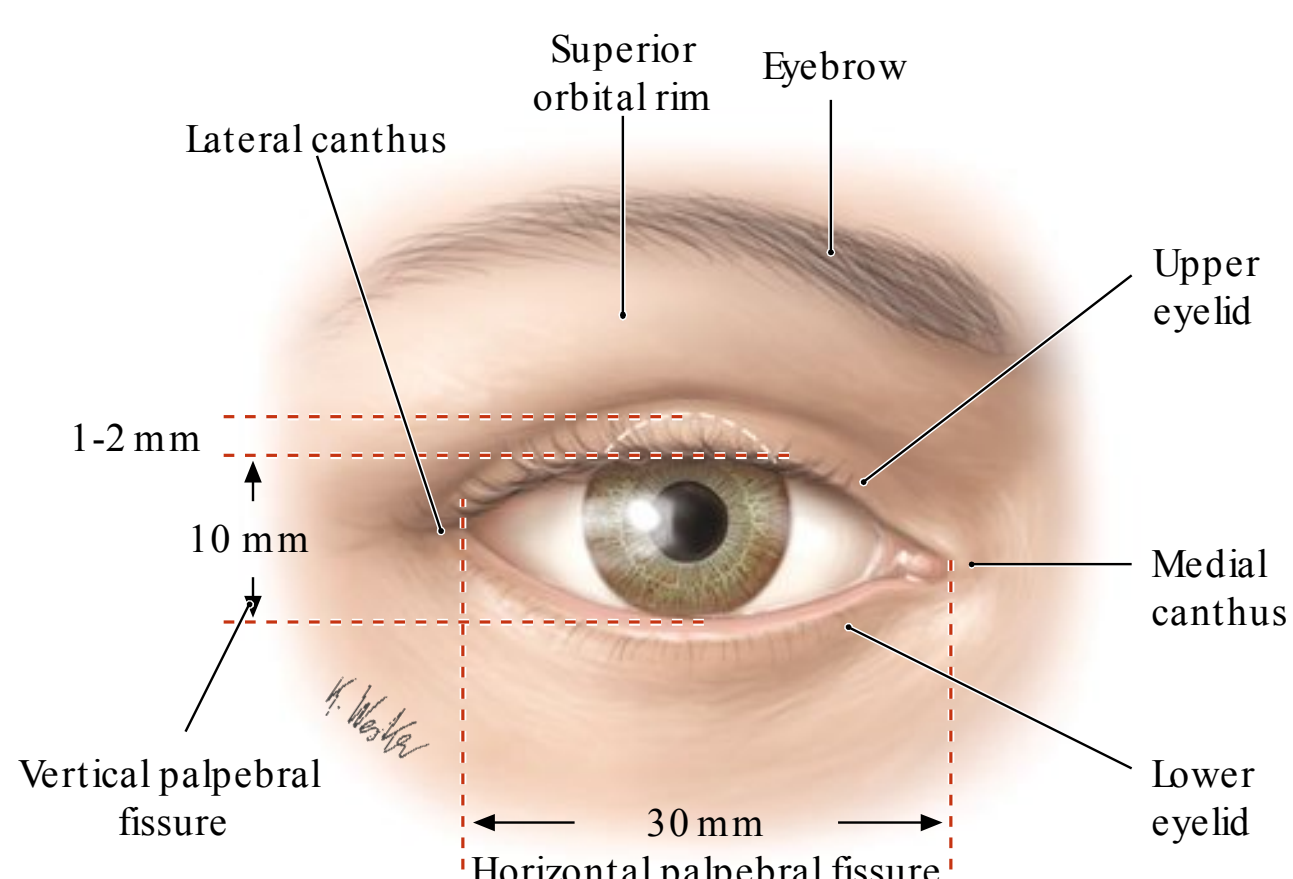


Fig. 15.1 Surface anatomy of periorbital region. Right eye, anterior view. (Modified from THIEME Atlas of Anatomy, Head and Neuroanatomy. © Thieme 2010, Illustrations by Karl Wesker.)

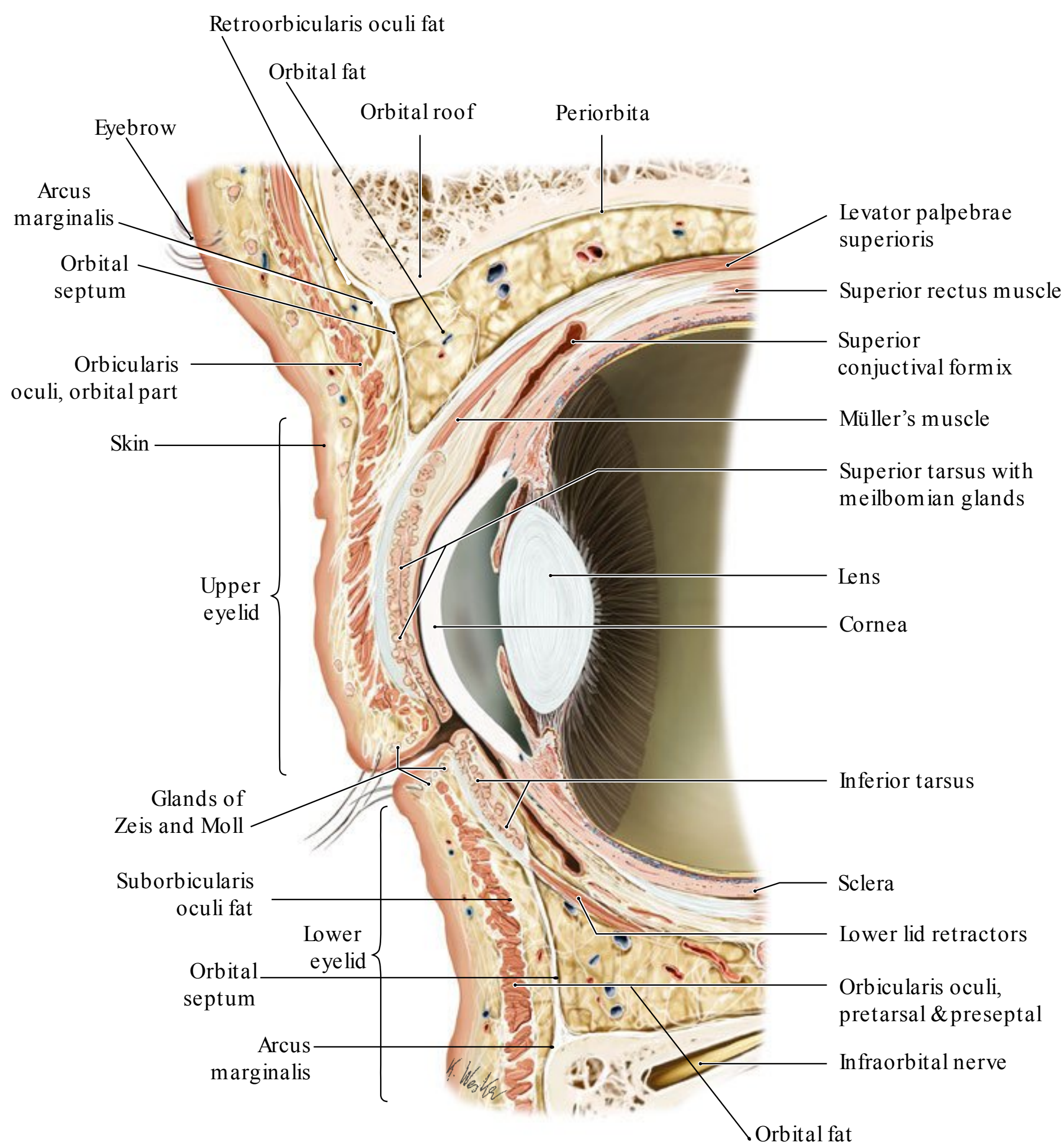
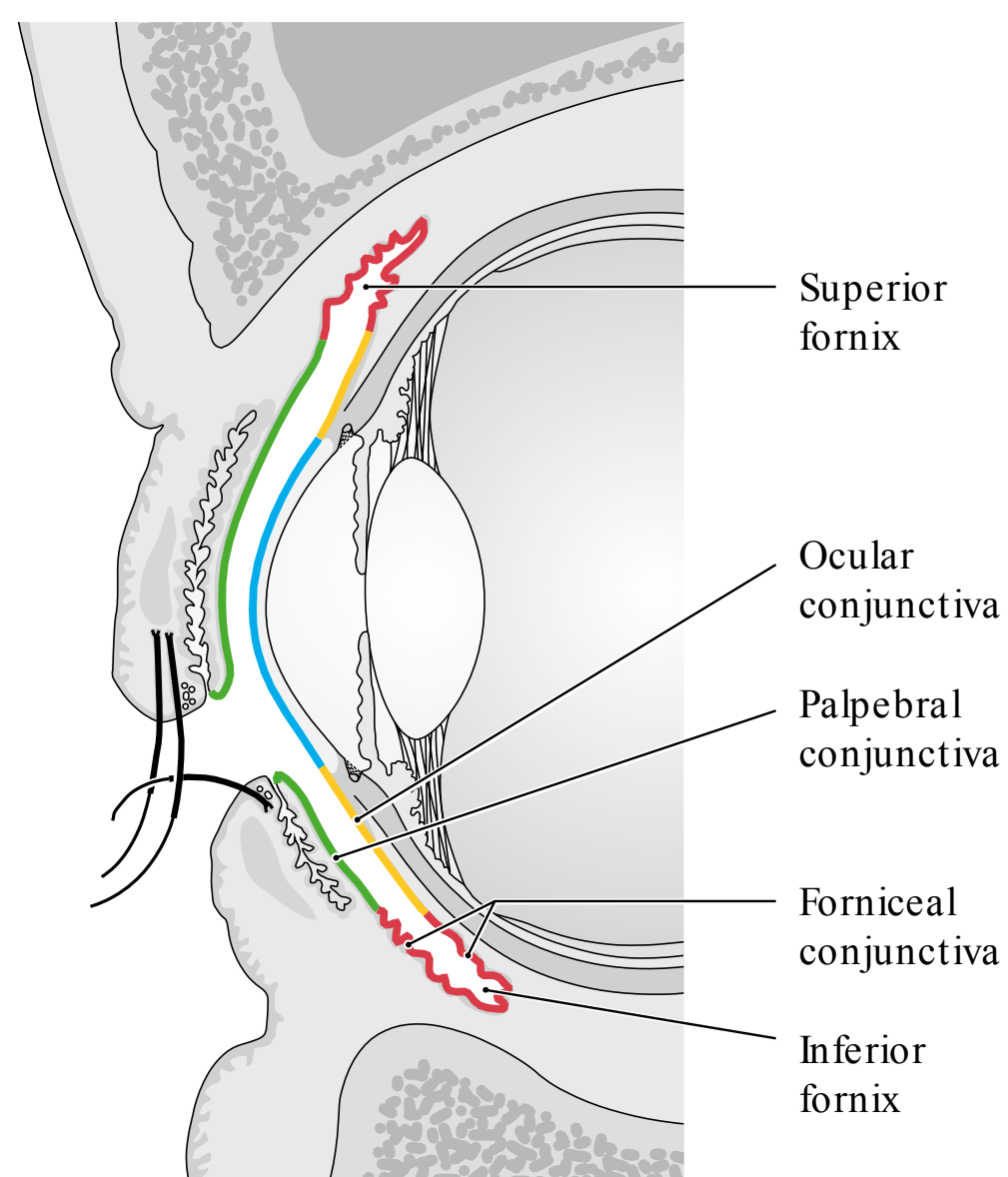
**a****b**

Fig. 15.2 Structure of eyelids and conjunctiva. (a) Sagittal view of eyelids and surrounding structures. (b) Anatomy of conjunctiva. (Modified from THIEME Atlas of Anatomy, Head and Neuroanatomy. © Thieme 2010, Illustrations by Karl Wesker.)